The Phases of Butane:
An Investigation by Computer Simulation and Neutron Diffraction

Thesis

Submitted by

Keith Refson

for the degree of

Doctor of Philosophy

University of Edinburgh

January 1986

I declare that this thesis is entirely my own work.

Acknowledgements

I am indebted to the following people and organisations who have helped me to produce this thesis - My supervisor, professor G. S. Pawley who initiated the project and who was always ready with advice or encouragement when it was needed. He read the manuscripts and showed me how to substitute an elegant phrase for a clumsy one; Dr Martin Dove, some of whose enthusiasm for the field of plastic crystals has rubbed off onto myself, Dr A. W. Hewat who rendered invaluable assistance as a scientific contact at the Institut Laue-Langevin and the staff of the physics department for the facilities thereof and especially Professor D. Wallace whose tireless pursuit of funding keeps the DAP computers running.

The Edinburgh Regional Computing Centre and its staff deserve a special mention for support of the DAPs and other computers, for the graphics and text processing facilities on which this thesis was composed and for the consistenly helpful attitude of the staff.

I am also grateful to the Science and Engineering Research Council for financially supporting the DAP computers and the ILL and its facilities and the Carnegie Trust for the Universities of Scotland for maintaining me and paying my fees.

"And are you not a greater analyst than the Googleplex Star Thinker in the Seventh Galaxy of Light and Ingenuity which can calculate the trajectory of every single dust particle throughout a five-week Aldebaran sand blizzard?"

"A five-week sand blizzard! You ask this of I who have contemplated the very vectors of the atoms in the Big Bang itself? Molest me not with this pocket calculator stuff."

Conversation between Fook and the computer Deep Thought from *The Hitch-Hiker's Guide to the Galaxy* by Douglas Adams.

Abstract

This thesis is a study of the solid phases of *n*-butane and in particular the orientationally disordered phase.

The crystallographic structures of all three phases were solved by neutron powder diffraction which showed them each to contain two molecules in the unit cell with space group $P2_1/c$. The molecular packing in form III is such that the long axes of the symmetry related molecules are roughly parallel whereas in both forms II and I they are almost perpendicular. Phase I is orientationally disordered about an axis along the longest dimension of the molecule.

The major part of this study was a molecular dynamics simulation of 2048 molecules of *n*-butane implemented in the ICL DAP computer. The simulation model included three internal molecular degrees of freedom and is unusual in that it was implemented using generalised co-ordinates. This large system together with the Parrinello and Rahman zero stress algorithm freed the system from the constraining effects of the periodic boundary conditions and allowed structural transformations to take place.

The experimental structures of all three solid phases were reproduced in the simulation and a transition from the ordered phase II to the disordered phase I was demonstrated. The simulated orientational distribution function agreed well with that obtained in the experiment. It is shown that in phase I the molecules librate about the disorder axis with large amplitude and that reorientations between the maxima of the orientational distribution function take place.

Contents

Chapter 1

Molecular Crystals, Orientational Disorder and Butane

§1.1 Molecular Crystals and the Plastic Phase

In recent years there has been a great deal of interest in the physics of molecular crystals. The term *molecular crystal* applies to an enormous range of substances which varies from the diatomic gases, simple hydrocarbons and halocarbons such as methane and carbon tetrachloride, through to very large molecules such as the long chain hydrocarbons, and includes ammonium and other salts with polyatomic ions. The feature which classifies a crystal as molecular is the unambiguous identification of some molecule or ion which is sufficiently tightly bound to exist independently of its surroundings and is therefore also present in the liquid and gas phases. The existence of distinct molecules in the solid state is due to the presence of two different kinds of interatomic forces, the strong covalent forces which bind atoms into a molecule and the much weaker external forces, either Van der Waals or electrostatic which bind the molecules to form a crystal.

Molecular crystals which are bonded mainly by Van der Waals (or dispersion) forces have certain common physical and electrical properties. Since the intermolecular binding forces are weak these solids have rather low melting points, especially those composed of light molecules whose solid phases exist only at well below room temperature. Van der Waals crystals are all insulators because the outer atomic electrons are highly localised in the covalent bonds and collective electronic properties are not important. Examples of this type of bonding are the crystals of the aromatic and aliphatic hydrocarbons, substituted hydrocarbons and the diatomic gases.

Because of the stronger intermolecular forces, ionic molecular crystals have much higher melting points than Van der Waals crystals, often over 1000K. Like the Van der Waals systems there are no conduction electrons, but there is a very important class of solids where certain ions are sufficiently mobile to conduct electricity. These are known as superionic or fast ion conductors. Ionic molecular crystals include potassium cyanide, ammonium sulphate and the superionic lithium sulphate.

Despite the macroscopic differences the presence of tightly bound molecular units means that the microscopic dynamics of these two classes share a number of properties which are not found in other systems. These all arise from the rotation

or libration of the molecule as a whole and the competition between the forces acting between different pairs of atoms belonging to the same molecules.

The crystallography of molecular solids is often rather interesting. In many cases the number of possible molecular arrangements is limited by the need to avoid molecular overlap, and geometrical packing considerations become important for all but the smallest molecules. Furthermore because atoms do not have the freedom to move independently there is competition between the interatomic forces. As a result the crystallographic unit cells are often large and have low symmetry. For example the low temperature phase of carbon tetrabromide is monoclinic and has 32 molecules in the unit cell (Finbak & Hassel, 1937; More *et al* 1977).

The effects of complex intermolecular interactions in a molecular crystal are manifest not only in the crystal structures, but also in the properties in all regions of the phase diagram. Molecular crystals therefore often have several solid phases and concomitant transitions. An extreme case is ice which has ten known crystalline phases (Polion & Grimsditch, 1984). Structural phase transitions have been studied extensively for many years, revealing a rich variety of behaviour. This has inevitably included a great deal of work on molecular solids. It would be inappropriate to review the fascinating phenomenology of molecular crystals here but a brief mention of some of the categories of phase transitions is in order. There are the ferroelectric (Bruce & Cowley, 1981) and incommensurate (Cailleau, 1984) transitions. These are examples of displacive transitions where the two phases are related by a small change in the position or orientation of part of the crystal basis. In contrast, there are reconstructive transitions where there is no such simple relationship between the phases. The annealing transition between phases III and II of *n*-butane described in chapter 4 of this work is a good example. There is a gross molecular reordering from a phase in which the two molecules in a unit cell are nearly parallel to one in which they are almost perpendicular. There also exists a transition between the insulating and conducting phases of superionic crystals. Of particular interest is the behaviour of those superionic systems which contain polyatomic ions such as lithium sulphate (Aronsson *et al.*, 1980; Impey *et al.*, 1985) and sodium uranium bromide (Hewat, 1984). The large SO_4 or UBr_6 ions rotate co-operatively in the high temperature phase in such a manner as to facilitate the passage of the smaller ions in a 'turnstile' effect.

However the rotation of molecules or ions in a crystal is of much wider significance than just the above examples. It is one of the most widespread phenomena observed in molecular crystals as a whole and the dynamics of such orientationally disordered phases is the subject of intense study.

An *orientationally disordered* or *plastic* phase is one in which the molecular centres of mass continue to occupy lattice sites but are oriented in some random way. It is a state which is intermediate between a crystalline solid where there is both orientational and translational order and a liquid where there is neither. Plastic phases occur commonly with molecules which are small or nearly spherical but are by no means unique to such systems. A contrast may be drawn with the liquid crystal state which is formed from large and very anisotropic molecules. These are rotationally ordered but translationally disordered, the reverse of the situation in a plastic crystal.

The concept of an orientationally disordered phase was first introduced by Simon and von Simson in 1924 in order to account for the large increase in heat capacity at the phase transition in hydrogen chloride. It was subsequently applied to other similar substances but the first proper classification of plastic phases was done by Timmermans (1935; 1938). He found that a number of crystals with nearly spherical molecules undergo a solid-solid phase transition to a high temperature phase which is very soft and plastic. The entropy of transition is high and the entropy of fusion low, less than 5 e.u.(c mol^{-1} K^{-1}) which indicates a highly disordered phase. He coined the term *plastic crystal* for these substances. The terms *plastic*, *orientationally disordered* and *rotator* phases are now used interchangeably and will be regarded as synonyms for the remainder of this work.

Although Timmermans only included Van der Waals bonded crystal in his definition of the plastic phase, many ionic crystals also have orientationally disordered phases. For example there are the ammonium salts and the much studied alkali cyanides (Luty, 1981; Lynden-Bell *et al*, 1983) The disorder in lithium sulphate is particularly intriguing as the rotational motion of the sulphate ions is very closely associated with the hopping motion of the lithium ions, linking the orientational disorder to the superionic conduction.

The disorder can not be of a static nature because all plastic crystals exhibit a low temperature ordered phase. It was assumed by Timmermans that the molecules undergo rotational motion of some sort. Packing considerations imply that in most cases the molecular rotation can not be free since rotation of a single molecule in the crystal would result in close approaches between its atoms and those belonging to the surrounding molecules. There are therefore potential barriers to rotation which are often very much larger than thermal energies. This means that the rotation is always hindered to some extent. The motion is therefore likely to involve co-operative effects where a cage of molecules move apart briefly allowing the central molecule to spin freely.

The disorder has serious consequences for the experimental determination of the crystal structures of plastic phases. The Debye-Waller factors for x-ray and neutron diffraction are large, which reduces the intensity of the Bragg peaks and eliminates high order reflections entirely. This is often compounded by intense diffuse scattering which appears as a strong background. The combination of these effects can be very severe. In the powder spectrum of neopentane for example only four peaks are visible (Mones & Post 1952) and in cyclobutane (Carter & Templeton 1953) there is only one. Fortunately such extreme cases are exceptional and there is usually enough information in the diffraction data to make a structure determination possible.

It is common for the plastic phase structure to have a higher symmetry than the ordered phase and in some cases higher than the molecular symmetry would support. If, for example, molecules reorient between non-equivalent sites which have equal probabilities of occupancy, the site symmetry is combined with the molecular symmetry to give the observed point group symmetry. It is for this reason that many plastic phases are face centred cubic *eg* methane, hydrogen chloride and carbon tetrachloride, in contrast to the lower symmetry ordered phases which for the above molecules are orthorhombic, tetragonal and monoclinic respectively.

§1.2 Classification of Disorder

The subject of this thesis is a study of orientational disorder in *n*-butane. However one system should not be considered in isolation and a comparison with other disordered molecular systems is valuable. Similarities in the microscopic properties may admit of a similar explanation and any universal aspects of these systems may be revealed. On the other hand one of the reasons for embarking on this study is that it may uncover new and interesting aspects of disordered systems.

Despite the ubiquitous occurrence of disordered phases the microscopic descriptions of the molecular disorder do differ considerably. The remainder of this section is a brief summary of some of the different types of orientationally disordered systems. It is not intended as a review, but simply to use selected examples to illustrate the kind of properties which are of interest and to provide a framework in which to discuss the disorder in *n*-butane.

Nearly Free Rotators

A few molecules show nearly free rotation in their plastic phases. The torques acting on the molecules in the crystal environment must therefore be small, which requires that two conditions be satisfied. Firstly the molecule should be small compared to the intermolecular spacing. In this way the moment of the intermolecular forces is small. Secondly, anisotropic electrostatic interactions must be insignificant, so that only non-polar and usually highly symmetric molecules display this behaviour. Examples are the hydrogen halides (See Dunning, 1979; Cole & Havriliak, 1951) except for HF whose large dipole moment prevents the existence of a plastic phase.

The effect of electric quadrupole interactions is clearly demonstrated in the case of nitrogen. It is experimentally observed that nitrogen has an ordered phase below 35K, the α phase. It has been found that model calculations must include the quadrupolar interaction otherwise they predict that this phase is disordered (Murthy *et al.*, 1981; Weis & Klein, 1975).

An interesting case is that of methane, CD_4. In Phase II there is partial disorder; 2 out of the 8 molecules in the primitive unit cell show free rotation while the other 6 are ordered (Bol'shutkin *et al.*, 1971). James and Keenan (1959) predicted the existence of just such a phase using a model which only considered quadrupolar interactions. The molecule is too small for steric hindrance to be

significant and the quadrupolar forces cancel for two of the sites by crystal symmetry, which leaves those molecules free to rotate.

Tetrahedral Molecules

There are many crystals composed of molecules of the type AX_4 which have similar plastic phases. In the *fcc* phase I molecules with T_d symmetry sit at sites with O_h symmetry. The site symmetry is due to the molecules disordering between non-equivalent orientations. Dolling *et al.* (1979) measured elastic neutron diffraction and the diffuse scattering from carbon tetrabromide. They established the form of the orientational distribution function (ODF) of the molecules and showed that it has O_h symmetry. It was assumed that this is a case of a system where molecules librate about one of a choice of orientations between which they occasionally make rotational jumps. However recent simulation results (Dove, 1986) have cast doubt on such an interpretation and suggest that rotational diffusion is a better model.

Octahedral Molecules

Sulphur hexafluoride is an octahedral molecule which occupies sites of the same symmetry in a body centred cubic plastic phase. In contrast to CBr_4 the disorder is not associated with a discrepancy between the point group symmetries of molecule and structure. Neutron experiments (Dolling *et al.*, 1979) show that the main lobes of the ODF for the S-F bonds lie along the cubic 100 directions but that there is a significant probability of finding molecules at all other orientations. Dove and Pawley (1983) have shown that in this case the disorder arises from what they term *orientational frustration.* The interaction between nearest neighbour molecules tends to order the molecules so that the S-F bonds lie in the (100) directions, which results in close contacts between the fluorine atoms of next nearest neighbours. These give rise to strongly repulsive forces which favour other orientations and it is the competition between nearest and next-nearest neighbour forces which is the ultimate cause of the disorder.

One Dimensional Rotators

A number of systems display one dimensional disorder, where the molecules are randomly oriented about a single axis. In contrast to the examples above they are usually long chain molecules. Hydrocarbon chains, C_nH_{2n+2} with n=11-35 have been much studied by various experimental techniques (Strobl *et al.*, 1974; Ewen *et al.*, 1974; Zerbi *et al.*, 1981, Ewen & Richter, 1978). They exhibit hexagonal rotator

phases where the molecules disorder about the long molecular axis. Monte Carlo simulation (Yamamoto, 1985) indicates that the molecules jump by 180°, and other evidence (Zerbi *et al.*, 1981) show that the reorientations are often coupled with translations of 2 methylene units along the axis. It has been suggested that the molecules are not always in the elongated *trans* conformation and that the transformation from *trans* to *gauche* bonds plays an important part in the motion.

A few relatively small molecules also show one dimensional disorder. Pivalonitrile, $(CH_3)_3CCN$, has a single axis of threefold symmetry about which the molecules disorder. A further example, 1,2-dichloroethane is rather unusual in that the molecules disorder not about a symmetry direction but along the line joining the two chlorine atoms. It is also unusual in that the disorder does not increase the symmetry; phase I is monoclinic as is phase II (Milberg & Lipscomb, 1951; Reed & Lipscomb, 1953). This feature may be connected in some way with the absence of a discontinuity in the specific heat curve between phases I and II (Pitzer, 1940). Instead of the expected singularity there is a continuous rise to a peak at 180K and therefore no true phase transition.

It is notable that because of the incomplete disorder the entropies of fusion of both these materials are rather high at 7.6e.u. and 8.9e.u. respectively, which places them outside Timmermans' strict definition of a plastic crystal.

§1.3 Theory, Experiment and Dynamics

One of the most interesting aspects of the solid state is the dynamic behaviour of the constituent particles. This has been widely investigated for many years and a variety of theoretical models and experimental techniques have been developed. We are concerned here with the extension from atomic and simple ionic solids to condensed molecular phases. Any theory should address the variety of new and complex behaviour which is seen in molecular systems, in particular the phenomenon of orientational disorder. Such behaviour goes beyond the description of microscopic dynamics which sufficed for atomic systems and the theory needs revising and extending. Unfortunately no comprehensive theoretical model has been found which is capable of describing the dynamics of molecular systems in general and in particular there is still no good model of orientational disorder.

The standard approach to motion in crystals is lattice dynamics (See for example Born & Huang, 1954) which is a general description taking full account of the collective motion. It yields the dispersion relations for phonons from which all thermodynamic properties may be calculated, and theoretically it can be applied to any crystal. However it is a harmonic approximation which assumes small displacements and it is therefore a low temperature theory. Since anharmonic interactions play a predominant role in most phase transitions, the harmonic approximation is only valid well below any such transition. The theory may be extended by the inclusion of anharmonic terms (for a review see Cochran & Cowley, 1967). It can then account for such phenomena as thermal expansion and the temperature dependence of phonon frequencies. The field of lattice dynamics reached maturity by 1960 with the development of neutron inelastic scattering in parallel with the theory. Using this technique it became possible to measure dispersion curves experimentally at all wavevectors, a significant advance over light scattering which can measure frequencies only at $\mathbf{q}=\mathbf{0}$. Lattice dynamics provides the model by which the neutron data can be interpreted, and the experiment allows refinement of the theory and evaluation of the force constants.

However the Born von Karman theory of lattice dynamics is difficult to interpret when applied to molecular crystals as it does not distinguish between the inter- and intramolecular forces. There are a large number of interatomic interactions, internal and external, which are involved in the dynamics of molecular crystals. The nature and strength of the forces is not known *a priori* and it is therefore necessary to use a potential with adjustable parameters which are fitted to experimental data. Both the number of parameters and the size of the dynamical matrix grow rapidly with

the complexity of the crystal and the calculation becomes unmanageable for all but the simplest systems. However most of the modes involving internal vibration are of a much higher frequency than the lattice modes because of the high strength of the covalent intermolecular forces. These internal modes are fairly independent of **q** and are not very different in frequency from those in an isolated molecule. It is not these modes but the lower frequency lattice modes which are of interest.

The approach of Cochran and Pawley (1964) takes advantage of this by only considering relevant modes. The molecule is treated as a unit (initially rigid) with only six degrees of freedom. The lattice dynamics is formulated in terms of three translational and three rotational co-ordinates per molecule. The resulting model has a much smaller number of unknown force constants which number may be further reduced by symmetry considerations. This is a practicable approach to the lattice dynamics for highly symmetrical molecular systems. Using this method Cochran and Pawley calculated dispersion curves for hexamethylenetetramine which compare well with those measured using neutron scattering by Dolling and Powell (1970).

There are two possible approaches to the question of force constants. The first is the method used by Cochran & Pawley for hexamethylenetetramine in which the force constants were fitted to experimental data. The disadvantage is that the constants can not be transferred to other systems. The other method is to synthesize the intermolecular forces from a sum of atomic pair forces calculated from a simple model potential. The adjustable parameters of the potential can be fitted to a range of experimental data. The great strength of this approach is transferability as the same potential can be used in calculations on different phases, or even on different molecules with the same atoms. This type of model has also been extensively and very successfully used in simulation calculations and will be discussed in greater detail in § 2.2.1.

The use of anharmonic expansions allows the dynamics of a crystal to be calculated at non-zero temperatures. The theory works at high enough temperatures to describe certain displacive transitions which have an associated soft mode. Although the calculations are difficult it has been shown that certain phonon frequencies go to zero at the transition temperature (Cowley, 1965). However reconstructive transitions can not be explained in this manner and lattice dynamics fails for plastic transitions in particular.

The presence of competing interactions and molecular libration means that the dynamics of molecular crystals is often highly anharmonic. In the case of an

orientationally disordered phase there is a catastrophic breakdown of lattice dynamics. The eigenvalues of the dynamical matrix are negative for certain modes indicating a structural instability of the crystal which is not observed. This happens in the case of sulphur hexafluoride (Pawley, 1981). Because the motion in such systems is not confined to libration and vibration about some mean, the perturbational approach of the anharmonic theory can not help.

The inappliccability of lattice dynamics has serious consequences for the experimental investigation of plastic phases. No experiment can yield a complete picture of crystal dynamics, so that all results must be interpreted on the basis of some model. In the case of inelastic neutron scattering this model has been lattice dynamics. It is therefore necessary to find new models in order to interpret the experimental results.

A number of models of molecular disorder have been used to interpret experimental results. To achieve a model which is analytically tractable only single particle motion is considered and the collective aspect of molecular motion as given by lattice dynamics is lost. In these 'Einstein models' the disorder is assumed to be independent of the surrounding molecules and also of the molecular centre of mass position.

Nevertheless a great deal can be learned about the dynamics of orientational disorder within the 'single molecule' model. There are several experimental methods which contribute including Raman and infra-red spectroscopy and nuclear magnetic resonance but one of the most exciting is the relatively new technique of quasi-elastic incoherent neutron scattering. Using high resolution instruments this technique can measure many interesting quantities such as rotational jump rates and amplitudes, orientational distribution functions and rotational diffusion constants. For a brief review see Leadbetter& Lechner (1979).

The evidence is accumulating that intramolecular and rotation - translational coupling do play an important part in the dynamics of plastic phases. Press *et al* (1979) re-interpreted the neutron scattering data of More and co-workers on CBr_4. They found a significant difference when rotation - translation coupling was included. Using a molecular dynamics simulation, Dove and Pawley (1983) found that in the case of SF_6 scattering from the rotation-translation coupling is of the order of 25% of the total. The neglect of the intramolecular and rotation-translation coupling is therefore a serious deficiency and a barrier to our understanding of the plastic phase.

It is for these reasons that computer simulations are playing an increasingly important part in the investigation of orientational disorder. There is no serious approximation involved and the collective dynamics are treated correctly. Single particle and co-operative effects can be separately identified and analysed by a number of techniques. As in the work of Dove and Pawley (1983; 1984) the scattering $S(\mathbf{Q},\omega)$ may be evaluated numerically and separated into its various contributions, which is of great value in the interpretation of experimental data. MD simulations can also provide detailed information on the dynamics of molecules that is inaccessible to any experiment. However, perhaps the most important role of MD is that it may suggest suitable models by which experimental data may be interpreted.

§1.4 Butane

N-butane is a saturated hydrocarbon of structural formula CH_3-CH_2-CH_2-CH_3. Figure 2.4 shows the molecular geometry. It is rather surprising that there is no report of the crystal structure of such a simple molecule in the literature. The lack of a known structure proved an impediment to progress with the computer simulations which form the major part of this study. A structural investigation using neutron powder diffraction was therefore undertaken and was very successful, the results of which are presented in chapter 4.

N-butane has a solid-solid phase transition at 108K and melts at 135K. The transition is strongly first order with a large entropy of 4.59eu. The entropy of fusion is 8.225eu (Aston & Messerly, 1940) placing it outside the range of plastic crystals defined by Timmermans. However phase I which exists between 108K and 135K is disordered. This is suggested by the large entropy of transition and confirmed by Raman and infra-red spectroscopy (Cangeloni & Schettino, 1975) and by nuclear magnetic resonance (Hoch, 1976). The spectroscopic measurements also show that there are two phases below the transition which exist in the same range of temperature. Phase II is metastable and may be produced by rapid cooling of phase I. It anneals to the stable phase III between 85K and 90K.

It is well known that hydrocarbon molecules may distort by twisting about a carbon-carbon bond, and butane is no exception. One reason for choosing butane as the subject of this study is that it is the smallest hydrocarbon in which this internal twist changes the shape of the molecule significantly. Such rotation is not free as a considerable potential arises from exchange forces on the bond electrons and from nonbonded interatomic interactions. This is considered further in §2.2.2 and a model potential is plotted in fig 2.3. It has three minima which correspond to the three observed molecular conformations. There is the *trans* conformation in which the molecule is planar and extended and the two *gauche* modifications which in the notation of §2.2.2 have $\Psi = \pm 31.5^\circ$. Although the gas contains molecules in both conformations, the spectroscopic data (Cangeloni & Schettino, 1975) show that in the solid state all molecules are *trans*.

Very little was known about the nature of the orientational disorder in *n*-butane prior to this study. The only direct experimental evidence is the nuclear magnetic resonance data of Hoch (1976). The measured absorption line widths are intermediate between the values expected for an ordered system and a completely disordered system which suggests that single axis rotation is taking place. These

results were well fitted by a model in which the molecules make jump reorientations about the molecule's long axis between two sites separated by 180°. This conclusion is supported by the magnitude of the entropy of fusion which at 8.225e.u. is similar to those of pivalonitrile (7.6e.u.) and 1,2-dichloroethane (8.9e.u.) which are both single axis rotators.

It was seen in § 1.2 that the charge distribution and the shape and size of the molecule determine the nature of the disordered phase. In this case the molecule is neutral and in the *trans* conformation has inversion symmetry. The smallest non-zero moment is therefore the quadrupole which is small as the atomic charges in hydrocarbons do not exceed 1.5e (Williams & Starr, 1977). The molecule is sufficiently large that quadrupole forces do not play a significant role so that the dominant interactions are the short range Van der Waals forces. Because of the competition between these atomic pair forces it is the shape of the molecule which determines the dynamic behaviour.

The only molecular symmetry is a twofold axis plus, in the *trans* conformation, an inversion centre. The molecule is over twice as long along the line joining the end carbon atoms as it is in any orthogonal direction so there is no similarity to any of the near-spherical systems discussed in § 1.2. In a close packed crystal, rotation about either of the shorter axes will be strongly hindered by steric repulsion, and reorientation about the long axis will be favoured.

Because they are built from the same methyl units it is natural to compare butane with some of the longer *n*-alkanes which also have rotator phases. However as will be shown in chapter 4, the molecular packing is quite different and there is therefore only a slight similarity in the nature of the disorder.

The purpose of this work is to investigate the molecular crystal of *n*-butane and in particular the disordered behaviour in phase I. Butane is of special interest as it falls outside the mainstream of plastic crystals which are usually composed of globular molecules. The crystal structure will be studied by neutron diffraction and hopefully some information on the disorder will be obtained. However the main thrust will be the use of molecular dynamics simulations to describe and characterize the plastic phase. It is hoped to establish a good model of the disorder and in particular to check whether the rotation is about a single axis. It is also intended to use the power of MD simulation to study the dynamics of the molecules in the plastic phase.

There are also some longer term aims. Within the next few years computers will be very much more powerful than today's machines and it is vital that when they arrive suitable problems have been identified and the techniques for modelling them devised. There is certainly no shortage of large dynamical problems which would benefit from simulation studies given enough resources.

Two striking examples are biphenyl and liquid crystals. Biphenyl C_6H_5-C_6H_5 has an incommensurate phase at low temperatures with different incommensurate periods in two directions. The wavevectors of the distortion in these directions are 20 and 12 lattice translations and a simulation would require a MD cell with dimensions several times that in order to reproduce this phase. It has been suggested (Cailleau, 1984) that the incommensurate behaviour is associated with the double well potential to internal rotation about the bond joining the two benzene groups. Liquid crystals, on the other hand are composed of very long chain molecules, usually with some large molecular group on one end or in the middle. Despite the technological interest of these substances the microscopic dynamics is still not well understood.

In general larger molecules are more flexible that small ones so the rigid molecule approximation becomes less valid with increasing size of the molecules. This is clearly demonstrated in the two examples above where the internal motion plays an important part in the dynamics. An additional aim of this work is to establish the feasibility of simulating systems like these which contain very large numbers of molecules and/or large molecules with internal rotation so that the techniques and experience to make good use of the anticipated leap in computer power are available.

Chapter 2

Molecular Dynamics Simulations – Theory and Implementation

§2.1 Introduction to Molecular Dynamics

It is well known that many body problems using simple interparticle interactions can give rise to behaviour of extreme complexity. Many analytic techniques for calculating both dynamic and static properties of such systems have been developed, from sophisticated theories in statistical thermodynamics to the harmonic and anharmonic theories of lattice dynamics. These have had enormous success in correctly describing the properties of diverse forms of condensed matter including magnetic and crystalline solids. However there still remain many systems for which no satisfactory analytic techniques exist, which typically display a considerable degree of disorder. Examples include liquids, liquid crystals, superionic conductors and, importantly for the present work, molecular crystals with plastic phases.

With the advent of digital computers in the 1950's it became possible to perform numerical calculations on models of such systems, a technique which is known as computer simulation. The word 'simulation' is used because such methods involve an internal representation of the system under study as distinct from simple numerical integration or solution of differential equations. The strength of simulation methods is that, in principle, they allow the calculation of any thermodynamic property, statistical average or correlation function from the microscopic co-ordinates of the system. In practice some quantities are not so easily evaluated, entropy for example, but the vast majority of simply defined properties are easily accessible. In this way simulation calculations can yield numerical predictions from a theoretical model which is otherwise intractable.

An alternative view of a simulation is that of a 'computer experiment'. This interpretation is a natural one partly because the results are numerical with statistical fluctuations and partly because the results can be made to model a 'real' system so closely that a calculation can be treated as a measurement on the model system. From this point of view a simulation can yield much information on the microscopic level which is not available in any real experiment.

One of the simpler numerical methods is static energy minimisation. Given a set of particles with interactions defined between them the configuration of lowest internal energy (crystal structure) may be found by an iterative method. Crystal

structures, defect energies and surfaces have all been investigated using this method. However its use is limited by a major drawback; it is a simulation at zero temperature. Thus problems such as dynamic disorder in liquids, liquid and plastic crystals are not accessible, nor is the rich field of phase transitions.

The Monte Carlo method due to Metropolis *et al* (1953) provides a means of including temperature in the simulation. Without going into details, random numbers are used to generate configurations of the model system which are representative of the Boltzmann distribution for the chosen temperature. Ensemble averages of quantities of interest may be evaluated by a simple average over a sufficient number of configurations. The computer programs to do this are short and simple. Magnetic models, liquids and solids both ordered and disordered have all been extensively studied using Monte Carlo which has contributed enormously to our understanding of these systems. It is limited though to the calculation of static canonical ensemble averages and as such can provide no information on time dependent behaviour or dynamics.

The next logical step is the molecular dynamics simulation in which the ensembles are not generated at random but by the time evolution of the system from a pseudo-random start according to a set of equations of motion. Dynamic properties such as velocity autocorrelation functions, molecular reorientation rates and many more may all be calculated from the time- related configurations. The method is by no means restricted to equilibrium physics and has indeed been extensively used in the study of such non -equilibrium processes as shear viscosity, heat propagation and so on. These gains over the Monte Carlo method are at the expense of increased complexity of the programs and a considerable increase in the computer time required.

Molecular dynamics simulation was first used by Alder and Wainwright (1959) who used a very simple model in which the only interactions were elastic collisions between hard spheres. In such a case the time evolution is easily calculated: all the velocities are constant except at the instant of a collision where those of the particles involved change discontinuously. The problem is then reduced to identifying the time of the next collision, re - evaluating all positions and the changed velocities and repeating this procedure for every collision. However this is a poor model of the way that atoms interact in condensed phases and the extension to a continuous potential was made by Rahman (1964) in a paper which essentially defined the technique of molecular dynamics as it is used today. The method is described in detail in §2.1. It has been used in a systematic study of fluids by Verlet and Levesque (Verlet 1967,1968; Levesque & Verlet 1970; Levesque *et al*

1973) and many others. Dickey and Paskin (1969) first applied MD to the study of the solid state in an investigation of the anharmonic properties of a Lennard - Jones crystal. The method has since had wide application to solids ranging from metals (Parrinello & Rahman 1980,1981), superionic conductors (Dixon & Gillan, 1978; Impey *et al*, 1984) and disordered molecular crystals which are especially suited to MD simulation because of the short range nature of the potentials.

Throughout the 1970's and 1980's the increase in the available computer power allowed the simulation of systems of increasing complexity. (For pair interactions the CPU time is proportional to the square of the number of atoms in a molecule and the memory requirement is linearly related. Molecular crystals which have been simulated range from N_2 (Klein & Weis 1977) and NaCN (Lynden-Bell *et al*, 1983) through methane (Bounds, Klein & Patey 1980), carbon tetrachloride (McDonald, Bounds & Klein 1981), sulphur hexafluoride (Dove and Pawley 1983) to bicyclo(2.2.2)octane (Neusy, Nose & Klein 1983) and napthalene (Della Valle & Pawley 1984). The aforementioned systems are typical of the type of molecular crystals which have been simulated and they have several common features. All except napthalene have plastic phases, are composed of highly symmetrical molecules and are treated in the rigid molecule approximation. It was partly in order to investigate a molecular crystal of a low symmetry unit and one in which the internal degrees of freedom may be significant that n-butane was chosen as the subject of this study. The symmetry of the molecule is low and its two halves can rotate about the central carbon - carbon bond. These internal vibrations have rather a low frequency, less than 200 cm^{-1} (Durig & Compton 1979) and hence are much more likely to interact with lattice modes than are the faster bond stretch and flex modes.

§2.1.1 First Principles

Given a set of N particles with initial positions $\{\mathbf{r}_i(t)\}$, velocities $\{\mathbf{v}_i(t)\}$ which interact with via a potential $\Phi(\mathbf{r}_1, \ldots, \mathbf{r}_N)$, the aim of a molecular dynamics simulation is to solve the classical equations of motion

$$m_i \ddot{\mathbf{r}}_i(t) = -\nabla\Phi(\mathbf{r}_1(t), \ldots, \mathbf{r}_N(t)) \tag{2.1}$$

for all times t. An exact solution is not possible for all but the most trivial potentials so the time evolution is calculated as follows. Given the co-ordinates at time t, calculate a good approximation to them at $t+\delta t$, re-evaluate the forces and repeat the process to generate configurations at $t+2\delta t$, $t+3\delta t$ and so on. In this way the continuous trajectory of the particles in phase space is replaced by jumps between discrete points. To do this the differential equation (2.1) must be replaced by a difference equation (commonly known as an integration algorithm) which must generate a set of positions and momenta which lie very close to the true phase space trajectory. The interval δt is called the *timestep* and its value is of crucial importance for the accuracy of the simulation. Some of the various algorithms available will be discussed in §2.1.3 but for now, consider one due to Verlet (1967) which because of its simplicity and economy of storage and computation is very widely used. The Taylor expansion of $\mathbf{r}_i$ about t is

$$\mathbf{r}_i(t\pm\delta t) = \mathbf{r}_i(t) \pm \delta t\dot{\mathbf{r}}_i(t) + (\delta t^2/2!)\ddot{\mathbf{r}}_i(t) \pm (\delta t^3/3!)\dddot{\mathbf{r}}_i(t) + O(t^4). \tag{2.2}$$

Adding the expansions for $t+\delta t$ and $t-\delta t$ and ignoring terms of order t^4 and higher gives

$$\mathbf{r}_i(t+\delta t) = 2\mathbf{r}_i(t) - \mathbf{r}_i(t-\delta t) + \delta t^2\ddot{\mathbf{r}}_i(t). \tag{2.3}$$

If the last term is evaluated from (2.1) then (2.3) is a prescription for a new $\mathbf{r}_i$ in terms of its current and past values. The velocities do not appear explicitly in (2.3) and if required may be calculated to order t^2 from

$$\mathbf{v}_i(t) = \left(\mathbf{r}_i(t+\delta t) - \mathbf{r}_i(t-\delta t)\right) / (2\delta t). \tag{2.4}$$

The potential is usually of the form of a sum of pair interactions

$$\Phi(\mathbf{r}_1, \ldots, \mathbf{r}_N) = \sum_{i=1}^{N}\sum_{j=i+1}^{N} \phi(\mathbf{r}_j-\mathbf{r}_i) \tag{2.5}$$

where $\phi(\mathbf{r}_j-\mathbf{r}_i)$ is typically a Lennard-Jones interaction

$$\phi(\mathbf{r}_j-\mathbf{r}_i) = \phi(r_{ij}) = \varepsilon\left((\sigma/r_{ij})^{12} - (\sigma/r_{ij})^6\right). \tag{2.7}$$

The evaluation of this potential, or rather its derivatives, is usually the largest part of the computation in a MD simulation. Equation (2.5) has $N^2/2$ terms in the sum so that the time required to evaluate it is proportional to N^2. This clearly

limits N rather severely. However if the force, $\nabla\Phi$ decreases rapidly with r and is negligible outside some small radius r_c then no interactions outside this 'cut-off' radius need be evaluated. The computation time is then proportional to $r_c^3 N$.

The maximum number of particles in a practical simulation is of the order of 250-10000, which number would form a cluster with a diameter of at most 16 inter-particle spacings. Any properties calculated from such a cluster will therefore be dominated by surface effects. Periodic boundary conditions are usually imposed so that each particle is surrounded by others as in the bulk. The particles are confined to a box called the molecular dynamics cell which is periodically repeated to fill space. This cell is often, though not always, cubic and so each particle 'sees' images of itself at intervals of L where L is the dimension of the MD cell.

This choice of topology means that the density and volume of the simulated system are constant, and the equations of motion require that the energy is constant too. Thus all properties are evaluated in a microcanonical or (N,V,E) ensemble. This can lead to structural phase transitions being inhibited and in §2.1.5 an extension of the method to isobaric or (NpH) ensemble is described.

It is important to have some measure of the accuracy and correctness of a calculation. There is no easy way of doing this in general since if the solutions to the equations of motion were known there would be little point in doing a simulation. However the conserved properties of the system may be used as an indicator of correctness, though not a proof. In particular if the particle trajectories are solutions of the exact, continuous equations of motion then the total energy will be exactly constant. Any change with time must therefore be due to an error in the program or integration algorithm.

If the program and algorithm are correct then the accuracy of the integration depends on the value of the timestep chosen. If the step is too large then the trajectories produced will be incorrect especially if the forces are large. This leads to fluctuations and drift in the total energy since the change in potential energy of a particle on each step will not be cancelled by the correct change in kinetic energy. Too small a timestep is wasteful of computer time and may not allow runs which are sufficiently long to reproduce the physics. For molecular systems the value is usually around 10^{-14}s, but there is an obvious need for some objective criterion.

One suggestion for such a criterion is that the fluctuations in total energy should not exceed a 'few' percent of those in the kinetic energy (Fincham 1985). I propose

another criterion which is based on the dynamics of the system under study. The trajectory of a particle undergoing harmonic motion can not be reasonably reproduced with less than 20 steps in a cycle. Therefore if the timestep is less than $^1/_{20}$ of the period of the highest frequency mode in the system the trajectories will be reasonably well reproduced. Even if the system is highly anharmonic there will still be some 'fastest' motion, be it an occasional molecular reorientation. The criterion then becomes that the velocities should not change by more than (say) 5% of their value in one step.

This is a more stringent condition than Fincham's since in a complex system only a small fraction of the energy will reside in the highest frequency modes and even a large error could give a small discrepancy in the total energy. In addition it can be shown (Hockney and Eastwood 1983) that although the trajectories may be wrong, a harmonic simulation will only become unstable when the timestep exceeds half the period.

§2.1.2 Application to Rigid and Flexible Bodies

The simulation described in the previous section assumed a system of N identical point masses interacting by a simple pair potential. Such a description is inadequate for a molecular system in a condensed phase since the covalent intra-molecular forces are very much stronger than the Van der Waals inter-molecular forces. Thus the system has a very wide range of vibration frequencies. However the high frequency internal modes are often decoupled from the lower frequency lattice modes and in such cases the motion can be frozen and the extra degrees of freedom eliminated from the equations of motion. In most cases these modes are properly described only by quantum mechanics and the classical approximation is invalid. Appropriate constraints must therefore be applied to the system.

In the 'rigid molecule' approximation all the internal modes are frozen whereas for the simulation of large proteins, for example, only the bond vibrations are eliminated as the bond flex modes are essential to the dynamics (Berendsen and van Gunsteren 1983). The main advantage of freezing the 'hard' degrees of freedom is that it is possible to use a much larger timestep and depending on the method used there may be a saving in the amount of computation. The physical validity of applying constraints is discussed in §2.2.

There are two possible approaches to the calculation of the dynamics of a constrained system. Either the redundant degrees of freedom are eliminated and the equations of motion are reformulated in terms of a smaller number of generalised co-ordinates, or they are augmented using the method of Lagrange multipliers. The latter technique (Berendsen and van Gunsteren 1983) requires some extra calculation to evaluate the forces of constraint. Although it is conceptually simple it requires considerably more storage than the generalised co-ordinate method since dynamic variables corresponding to redundant as well as necessary degrees of freedom are included. For example consider a system of N molecules each with n atoms using the Verlet algorithm (2.3). The Lagrange multiplier method requires at least 15nN words of store, 5×3 per atom whereas only 5N×6 (degrees of freedom) = 30N are used by generalised co-ordinates. As the number of constraints increases and the model approaches a rigid molecule approximation the generalised co-ordinate method becomes increasingly attractive.

Consider the equations of motion in the rigid body approximation. It is necessary to choose some set of parameters to represent the orientational degrees of

freedom of the system. Their time derivatives must be calculated in terms of the angular velocity, $\boldsymbol{\omega}$ in order to integrate the equations of motion, a generalisation of (2.3). An obvious choice which has been extensively employed is the Euler angles ϕ,θ,ψ. They are related to the angular velocity, $\boldsymbol{\omega}$ by

$$\boldsymbol{\omega} = \begin{pmatrix} \cos\psi & \sin\theta\sin\psi & 0 \\ -\sin\psi & \sin\theta\cos\psi & 0 \\ 0 & \cos\theta & 1 \end{pmatrix} \begin{pmatrix} \dot{\theta} \\ \dot{\phi} \\ \dot{\psi} \end{pmatrix} \equiv \Xi.\dot{\boldsymbol{\alpha}} \tag{2.8}$$

In order to perform a timestep the inverse equation is required.

$$\dot{\boldsymbol{\alpha}} = \Xi^{-1}.\boldsymbol{\omega} \tag{2.9}$$

However if $\theta = 0$ then Ξ is singular and the co-ordinates ϕ and ψ are no longer independent. This requires that the simulation must test for θ approaching zero and take special action to avoid a computational catastrophe. Such special action may take several forms but is invariably complicated.

Evans (1977) pointed out that the quaternions of Euler are a much better choice of orientation parameters. They allow a set of equations of motion which are free of any singularity plus an elegant representation of molecular symmetry operations. A brief description of the properties of quaternions is given below without proof, which may be obtained in Du Val, 1964.

A quaternion is defined as an ordered number quartet, a logical extension of the complex numbers. For the purposes of defining its properties a quaternion $\mathbf{q}$ will be represented by a scalar plus a vector in a three dimensional space known as the imaginary prime although this does obscure the symmetry of the four parameters. If $\mathbf{q} \equiv (w,\mathbf{v})$ then addition and multiplication are defined by

$$\begin{aligned} \mathbf{q} + \mathbf{q}' &= (w+w',\mathbf{v}+\mathbf{v}') \\ \mathbf{q}\mathbf{q}' &= (ww'-\mathbf{v}.\mathbf{v}',\ w\mathbf{v}'+w'\mathbf{v}+\mathbf{v}\times\mathbf{v}'). \end{aligned} \tag{2.10}$$

It is easily shown that quaternion multiplication is associative but is not commutative. It is also clear that there is a unit quaternion and if the norm of $\mathbf{q}$, defined in the obvious way, is non zero that an inverse quaternion exists.

$$\begin{aligned} \mathbf{1} &= (1,0) \\ |\mathbf{q}| &= \surd(w^2 + \mathbf{v}^2) \\ \mathbf{q}^{-1} &= |\mathbf{q}|^{-2}\ (w,-\mathbf{v}) \end{aligned} \tag{2.11}$$

In order to represent a three dimensional orientation only three parameters are required and so an arbitrary rotation can be described by quaternions with a norm of one. Any such unit quaternion may be written $\mathbf{q} = (\cos(\alpha/2),\mathbf{l}\sin(\alpha/2))$ where $\mathbf{l}$ is a unit vector. Du Val (1964) shows that if $\mathbf{p} = (0,\mathbf{r})$ for any vector $\mathbf{r}$ and $\mathbf{q}$ is

defined as above then the product

$$\mathbf{p}' = (0,\mathbf{r}') = \mathbf{q}\mathbf{p}\mathbf{q}^{-1} \tag{2.12}$$

corresponds to a rotation of $\mathbf{r}$ about $\mathbf{l}$ by an angle α. This clear prescription of the quaternion corresponding to an arbitrary rotation has another benefit in the description of compound rotations. For if in addition to the definitions above,

$$\begin{aligned}\mathbf{p}'' = (0,\mathbf{r}'') \quad &= \mathbf{q}'\mathbf{p}'\mathbf{q}'^{-1} \\ &= \mathbf{q}'(\mathbf{q}\mathbf{p}\mathbf{q}^{-1})\mathbf{q}'^{-1} \\ &= (\mathbf{q}'\mathbf{q})\mathbf{p}(\mathbf{q}'\mathbf{q})^{-1}\end{aligned} \tag{2.13}$$

so that a compound rotation is represented by the quaternion product of the individual ones. This result may be used to find the relative orientations of two separate molecules; if they are described by $\mathbf{p}$ and $\mathbf{q}$ then the operation $\mathbf{p}\mathbf{q}^{-1}$ will rotate $\mathbf{q}$ into $\mathbf{p}$.

Another relationship is required to make use of quaternions in a molecular dynamics simulation. In order to increment a quaternion its time derivative must be evaluated in terms of the vector angular velocity. This is given by (Pawley, 1981)

$$2\dot{\mathbf{q}} = (-\boldsymbol{\omega}.\mathbf{v},\ \boldsymbol{\omega}w + \boldsymbol{\omega}\times\mathbf{v}).$$

or

$$2\dot{\mathbf{q}} = (0,\ \boldsymbol{\omega})\mathbf{q} \tag{2.14}$$

Differentiating (2.14) and substituting (2.14) in the result gives

$$2\ddot{\mathbf{q}} = (0,\ \dot{\boldsymbol{\omega}})\mathbf{q} - 1/2\omega^2\dot{\mathbf{q}}. \tag{2.15}$$

The angular acceleration $\dot{\boldsymbol{\omega}}$ is given by the Euler equations which are conveniently expressed in vector form

$$\mathbf{I}.\dot{\boldsymbol{\omega}} + \boldsymbol{\omega}\times\mathbf{I}.\boldsymbol{\omega} = \mathbf{N} \tag{2.16}$$

where $\mathbf{I}$ is the inertia tensor. By (2.15) $\ddot{\mathbf{q}}(t)$ can not be evaluated from $\dot{\boldsymbol{\omega}}$ without a knowledge of $\boldsymbol{\omega}(t)$. This means that equation (2.3) can not be consistently applied to quaternions and a more sophisticated integration algorithm is necessary. This will be discussed further in §2.1.3 but for now let us assume that it is possible to evaluate $\mathbf{q}(t+\delta t)$ consistently.

If the four components of the quaternion are treated as independent parameters and incremented separately at each timestep the question arises as to whether the new quaternion is correctly normalised to unity. It is easy to show using (2.14) that the time derivative of the norm is always zero. However the equations of motion are not solved exactly so some error may be introduced. The procedure followed here was suggested by Evans (1977) which is that after each timestep the components of $\mathbf{q}$ be scaled so that $|\mathbf{q}| = 1$.

Thus a simulation of a system of rigid molecules can be implemented using quaternions to describe the molecular orientations and whose dynamics are given by the Euler equations (2.16) for rotation and Newton's equations for the centre of mass. This will not suffice for the proposed model of n-butane which has three additional degrees of freedom for internal motion. The appropriate equations of motion are derived from the Lagrangian and may be written in the following general form. Let q_k $(k=1,...n)$ be the generalised co-ordinates, and $\mathbf{r}_i$ the cartesian atomic co-ordinates. The potential function is decomposed into two parts, an intermolecular part which depends only on $\mathbf{r}_i$ and an intramolecular part which is an explicit function of the generalised co-ordinates only.

$$\Phi = \Phi_{ext}(\mathbf{r}_i) + \Phi_{int}(q_j)$$

This gives rise to the external cartesian forces $\mathbf{F}_{i\ ext} = -\nabla\Phi_{ext}$ and the internal generalised forces $Q_j = -\partial\Phi_{int}/\partial q_j$. The subscripts int and ext will be dropped from now on.

Defining $\mathbf{r}'_{ij} = \dfrac{\partial \mathbf{r}_i}{\partial q_j}$ and $\mathbf{r}''_{ijk} = \dfrac{\partial^2 \mathbf{r}_i}{\partial q_j \partial q_k}$

the chain rule for differentiation gives

$$\dot{\mathbf{r}}_i = \sum_j \mathbf{r}'_{ij}\dot{q}_j,$$

$$\dot{\mathbf{r}}'_{ij} = \sum_k \mathbf{r}''_{ijk}\dot{q}_k \qquad \text{and}$$

$$\ddot{\mathbf{r}}_i = \sum_j \dot{\mathbf{r}}'_{ij}\dot{q}_j + \sum_j \mathbf{r}'_{ij}\ddot{q}_j$$

$$= \sum_j\sum_k \mathbf{r}''_{ijk}\dot{q}_j\dot{q}_k + \sum_j \mathbf{r}'_{ij}\ddot{q}_j. \qquad (2.17)$$

Lagrange's equations for this system may be written in the form

$$\frac{d}{dt}\left(\frac{\partial T}{\partial \dot{q}_j}\right) - \frac{\partial T}{\partial q_j} = \sum_i \mathbf{F}_i.\mathbf{r}'_{ij} + Q_j \qquad (2.18)$$

Now the kinetic energy

$$2T = \sum m_i \dot{\mathbf{r}}_i^2 \qquad \text{so that}$$

$$\frac{\partial T}{\partial q_j} = \sum_i m_i \dot{\mathbf{r}}_i.\dot{\mathbf{r}}'_{ij} \qquad \text{and}$$

$$\frac{\partial T}{\partial \dot{q}_j} = \sum_i m_i \dot{\mathbf{r}}_i.\mathbf{r}'_{ij}.$$

so from (2.17) and (2.18)

$$Q_j + \sum_i \mathbf{F}_i.\mathbf{r}'_{ij} = \sum_i m_i \ddot{\mathbf{r}}_i.\mathbf{r}'_{ij},$$

$$= \sum_i m_i \mathbf{r}'_{ij} \cdot \Big(\sum_k \sum_l \mathbf{r}''_{ikl} \dot{q}_k \dot{q}_l + \sum_k \mathbf{r}'_{ik} \ddot{q}_k \Big),$$

$$= \sum_i \sum_k \sum_l m_i \mathbf{r}'_{ij} \cdot \mathbf{r}''_{ikl} \dot{q}_k \dot{q}_l + \sum_i \sum_k m_i \mathbf{r}'_{ij} \cdot \mathbf{r}'_{ik} \ddot{q}_k$$

Therefore

$$Q_j + \sum_i \Big(\mathbf{F}_i - m_i \sum_{k,l} \mathbf{r}''_{ikl} \dot{q}_k \dot{q}_l \Big) \cdot \mathbf{r}'_{ij} = \sum_k M_{jk} \ddot{q}_k \tag{2.19}$$

where $M_{jk} = \sum_i m_i \mathbf{r}'_{ij} \cdot \mathbf{r}'_{ik}$ is a generalised inertia matrix.

The index i runs over all atoms in the molecule and j,k run over the generalised co-ordinates. The constraint forces are given by the second term within the summation over i. M_{jk} is a symmetric $n \times n$ matrix whose entries are a function of the internal, rotational and translational co-ordinates of the molecule, and is different for each independent molecule. The equations (2.19) are solved for q_k by evaluating the left hand side and multiplying by the inverse of M_{jk}. The kinetic energy is given by the expression

$$T = 1/2 \sum_j \sum_k M_{jk} \dot{q}_j \dot{q}_k. \tag{2.20}$$

As written there are n coupled equations. However they may be separated into 3 representing the centre of mass motion and $n-3$ for the rotational and internal motion. For if q_1, q_2, q_3 are the centre of mass positions and $k=1,2,3$, $(\mathbf{r}'_{ij})_k = \delta_{jk}$, $\mathbf{r}''_{ikl}=0$ and M_{jk} is of the block diagonal form

$$\begin{pmatrix} \mathbf{1} \sum m_i & \mathbf{0} \\ \mathbf{0} & M_{lm} \end{pmatrix} \quad l,m = 4,..n.$$

The off diagonal zeros decouple the translational co-ordinates whose equation of motion reduces to Newtons equation

$$\sum_i \mathbf{F}_i = \ddot{\mathbf{r}} \sum_i m_i \tag{2.21}$$

and the rotation and internal motion are given by (2.19). This separation has two benefits which accrue from reducing the size of M_{jk}. There is a considerable saving in storage required and in the computational effort needed to invert the matrix.

The correctness of (2.19) is confirmed by considering a rigid body where j and k run only over the three rotational co-ordinates. If the constraint forces $\mathbf{r}''_{ijk}$ and the projection matrix $\mathbf{r}'_{ij}$ are evaluated then $\mathbf{M}_{jk}$ is identical to the inertia tensor and the Euler equations can be recovered from (2.19).

It is of some significance that this equation contains terms which depend on the generalised velocities $\dot{q}$, which include the angular velocity $\boldsymbol{\omega}$. The integration algorithm (2.3) does not permit an accurate determination of velocities and so is unsuitable for use with a rigid or flexible molecule model. A suitable algorithm is discussed in the next section.

§2.1.3 Integration Algorithms

In §2.1.1 a simulation of point masses was discussed and a simple method of integrating the equations of motion, the Verlet algorithm (2.3) was described. It was extended to a set of interacting rigid bodies in §2.1.2 where it was assumed that a suitable algorithm could be found. It is clear that the simple approach of replacing the cartesian co-ordinates in (2.3) with the appropriate generalised co-ordinates will not work. For the equations of motion (2.16) yield $\dot{\boldsymbol{\omega}}$, and to evaluate the second derivatives of the generalised co-ordinates requires an expression like (2.15) or the derivative of (2.9) which involve the angular velocity $\boldsymbol{\omega}$. But (2.3) does not contain a term in $\boldsymbol{\omega}(t)$, which indeed is only known *after* $q(t+\delta t)$ has been evaluated and then only to order t^2.

There is another related but distinct problem. The equations of motion (2.16) or (2.19) contain terms in $\boldsymbol{\omega}$ or $\dot{q}$ so the generalised forces are velocity dependent. In the special case of rigid molecules with tetrahedral or higher symmetry the inertia tensor, $\mathbf{I}$ or M_{jk} is a multiple of the unit tensor, these terms are zero and the equation of motion simplifies to $\mathbf{I}\dot{\boldsymbol{\omega}} = \mathbf{N}$. Most of the molecular systems which have been the subject of simulation such as methane, adamantane, sulphur hexafluoride and so on fall into this class. However the proposed model of *n*-butane is both asymmetric and has internal degrees of freedom so the forces *are* velocity dependent.

Both of these problems can be addressed by the class of predictor - corrector or Gear algorithms. These will not be discussed here in detail (see Beeman, 1976) but in general they use more than one step during each integration cycle. The third order algorithm due to Beeman allows the use of generalised co-ordinates and has been widely used for the simulation of symmetric molecules. It also proved easily extensible to deal with velocity dependent forces. (The order of an algorithm is highest power of δt which is not dropped from the expansion. Thus the Verlet algorithm is of third order.)

The simplest form of the Beeman algorithm consists of a cycle of three steps:

$$\begin{aligned}
&\text{(a)} \quad q(t+\delta t) = q(t) + \dot{q}(t)\delta t + \{4\ddot{q}(t) - \ddot{q}(t-\delta t)\}\delta t^2/6 \\
&\text{(b)} \quad \text{calculate } \ddot{q}(t+\delta t) \text{ as a function of } \{q(t+\delta t)\} \\
&\text{(c)} \quad \dot{q}(t+\delta t) = \dot{q}(t) + \{\ddot{q}(t+\delta t) + 5\ddot{q}(t) - \ddot{q}(t-\delta t)\}\delta t/6
\end{aligned} \tag{2.22}$$

This can certainly be used consistently to represent angular motion. If the generalised co-ordinates q are replaced by the quaternions $\mathbf{q}$ then all the dotted

terms in (2.22a) can be substituted by equations (2.15) and (2.16). The angular velocity is available from (2.22c) on the previous cycle. Note that the derivatives updated in (2.22c) are the vector quantities $\boldsymbol{\omega}$ which must be converted to the quaternion form for step (a) of the next cycle.

It is fairly easy to combine the equations (2.22a,b,c) so as to reproduce the Verlet algorithm (2.3). Although the trajectories are exactly the same the velocities are known to order t^3 which is necessary for the accurate evaluation of temperature, pressure and other thermodynamic quantities.

This algorithm still can not be used for a system with velocity dependent forces, for it requires the evaluation of the forces in step (b) at a stage when the velocities at $t+\delta t$ are not available. This deficiency can be remedied by the insertion of an additional 'velocity predictor' step between (a) and (b) to calculate an approximation to them which is then corrected by (c).

$$\begin{aligned} &\text{(a1)} \quad \dot{q}'(t+\delta t) = \dot{q}(t) + \{3\ddot{q}(t) - \ddot{q}(t-\delta t)\}\delta t/2 \\ &\text{(b)} \quad \text{calculate } \ddot{q}(t+\delta t) \text{ as a function of } \{q(t+\delta t)\} \text{ and } \{\dot{q}'(t+\delta t)\} \end{aligned} \tag{2.23}$$

Steps (a1) to (c) may be iterated until convergence is reached. In the case of the present butane simulation it was found that with a suitable value for δt the velocities converged to about 5 decimal places in one iteration. Since evaluating the forces which is part of step (b) is by far the largest computation of the simulation, the algorithm was performed once through without any iteration in all the runs described.

Velocity dependent forces also arise when implementing the zero-stress algorithm of Parrinello and Rahman (1981). The above integration scheme allows a direct implementation of the equations as given in their paper, avoiding the need to reformulate them to eliminate the velocity dependent term.

§2.1.4 Calculating Thermodynamic Properties

In order that a simulation is performed under realistic conditions it is necessary to evaluate certain quantities such as the temperature, pressure and in some cases the stress tensor. These are evaluated as time averages over many timesteps and correspond to statistical averages in some ensemble. Intensive quantities such as those mentioned are independent of the ensemble used in the limit of large systems, although this does not apply to fluctuations.

The temperature is given by the equipartition theorem

$$T = 2<K>/(nNk_B) \tag{2.24}$$

where N is the number of molecules, n is the number of degrees of freedom per molecule and K is the instantaneous kinetic energy. A precondition for the evaluation of statistical averages is that the system be in thermal equilibrium. This is achieved by starting the simulation from an initial state close to the expected equilibrium configuration and running it for some time until equilibrium is achieved. If the 'temperature' corresponding to different degrees of freedom is calculated independently then the consistency is a good check on whether this condition is satisfied. The three translational and six rotational and internal degrees of freedom of the model butane molecule were treated separately for this purpose.

Another useful check on equilibrium is provided by the fluctuations in kinetic energy (δK^2) which are related in the microcanonical ensemble to the specific heat (Lebowitz *et al*, 1967). This quantity is large in a non -equilibrium condition and decreases to a minimum as equilibrium is approached. Note that neither of these checks provides any indication as to whether the system is in a true equilibrium state or merely a metastable one.

The pressure is calculated from the virial (see Hansen, 1976b)

$$p = \rho k_B T - 1/(3V) < \sum_{j>i} \mathbf{F}_{ij}.\mathbf{R}_{ij} > \tag{2.25}$$

where for a molecular system i and j vary over all pair interactions but $\mathbf{R}_{ij}$ is the corresponding *molecular* centre of mass vector. In a similar manner the stress tensor σ_{ij} can be written

$$\sigma_{kl} = \rho k_B T \delta_{kl} - 1/V <\sum_{j>i} (\mathbf{F}_{ij})_k (\mathbf{R}_{ij})_l > \tag{2.26}$$

where δ_{ij} is the Kronecker delta and the quantity in brackets is a dyad product.

Since the aim of a simulation is to investigate a system under specified conditions some method of setting the temperature and pressure to a desired value is necessary. However the equations of motion generate a (NVE) ensemble where the volume and energy are specified. Various methods have been devised for performing a simulation at constant temperature (Andersen, 1980; Nose, 1984) but the method adopted here is much simpler. Every few timesteps the particle velocities are all scaled (multiplied by a constant) so as to give exactly the kinetic energy required at the reference temperature. However there is no proof that this procedure produces configurations from the canonical ensemble and its effects on dynamic properties are unknown. It is therefore treated only as a method of setting the desired temperature. The simulation is run for some time with scaling applied. Once it has stabilised rescaling is switched off and the system allowed to re - equilibrate for a period. Only then are the trajectories analysed to calculate the results.

§2.1.5 Molecular Dynamics at fixed pressure

It was noted in the previous section that it is necessary to set the temperature during a simulation. It is also important that the pressure be fixed. Because of the sharply repulsive nature of the interatomic forces a very small error in the size of the MD cell can lead to a pressure of many kilobars. Such a pressure could easily force the system into a different region of the phase diagram than is wanted.

In order not to put any constraint on the crystal structure it is required not only that the internal pressure be zero but also the internal stress. These are difficult conditions to satisfy in a system with periodic boundary conditions as it requires that the MD cell translation vectors are also lattice translations of the crystal structure. In other words a suitable number of unit cells must fit exactly into the MD cell. The question of a simulation of a system with a phase transition then arises. If the lattice in one phase is commensurate with the MD cell, then in most cases the different lattice of another phase will not be. This is certainly true for plastic phase transitions in molecular crystals in general and butane in particular. Thus to have any chance of success in simulating a phase transition the size and shape of the MD cell must be allowed to change in response to the internal stress.

A method to do this was devised by Parrinello and Rahman (1980; 1981). This is a modification of one due to Andersen (1980) which allowed only for an isotropic change in volume of the MD cell. Briefly, the method introduces the new dynamic co-ordinates $\mathbf{s}_i$. These are known as *scaled* co-ordinates and are related to the cartesian co-ordinates $\mathbf{r}_i$ by

$$\mathbf{r} = \mathbf{hs} = s_1\mathbf{a} + s_2\mathbf{b} + s_3\mathbf{c} \qquad (2.27)$$

where the columns of $\mathbf{h}$ are the MD cell edge vectors $\mathbf{a}$, $\mathbf{b}$ and $\mathbf{c}$. In the simulation, the co-ordinates $\mathbf{r}_i$ are replaced by $\mathbf{s}_i$ and the components of $\mathbf{h}$ are treated as additional dynamical variables with their own equations of motion.

The equations given below (2.28) are an extension to Parrinello and Rahman's method which works for molecular systems. Only the centre of mass co-ordinates $\mathbf{r}_i$ are scaled; the other degrees of freedom are represented by unscaled generalised co-ordinates exactly as in §2.1.2. Thus their original Lagrangian is augmented by an additional kinetic energy term for the rotational and internal generalised co - ordinates.

There is another slight modification in that $\mathbf{h}$ represents a notional lattice, a sub-multiple of the MD cell so that in this case the MD cell volume $\Omega = N \det(\mathbf{h})$

rather than just det($\mathbf{h}$). The equations are otherwise identical. This is merely for convenience in the parallel implementation since the molecule positions are stored as displacements from this lattice rather than as absolute positions.

The motion is governed by the Lagrangian

$$L = 1/2 \sum_i m_i \dot{\mathbf{s}}_i' \mathbf{G} \dot{\mathbf{s}}_i + 1/2 \sum_{i} \sum_{j,k} \dot{q}_{ij} M_{jk} \dot{q}_{ik} - \sum_{j>i} \phi(r_{ij}) + 1/2 W \, \mathrm{Tr}(\dot{\mathbf{h}}'\dot{\mathbf{h}}) - p\Omega. \quad (2.28)$$

The crucial feature is the last two terms which represent the kinetic and potential energy of the MD cell. This yields equations of motion for the molecular centre of mass and the unit cell matrix

$$\begin{aligned} \ddot{\mathbf{s}}_i &= M_i^{-1} \mathbf{h}^{-1} F_i - \mathbf{G}^{-1} \mathbf{G} \dot{\mathbf{s}}_i \\ W \ddot{\mathbf{h}} &= \Omega(\pi - p) \mathbf{h}'^{-1} \end{aligned} \quad (2.29)$$

where $\mathbf{F}_i = \sum \mathbf{f}_i$ is the cartesian force on the centre of mass, M_i is the molecular mass and

$$\Omega\pi = \sum_i M_i (\mathbf{h}\dot{\mathbf{s}}_i)'(\mathbf{h}\dot{\mathbf{s}}_i) - \sum_{k,l} \sum_{j>i} (\phi'/r_{ij}^{kl}) r_{ij}^{kl} R_{ij}. \quad (2.30)$$

The indices i and j run over all pairs of molecules and k,l over all atoms within a molecule. The time average of (2.30) is just (2.26) showing that $<\pi> = \sigma_{ij}$, the microscopic stress tensor. Thus the MD cell $\mathbf{h}$ changes shape in response to the imbalance between the applied pressure p and the internal stress.

The equation of motion for the molecular centre of mass (2.29) is just Newton's equation (2.21) augmented by an extra term which depends on both the particle and the MD cell velocities. This requires the integration algorithm of (2.22) and (2.23) irrespective of the internal motion. It follows from the Lagrangian that the rotational and internal motion is governed by (2.19) as before.

The conserved quantities of these equations are the pressure and the enthalpy (Parrinello & Rahman, 1981) so the method generates a (p,H,N) ensemble.

There is a problem which arises because the MD cell matrix $\mathbf{h}$ is overdetermined. It contains nine entries whereas only six quantities suffice to define the size and shape of the MD cell. The other three degrees of freedom correspond to the absolute orientation of the cell. That they have no effect on the physics is easily

verified by multiplying $\mathbf{h}$ by an orthogonal rotation matrix and substituting this into (2.28). The Lagrangian and the corresponding Hamiltonian are invariant as are the equations (2.29) and (2.30).

In the microcanonical ensemble the total energy E, momentum **P** and angular momentum **L** are conserved quantities. The ensemble generated by (2.27) has as constants the enthalpy H (this is only approximate) and the quantity $\mathbf{h}'\mathbf{P}$ (Nose & Klein, 1983). There is however no analogue of a conserved angular momentum. Nose and Klein show that in a general molecular system the MD cell will rotate as a whole which complicates the analysis of structures and any other directional properties (*eg* $S(\mathbf{Q},\omega)$). They therefore eliminate the extra degrees of freedom by constraining $\mathbf{h}$ to be symmetric.

The author also encountered this problem as a result of early work on the simulation described here and adopted a different and more intuitive solution. Three of the components are constrained to zero so that $\mathbf{a}=(a,0,0)$, $\mathbf{b}=(b_x,b_y,0)$, $\mathbf{c}=(c_x,c_y,c_z)$. In contrast to the symmetrisation method where there is no obvious physical interpretation of the constraint, the method proposed here simply requires that the direction of **a** and the plane containing **a** and **b** be fixed. The implementation is trivial. The appropriate components of $\mathbf{h}$ and $\dot{\mathbf{h}}$ are set to zero at the beginning of the run and the corresponding components of $\ddot{\mathbf{h}}$ are zeroed every timestep. This procedure corresponds to the application of some undetermined constraint forces to the system. There is a useful analogy to this constraint; a crystal placed on a sloping surface with the **a** side lowermost and resting against a barrier. The constraint forces are simply the reaction pairs of the gravitational forces acting on the crystal.

§2.1.6 Parallel Implementation

The n-butane simulation was implemented on a specialised computer called a Distributed Array Processor (DAP) made by ICL. This is a parallel processor of the single instruction stream, multiple data stream (SIMD) type where the same instructions operate on many different data items simultaneously. It is composed of 4096 simple processors called processing elements (PE's). If the PE's are considered to lie on a two dimensional lattice then data can be communicated between neighbouring PE's. It is a massively parallel processor as opposed to one composed of a small number of more sophisticated processors.

This parallelism is made available to the programmer by an extension of the high level language FORTRAN called DAP FORTRAN. Parallel data structures called matrices are provided which are similar to arrays with a fixed number of elements (4096). The difference is that arithmetic is performed on any or all of the elements simultaneously. Logical masks may be set to allow or inhibit activity on each element individually and these are extremely powerful tools for controlling the parallelism. The interprocessor communication is made available through a class of operations known as *shifts*. These may be one or two dimensional where the matrix is considered as an array of either 4096 or 64×64 elements respectively. In both cases a shift of n may be thought of as bringing the element $(i+n)$ (or $(i+n,j+m)$) into position (i) (or (i,j)). The boundary conditions for shifts are either *planar* when elements brought in from outside the matrix are zero, or *cyclic* when the addition is modulo 4096 (64).

In order to obtain efficient use of the SIMD architecture it must be possible to divide the problem into many independent but identical tasks, that is tasks which require the same operations to be performed on different data. In programming terms the requirement is that the results of a computation within a loop should be independent of the previous cycles. The tasks can then be simultaneously performed by different processors to give the same results.

A Molecular Dynamics simulation *can* be split up in such a manner and thus is ideally suited to a parallel implementation. Equations (2.22) and (2.23) which describe the basic algorithm apply separately to each molecule. Only the calculation of the interatomic forces involves more than one molecule and hence inter-process communication.

The forces in this simulation are all pair forces which depend only on the vector displacement between two atoms. Now if the sequence of operations required to calculate $\mathbf{r}_{ij}$ is the same as $\mathbf{r}_{i+n,j+n}$ for all i then the i calculations can be done in parallel. In particular if the data pertaining to molecule i is stored in element i of a DAP FORTRAN matrix and if the shift required to obtain the data for molecule $i+n$ is the same for all i then the interatomic vector $\mathbf{r}^k_i - \mathbf{r}^l_{i+n}$ can be calculated simultaneously for all molecules i. Thus there is exactly the same degree of parallelism present as in the integration step (2.22). For this reason it is natural and efficient to simulate exactly 4096 molecules and store the data pertaining to each on a single PE. It still remains to calculate the forces and to loop over all *neighbour* molecules n and all atoms in both molecules k and l. Because these loops are executed serially the interatomic force calculation is usually the largest part of the simulation by far.

It is worthwhile to note that this procedure has by no means exhausted the parallelism of the problem. If the ni displacements $\mathbf{r}^k_i - \mathbf{r}^l_{i+n}$ are first evaluated, in parallel for all i and serially for each n, then the ni calculations of $\mathbf{F}(\mathbf{r})$ are identical and can be done in parallel. Since the actual force calculation involves much more arithmetic than a simple subtraction the total time required will not be increased much by the serial sum over n. The same procedure may be applied to the atomic indices j and k as well. By this means a simulation need not be confined to the same number of molecules as there are PE's but instead can use the parallelism to speed up the computation for a smaller number.

The model butane molecule is rather complex with 14 interaction centres and 9 generalised co-ordinates. It was found that the amount of store required to implement a simulation of 4096 molecules is around 4 MBytes, twice as much as the DAP actually possesses. For this reason the information relating to a single molecule was distributed between 2 processing elements. Therefore the simulation consists of only 2048 molecules. The scheme outlined above was used to parallelise the force calculation. That is the forces between an atom in the 'left' half of a molecule and the 'left' half of the neighbour molecule are evaluated simultaneously with those on the equivalent atoms on the 'right'. This is followed by the parallel calculation of the left/right and right/left forces.

It remains to be shown that interactions defined on a three dimensional lattice with periodic boundary conditions can be represented using one cyclic index as assumed above. It is not possible in general to represent normal 'straight' periodic boundary conditions in this way. However it was shown by Pawley and Thomas (1982) that what are called *skew cyclic* boundary conditions can be used to set up a

parallelopiped shaped MD cell. For almost all purposes this is just as good. The principle is illustrated in figure 2.1 for a 12 PE DAP in two dimensions. Coverage of two dimensional space is achieved by placing images of the string of PE's to the 'north' and 'south' of the original and shifting them 'east' and 'west' by three units. It will be seen that the 12 PE's appear in a rectangle which also can be repeated to fill space.

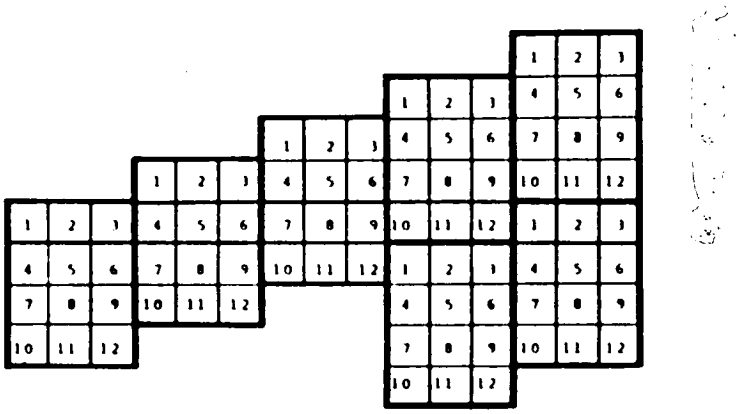

Figure 2.1. Skew cyclic boundary conditions with 12 PE's.

This arrangement certainly satisfies the parallel condition, for PE *i+1* is the neighbour to the 'east' of all PE's and *i+3* is the one to the 'south'. This is very different from the *straight* boundary conditions usually employed where *i+3* would just be the cyclic image of *i*. The MD cell translation vectors which join an element to its images are (3,-1) and (0,4) which generated a parallelopiped shaped MD cell The only significant consequence of this is that the allowed phonon wavevectors are different from the usual case. It is fairly obvious how this procedure may be extended to three or more dimensions.

The scheme is implemented by storing molecule positions relative to a notional lattice which is conveniently chosen to be the bravais lattice of the crystal. The program contains a table whose entries consist of the relative index of the PE and the translation on this lattice between the reference origins for the molecule and neighbour positions. There is one entry for each molecule-molecule interaction to be included and the program loops over this table to calculate all interactions. Thus for the scheme of figure 2.1 if nearest and next nearest neighbour interactions are included the table would be:

Table 2.1

i	index	Vector displacement
1	1	(1,0)
2	−3	(0,1)
3	-2	(1,1)
4	4	(1,-1)

There are 8 interactions in all; the other four are simply the negatives of the entries present.

This method is well suited to the Parrinello and Rahman zero stress algorithm since all positions are defined with respect to a lattice which will correspond to the **h** matrix used therein. To calculate the actual displacement between two molecule centres the vector from the neighbour list is added to the difference between the (scaled) centre of mass co-ordinates. This is multiplied by the **h** matrix to give $\mathbf{r}_{ij}$. Fig 2.2 and table 2.2 show the layout which was first used for the butane simulation. This is for a body centred lattice. Notice that the PE index goes between 1 and 2048 since each molecule is split between 2 PE's.

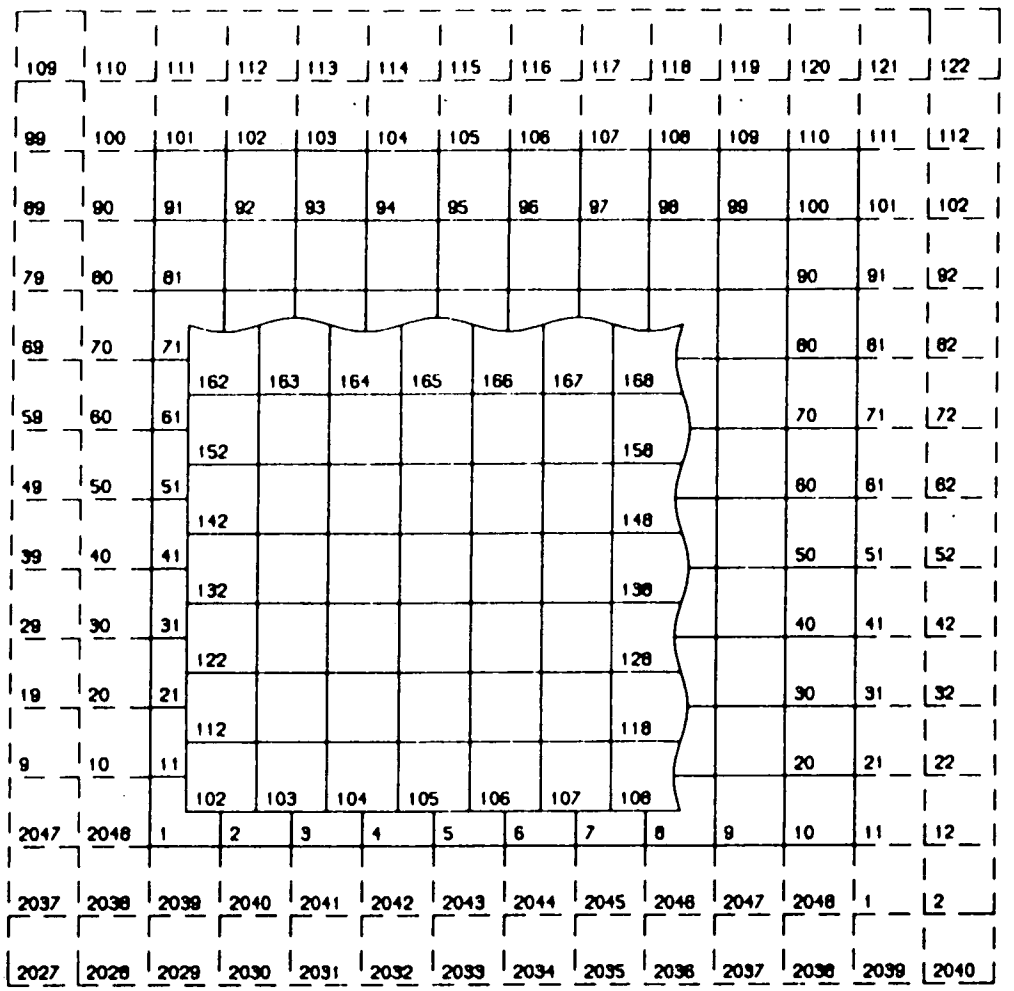

Figure 2.2. Boundary conditions used for n-butane simulation. The inset layer is of body centre molecules (0.5,0.5,0.5).

Table 2.2. Original neighbour list.

i	index	Vector displacement
1	1	(1,0,0)
2	10	(0,1,0)
3	191	(0,0,1)
4	90	(-0.5,-0.5, 0.5)
5	91	(0.5,-0.5, 0.5)
6	100	(-0.5, 0.5, 0.5)
7	101	(0.5, 0.5, 0.5)

§2.2 Models

This section deals with the physical models used to represent condensed molecular phases and their application to *n*-butane. The molecule is represented by a set of point masses (perhaps constrained) governed by classical equations of motion. It was shown in §2.1 how a simulation of such systems may be implemented. The following discussion concentrates on the potentials applied to the system.

Atoms experience forces which fall into two classes, bonded and nonbonded interactions. While bonded forces are entirely intramolecular by definition of a molecule, nonbonded interactions act both between and within molecules. The former are not usually important for simulation purposes since they are responsible only for high frequency bond flex and stretch modes. For example the lowest frequency deformation of the *n*-butane molecule is the CCC flex mode at 12.9 THz (Harada *et al*, 1977). This is much faster than the highest lattice modes at around 1THz and therefore weakly coupled with them. This is the justification for 'freezing' such modes as rigid bonds. However the dihedral modes which involve a rotation about the 3 C-C bonds are at the lower frequency of 3 to 6THz and are much more likely to be coupled to the lattice modes. Hence the inclusion of three extra degrees of freedom in the model *n*-butane molecule which represent rotation about the C-C bonds.

§2.2.1 Non Bonded Potentials

There are several contributions to the nonbonded forces. The London or dispersion forces are responsible for the attractive part of the potential. They arise from the fluctuating electric multipole moments of one atom which causes an induced moment in another. The potential may be expanded in powers of the interatomic spacing r_{ij} and the leading term is an induced dipole-dipole interaction which varies as r_{ij}^{-6}. Terms of the form $r_{ij}^{-8}, r_{ij}^{-10}$... from dipole-quadrupole and quadrupole-quadrupole interactions are also present, but they are usually neglected.

At short distances the forces become repulsive as the electron orbitals of the two atoms overlap. This part of the potential is represented by a term either of the form r^{-12} or $B\exp(-Cr)$. The first case gives a Lennard Jones potential (2.7) (1924) while the latter expression, first suggested by Buckingham (1938), arises from quantum mechanical calculations on hydrogen and helium atoms by Kitaigorodsky and Mirskaya (1972).

$$\phi(r_{ij}) = -A_{ij} r_{ij}^{-6} + B_{ij}\exp(-C_{ij} r_{ij}) \tag{2.31}$$

It is a basic assumption of this model that the parameters are transferable and species specific. That is the interaction between two carbon atoms, for example, is given by the same parameters and functional form irrespective of the atoms' molecular environment but is different from a H-H or C-H interaction. Assuming transferability the parameters A, B and C can be fitted to known quantities such as crystal structures, sublimation energies *etc*. This was done by Williams (1967) who obtained a set of parameters suitable for carbon and hydrogen atoms from a fit to a large number of hydrocarbon structures. (See table 2.3). These are the values used in the *n*-butane simulation for most of the runs.

However it is known that even simple hydrocarbons have net atomic charges which can exceed 0.1 electronic units. These may contribute as much as 10% of the lattice energy of some crystals. However an accurate measurement of lattice energy is not the purpose of a MD simulation and most of the effects are subsumed into the coefficients A, B and C by the fitting process. However it is of some interest to investigate the effects of including the electrostatic contribution and some runs were performed using a later set of potentials by Williams and Starr (1977). These include a coulomb term from a residual charge on each atom and have the form

$$\phi(r_{ij}) = -A_{ij} r_{ij}^{-6} + B_{ij}\exp(-C_{ij} r_{ij}) + q_i q_j e^2 r_{ij}^{-1}. \tag{2.31}$$

Table 2.3 Williams' parameters.
Set IV of 1967 without coulombic forces and set II of 1977 with.

Parameter	Set IV (1967)	Set II (1977)	
A_{CC}	2376.5	2414	$kJ\ mol^{-1}$
B_{CC}	349908	367250	"
C_{CC}	3.60	3.60	A
A_{CH}	523.0	573	$kJ\ mol^{-1}$
B_{CH}	36677	65485	"
C_{CH}	3.67	3.67	A
A_{HH}	114.2	136	$kJ\ mol^{-1}$
B_{HH}	11104	11677	"
C_{HH}	3.74	3.74	A
q (CH group)	0	0.153	*e.u.*

It should be emphasized that these models are rather crude approximations. Their form is isotropic whereas distortion of the electronic orbitals due to bonding will make the true potential directional. They act between two atoms only and are assumed to be independent of the presence of other atoms nearby. To take this into account really requires many body terms.

Despite these limitations, simple pair potentials have achieved great success in many different kinds of calculation (See Ramdas & Thomas, 1977) including Molecular Dynamics. In general they work rather better for larger molecules and ones which are non spherical for which the important properties are determined by the molecular shape. Only for small molecules such as N_2 for example have other terms such as quadrupolar interaction terms been found necessary (Murthy *et al*, 1980). It is therefore to be expected that a fairly large and asymmetric molecule such as *n*-butane will be well modelled by 6-exp potentials like (2.31).

Many studies of hydrocarbons (e.g. Ryckaert & Bellemans, 1975, Neusy *et al*, 1984) attempt to reduce the amount of calculation by replacing a CH_2 or CH_3 group with a single interaction centre using a suitably averaged potential. If each molecule has n atoms there are n^2 interactions per molecule pair and hence the time required to evaluate the forces varies as n^2. In the case of *n*-butane this would reduce this number from 196 to 16, a factor of 12 saving. However it may well be a very poor approximation in a close packed crystal where molecular rotation is hindered by close H-H contacts. It was found by Neusy *et al* (1984) that even for a nearly spherical molecule, bicylo(2,2,2)octane, there is a marked difference in reorientation rates between the full 22 site model and a reduced 8 site model. In view of the large computational saving it would be worthwhile to conduct an experimental comparison of the properties of the two models although at the time of writing this has not been done.

§2.2.2 Dihedral Bond Potential

It has been known since the 1930's that rotation of part of a molecule about a single bond is not free but in general has a considerable potential barrier. This potential arises both from nonbonded interactions between atoms belonging to the same molecule and from the distortion of the bond's electron orbitals. It is therefore necessary to find a simple model potential for inclusion in the MD simulation. The two approaches are via experimental spectroscopy and theoretical calculation. Although neither has provided a definitive result, a functional form quite adequate for simulation purposes is easy to come by.

There has been a great deal of interest in the last 20 years in the calculation of dihedral bond potentials and a multiplicity of techniques have been developed (See Musso and Magnasco, 1984 for a short review and references). Most of the effort has been directed towards calculating barrier heights. Although important in the gas phase these are of less relevance to the crystalline state where the lower thermal energy means that only the region close to the potential minimum is explored. The potential for rotation about the central C-C bond of *n*-butane was calculated by Scott and Scheraga (1966) from bonded and nonbonded contributions. This was used by Ryckaert and Bellemans (1975) in their simulation of liquid *n*-butane and is also used here for the simulation of the solid state. With a redefinition of the origin and scale of the dihedral angle Ψ (See § 2.3 for definition) the potential function is

$$\begin{aligned} V(\Psi) &= 154.2 - 201.8\cos\Psi - 217.9\cos^2\Psi + 50.81\cos^3\Psi \\ &\quad + 435.7\cos^4\Psi + 523.0\cos^5\Psi \times 10^{-22}\text{J}. \end{aligned} \tag{2.32}$$

This potential is plotted in figure 2.3.

The methyl group was allowed to rotate freely for all of the runs described in the remainder of chapter 2. It was later decided that a potential should be applied and this was implemented for the simulations in chapter 5. The first function tried was that of the CH_3 group of propane as calculated by Scott and Scheraga (1966) and has the form $V(\chi)=b(1-\cos 3\chi)$ with $b=236.4\times10^{-22}$J. However this results in an oscillation frequency for the symmetric methyl twist mode of 10.2THz, nearly twice that measured by Durig and Compton (1979) of 6.2THz. An extra term was therefore added to drop the frequency to around 6THz. This leaves the barrier height unchanged and gives the form.

$$V(\chi) = 192.1 - 236.4\cos 3\chi + 44.33\cos 6\chi \times 10^{-22}\text{J}. \tag{2.33}$$

Durig and Compton (1979) suggested a slightly different form for the internal potential involving a $\chi_1\chi_2$ cross term which gives approximately the same barrier

heights and frequencies. This was not used because of the arbitrary nature of the potentials; it was not felt that there would be a significant gain over (2.33). It is certainly true that at temperatures at which butane is solid the thermal activation is only sufficient for sampling a small region around the potential minimum. Since the potentials used are adjusted to reproduce the experimental frequencies the potential is good enough in that region.

It should be noted that with the potential models described above the motion of the internal degrees of freedom falls outside the regime where the classical approximation is valid. The temperature at which the classical equipartition value of the energy equals the quantum zero point energy is 174K for the Ψ torsion and over 300K for the antisymmetric methyl twist mode at 7.2THz. Thus in the plastic phase at around 130K classical mechanics is not a good approximation. In particular the average mode energy given by classical equipartition is only half the correct quantum energy for the methyl torsion modes. However the Ψ torsion is not too badly wrong and this is expected to be the most significant feature of the internal motion. This does not limit the simulation's validity as a classical model calculation but does necessitate caution when comparing some of the results with experiment.

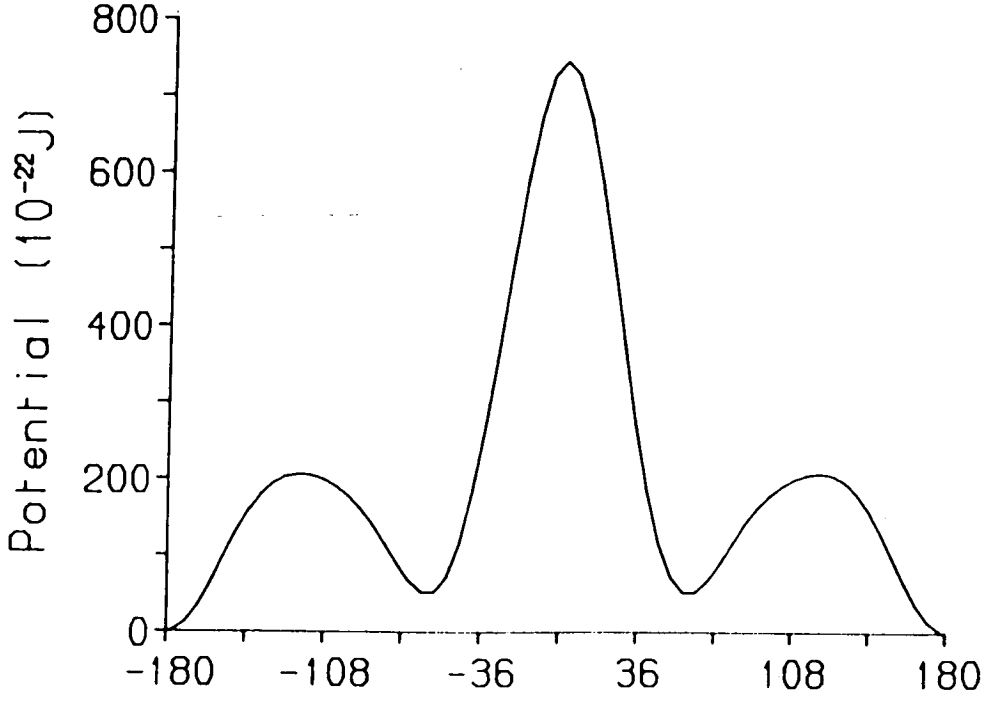

Figure 2.3. Potential as a function of internal rotation Ψ.

§2.2.3 Cut-off and Distant Stress

In a MD simulation the computation time is directly related to the number of atom-atom interactions considered, which should therefore be as small as possible. For most useful potentials the force drops off very rapidly, usually as the 7^{th} power of the distance. The interaction is therefore negligible outside about 10A. In the case of a liquid, a cut-off radius is usually defined beyond which any residual interactions are ignored. However in most solids, atoms or molecules are confined to fixed sites and only move away from these by small displacements. Thus it is more convenient to define a list of 'neighbour' molecules with which each molecule interacts, which remains fixed during the simulation run. It was shown in §2.1.6 that this method is ideally suited to a parallel implementation. However, the number and placing of such molecules is obviously structure dependent and the arrangement chosen will tend to favour certain structures at the expense of others with a different symmetry. This means that the 'true' structure (ie that calculated with a large interaction range) may not be stable in the restricted case and phase transitions between different structures may be inhibited. For example consider a simulation of a crystal phase transition from a *bcc* structure with 8 nearest neighbours to *fcc*, with 12 nearest neighbours. If the simulation considered only the original 8 then the *fcc* structure will not be stable and the transition will be inhibited. One way round this problem is to run the simulation with a large number of neighbours for an initial run. This is time consuming since run time is directly proportional to the number of neighbour interactions, but once the structure has been established the number may be reduced to be consistent with its symmetry.

Although the imposition of a suitable cut off has little effect on the system's dynamics the same is not true of the pressure calculation. There is a significant deviation which is easily evaluated by assuming that outside the cut-off radius the interaction is smeared out into a uniform distribution in space. A trivial integration gives the potential energy residue which is differentiated with respect to the cut off volume to yield the distant pressure term. Notice that under the assumption of uniform interactions the stress tensor is isotropic and identical to the pressure.

If the interactions are defined by a neighbour list then an equivalent cut-off may be defined. Given P molecules in the neighbour list and a molecular density $\rho=N/V$ the distant stress term is

$$\sigma_{ij\ dist} = 16\pi^2\rho^2/(9P+9)\sum A_{kl}\delta_{ij} \qquad (2.34)$$

where the sum is over all atom-atom interactions between a pair of molecules. The magnitude is usually of the order of 10^8 Pa. This term may be consistently

introduced into equation (2.29) as an external applied pressure p.

§2.2.4 The Model Molecule

The model molecule of *n*-butane is illustrated in figure (2.4) which shows the definitions of the dihedral angles χ_1, χ_2 and Ψ. Notice that Ψ rotates *both* ethyl groups and therefore varies over a range of only 180°. The bond lengths are 1.53A (C-C) and 1.08A (C-H) and for computational simplicity the bond angles all take the tetrahedral value of 109.47°. This is a simplified approximation to the shape of the molecule which is used for expediency. The dimensions of the butane molecule have been determined in the gas phase by electron diffraction (Bonham & Bartell, 1959; Kuchitsu 1961) and also in the solid state (See chapter 3). The true bond lengths are 1.533A or 1.539A (C-C) and 1.100A or 1.108A (C-H) respectively while the bond angles are 110.5(5)° for the CCH angle and 112.4(5)° for the CCC angle (gas phase) and 111.0(7)° (crystalline phase). The discrepancy is most apparent in the case of the CCC angle where there is 1.5°-2.5° difference giving an error of 0.06A in the position of the methyl group hydrogen atoms.

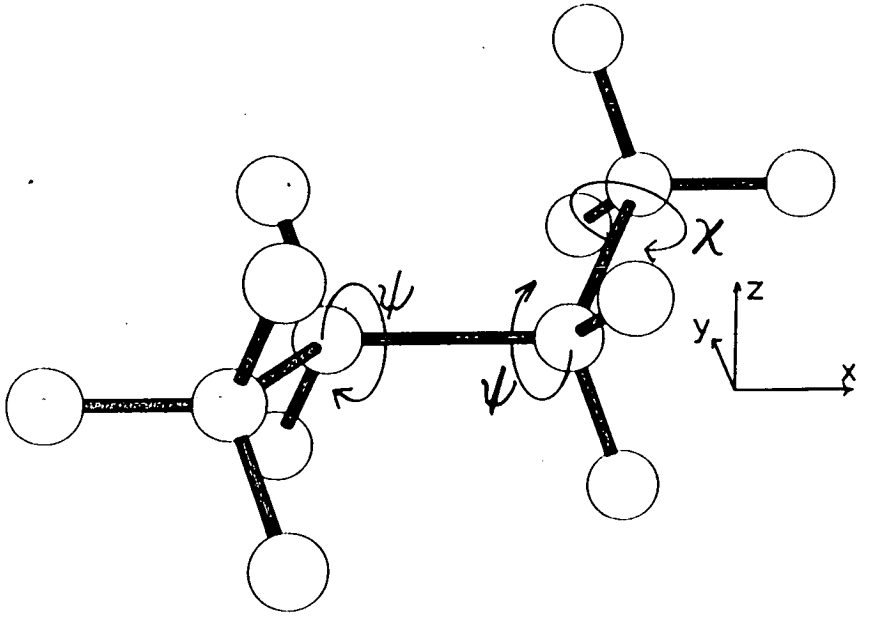

Figure 2.4 The model butane molecule.

In the 1977 paper Williams suggests that the interaction centre for a hydrogen atom should be shifted by 0.07A inward along the bond to account for the distortion of the electron orbitals by bonding. Thus the correct bond length to use with this potential is actually 1.04A.

When considering these points it should be borne in mind that this is a model calculation whose purpose is not to reproduce nature in all its detail, but to explain the main features of the system's behaviour with a simple model. Although a more

accurate model *would* be preferable the results, especially those of chapter 5, show that even our simple model is extremely successful and in good agreement with experiment.

§2.3 Computational Details

The model *n*-butane system is extremely complex and requires a large amount of storage for all the variables necessary to implement a simulation. Our DAP computer has only 2 MBytes of main store which is insufficient to implement the simulation in the most obvious manner. It was therefore necessary to use a few special techniques to squeeze the program into the space available. This inevitably entailed a more complex program and a considerable amount of time was needed to develop a working version.

The first method has already been mentioned in §2.1.6. The simulation consists of only 2048 molecules and information relating to atoms on the two halves of each molecule is stored on separate PEs. Non-atom-specific information is divided in an arbitrary manner. Logical masks are used to extract and separate information which is then processed serially. However as was shown in §2.1.6 the largest part of the computation, the force evaluation *does* use the full parallelism available.

The matrix M_{ij} defined in equation (2.19) is a large user of store. It has 6×6 entries for each molecule but as it is symmetric only 21 of these are distinct. It is stored as a 21 element array and is accessed via a 6×6 lookup table. Because it is symmetric and positive definite a Cholesky algorithm is used to invert it *in situ*.

There is a large saving in storage to be gained by exploiting the unusually comprehensive range of storage precisions available in DAP FORTRAN. All of the generalised co-ordinates, M_{ij} and the final generalised forces are held as 4 byte floating point data which gives an average precision of 1 part in 10^6. However many of the calculations in a simulation involve the addition of a small increment to a larger quantity. The increment may then be stored in a smaller length word without affecting the accuracy of the sum. For example consider an increment Δv to a velocity v such that $v=100\Delta v$ and both v and Δv are stored to 6 decimal places. Then the two least significant figures of Δv are less than the round off error in v and will be lost when Δv is added to v. It is therefore no disadvantage to store Δv to only four places.

The following quantities are stored as three byte floating point data which gives an average precision of 1 part in 2^{14}: the atomic positions relative to the molecular centre (which are small compared to the interatomic spacing), the quantities $\mathbf{r}^{*}_{ikl}$ of (2.19) and the cartesian forces $\mathbf{F}_i$. It might be objected that the forces which are the sum of many terms should be stored to a higher precision to avoid the

accumulation of truncation errors. On many computers that would be true. In such cases the result of an addition is truncated to fit the word length which gives a systematically low result for the sum. The error is proportional to the number of terms. However DAP arithmetic rounds the result and the errors on individual additions will tend to cancel. The error then goes as the square root of the number of terms. In a typical run there are of the order of 250 terms added to each force so that the error is approximately 16 times the individual round off. With a storage precision of 1 in 2^{14} the force is accurate to 1 part in 1000.

Confirmation that using reduced precision does not affect the simulation too much is provided by the fluctuations in the total energy. For a run at 25K using a timestep of 0.005ps $\surd<\Delta E^2>/<E>$ is less than 10^{-5}.

In order to evaluate such quantities as $<r^2>$ and $<v^2>$ the averages $<r>$ and $<v>$ should be zero. Even if these quantities are initially set to zero they will drift due to the accumulation of computational errors. They are therefore reset to zero periodically.

Several of the co-ordinates are multi-valued because of some symmetry of the molecule. χ_1 and χ_2 have three equivalent values in the range 0° to 360° and the quaternions, already double valued, are further doubled due to the 2 fold rotation symmetry of the molecule. For simplicity of analysis all of these are tested each time step and normalised to some range in which they are single valued. In the case of the orientation the use of quaternions allows this to be done simply and elegantly. A rotation of 180° about the z axis has a quaternion $\mathbf{q}_{180}=(0,0,0,1)$. If the molecule's orientation is given by $\mathbf{p}=(w,x,y,z)$ the symmetry rotated quaternion is $\mathbf{pq}=(-z,y,-x,w)$. This transformation must be accompanied by an interchange of χ_1 and χ_2. Recalling that $\mathbf{q}$ and $-\mathbf{q}$ describe the same orientation, single valuedness is enforced by the requirement that $w>0$ and $y>0$.

Chapter 3

Early Runs – Structures and Constraints

§3.1 Introduction

This chapter describes the early runs of the *n*-butane simulation. They were all carried out before the results of the neutron powder diffraction experiment were available, when the crystal structures of butane were unknown. The goal of these runs was to find the structure of lowest free energy of the model which at low temperatures is also the structure of lowest internal energy. The obstacles which were encountered to the formation of such a structure and their solution are of importance to any MD simulation of the solid phase. This is because the stable structure of the model is rarely known and will inevitably be slightly different from the structure of the real system. The simulation will only yield the properties of the model structure if no artificial constraints are imposed.

It should be recognised from the outset that the strength of the MD technique lies in the study of dynamic phenomena and that it is not necessarily the ideal method for finding structures. The molecular motion and co-operative dynamics depend strongly on the forces between adjacent or nearby molecules and much less on the interaction between distant ones. On the other hand two different structures may have similar internal energies. Their relative stability depends on a delicate balance between these energies which must therefore be very accurately evaluated by considering interactions at large distances.

The natural method of doing this is known as *lattice energy minimisation* or *static simulation*, which involves setting up a model structure, computing the potential energy and using an iterative fitting procedure to find the minimum. It is well known that the final structure is strongly dependent on the initial configuration. To obviate this problem many runs are needed from a wide range of initial states and the final energies should be compared to find the minimum. The necessity of multiple starts arises because there is no kinetic energy in the model, so that the method is essentially a zero temperature one. It can therefore address only low temperature phases and in particular is inapplicable to plastic phases.

In principle the inclusion of temperature in a MD simulation means that there is no need of multiple starting configurations. Thermal activation should overcome the potential barriers which block the evolution of states in a static simulation and the

dynamics should find the structure of lowest free energy. In practice the problem may not be completely ergodic on a timescale accessible to MD and some potential barriers may be too large to overcome. In particular it may not be possible for a reconstructive transformation to take place where the molecular packing is radically altered. This will be amply illustrated in this chapter by the stability of several 'wrong' structures for butane. However it should be noted that butane is a particularly difficult case because of the elongated molecule which cannot rotate freely in the crystal. This results in the existence of a long-lived metastable phase in the real system. Despite this proviso the number of configurations accessible to a MD simulation it still vastly greater than for a static simulation and probably only a very few starting structures are necessary.

It will be shown in this chapter that there are two other factors which restrict the formation of a stable phase in a MD simulation. They are both associated with the difference between an effectively infinite real system and a finite-sized model with periodic boundary conditions. The latter are needed to ensure that properties measured on a system which is no more than 11 lattice translations wide in any direction are those of the bulk. Their implementation in this case has been described in § 2.1.6.

These two factors are the geometry and the topology of the molecular dynamics cell. By *geometry* is meant the size and shape of the cell, that is the physical location of the periodic image molecules. Until recently all simulations used a MD cell of fixed shape and size. In such a case the pressure, or more generally the stress is not controlled and may take unrealistic values, in particular negative ones. This could force the system into a different point on the phase diagram than desired. The introduction of the 'new' MD by Parrinello and Rahman (see § 2.1.5) means that the stress may be set to any value, usually zero. Simulations of butane were done using both methods and the constraints imposed by the fixed geometry are clearly demonstrated.

The *topology* of the cell refers to the way that the image of a molecule is related in terms of lattice displacement to the original and is not altered by changing the shape of the MD cell in a zero stress simulation. In particular the choice of topology determines the number of molecules that may exist in a crystallographic unit cell. The peculiar topology of skew cyclic boundary conditions which are the most convenient for implementation on the DAP are shown to constrain the structure in this way although the more conventional straight cyclic conditions will also constrain though slightly differently.

In all of the following runs the rotation of the methyl groups was free, although there was a potential associated with Ψ as described in §2.2.2. This eliminated the fastest modes and allowed the relatively large timestep of 0.02ps to be used. Most of the runs used the set of neighbour interactions defined in table 2.3 which includes 6 nearest and 8 next-nearest neighbours.

§3.2 Low Temperature Simulation

The first objective was to find a stable low temperature phase. Although it is desirable to experiment with a number of different starting configurations it proved rather difficult in practice to find any which resulted in a stable simulation because of the irregular shape of the butane molecule. If the simulated model is at a realistic density there are only a small number of orientations that adjacent molecules may have if atoms on each are not to be too close. Such close approaches are disastrous as the 6-exp potential becomes attractive at separations of less than 1A whereupon the offending atoms experience enormous forces. The resultant accelerations are so large that the trajectory is evaluated too coarsely to sample the details of the potential and the discrete approximation of the integration algorithm breaks down. Thus when two atoms become too close, the molecules to which they belong suddenly fly apart at high velocities in opposite directions.

Because of this problem attempts were made to produce a stable configuration by running the simulation from a start in which the molecules were well separated, that is at low density. It was hoped that crystallites would form but unfortunately only disordered clusters were observed, so this approach was abandoned.

The first successful initial configuration was designed by an *ad hoc* procedure in which a qualitative assessment of molecular packing was considered. Eventually a body centred orthorhombic structure was arrived at with the molecules all in the same orientation. This packing was simply for expediency since there was no obvious molecular overlap. The simulation was then run for the equivalent of 72ps at 25K to allow thermal equilibrium to be reached and to give the system time to explore phase space. A representation of one layer of the final configuration is shown in fig 3.1 which appears to consist of two different structures. However when the packing of layers out of the plane of the diagram is considered the 'right hand' structure is seen to have split into two. These are characterised by the **c** axis which alternates between two directions with $\alpha \simeq 72°$ and $108°$ which is illustrated in fig 3.2 by distribution of unit cell angles over a single configuration. The three peaks in the α distribution correspond to these three structures.

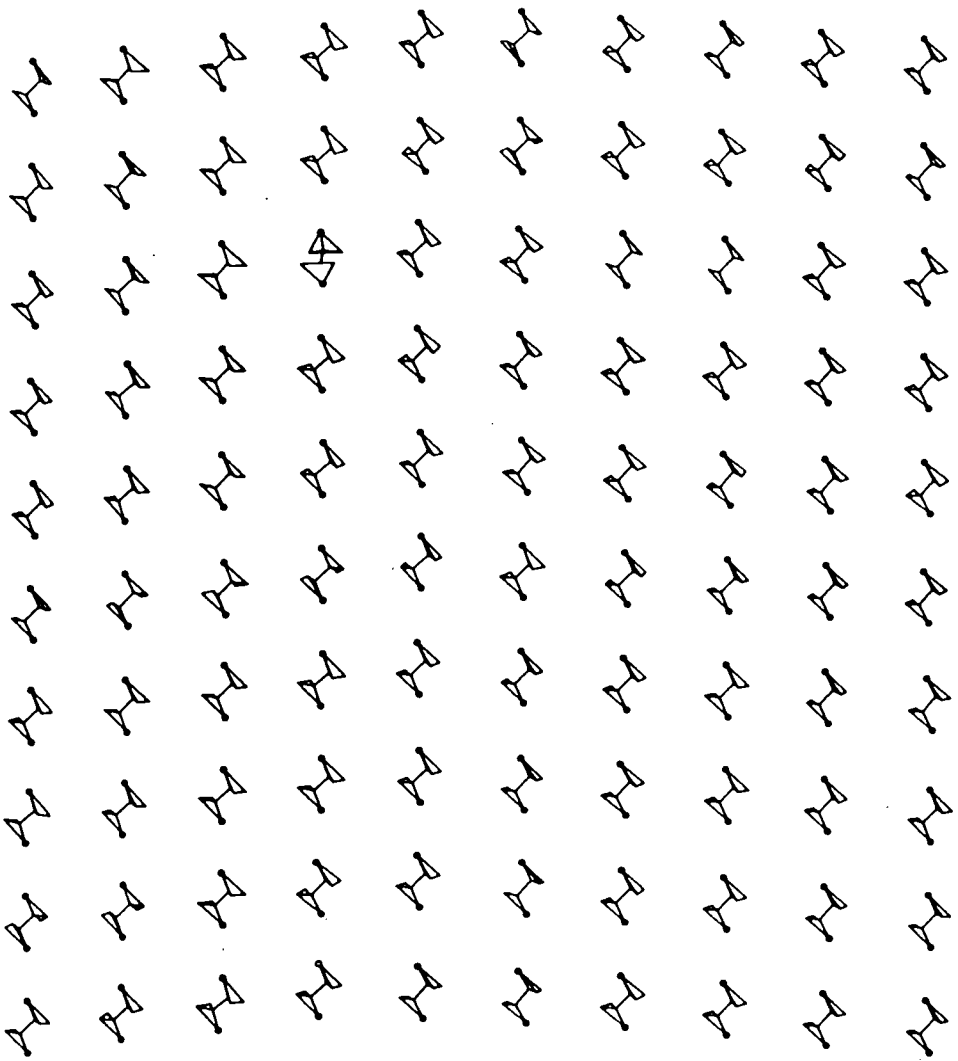

Figure 3.1 One layer of structure obtained using a fixed MD cell.

However there can only be one truly stable structure, so how can the other two be accounted for? In order for a single crystal of any structure to exist, it must be possible to exactly fill the MD cell with copies of the unit cell. This is clearly not the case for any of the three structures observed. Of the two which can be seen in fig 3.1, the leftmost one has an in plane unit cell angle γ which is acute whereas the rightmost one is obtuse. Only the presence of *both* allows the y displacement at both sides of the boundary to be the same and so satisfies the cyclic condition. Similarly the alternating direction of the unit cell vector **c** is necessary to satisfy the boundary condition in the z direction. The presence of three structures is therefore an artefact of the geometrical constraint imposed by the fixed boundary conditions.

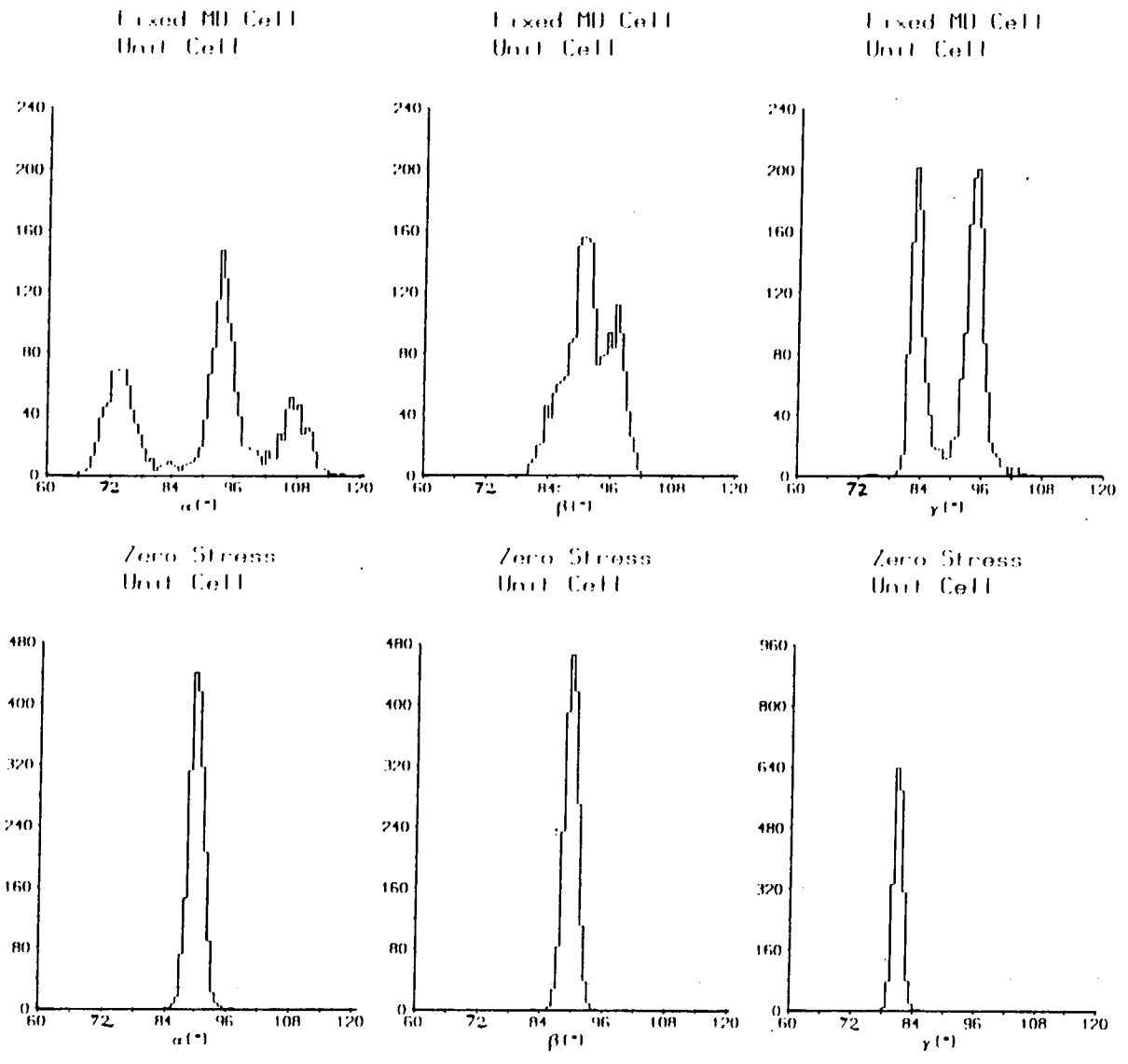

Figure 3.2 Comparison of unit cell angle distributions between fixed MD cell and zero stress simulations.

Given a large enough sample it must be possible for crystallites of the stable structure to form in several different orientations so as to satisfy the boundary conditions. Whether this can occur depends on whether the defect energy associated with the grain boundaries is lower than the free energy difference between the metastable and stable structures. It is not easy to predict how large a simulation is needed before this condition is satisfied, but it will clearly be larger for such an anisotropic system as butane than for cubic systems.

The effect of using a fixed shape MD cell clearly presents major difficulties to a simulation of the solid state. However the problems are now easily overcome by using the zero stress method of Parrinello and Rahman (see § 2.1.5) which allows the system to adjust the shape of the MD cell. By considering the parameters of cell as

dynamic variables the shape which minimises the free energy is chosen. For this reason the 'new' MD as it is sometimes called is being extensively used for solid state simulations.

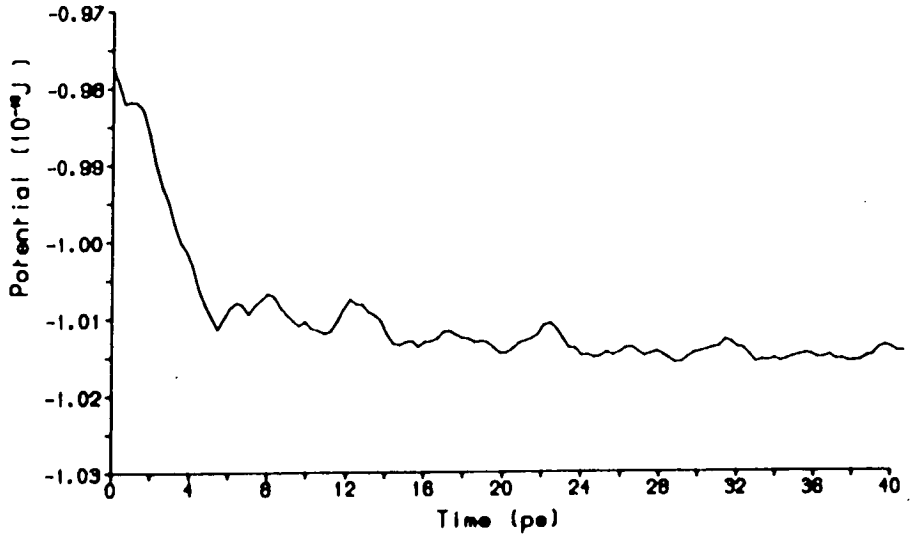

Figure 3.3 Potential energy during zero stress run.

The method as described in §2.1.5 was incorporated into the simulation which was then run for 2048 timesteps from the state at the end of the previous run. The potential energy decreased rapidly for around 5ps before settling down to fluctuate about a new value (see fig 3.3) which indicated that a structural transformation had taken place. The nature of the change is shown in fig 3.2 where the distribution of unit cell angles before and after this run are plotted. The peaks corresponding to the right hand structure of fig 3.1 disappeared entirely and those left were similar, though not identical to the left hand side. It is clear that the right hand structure was not merely metastable but was highly unstable with respect to the final structure since the rapid and monotonic decrease in the potential showed that there was no potential barrier to the transformation. In the new structure there are two angles, α and β which are very close to 90° although there is no corresponding structural symmetry. It is therefore triclinic with two molecules in the unit cell. A cross-section is shown in fig 3.4.

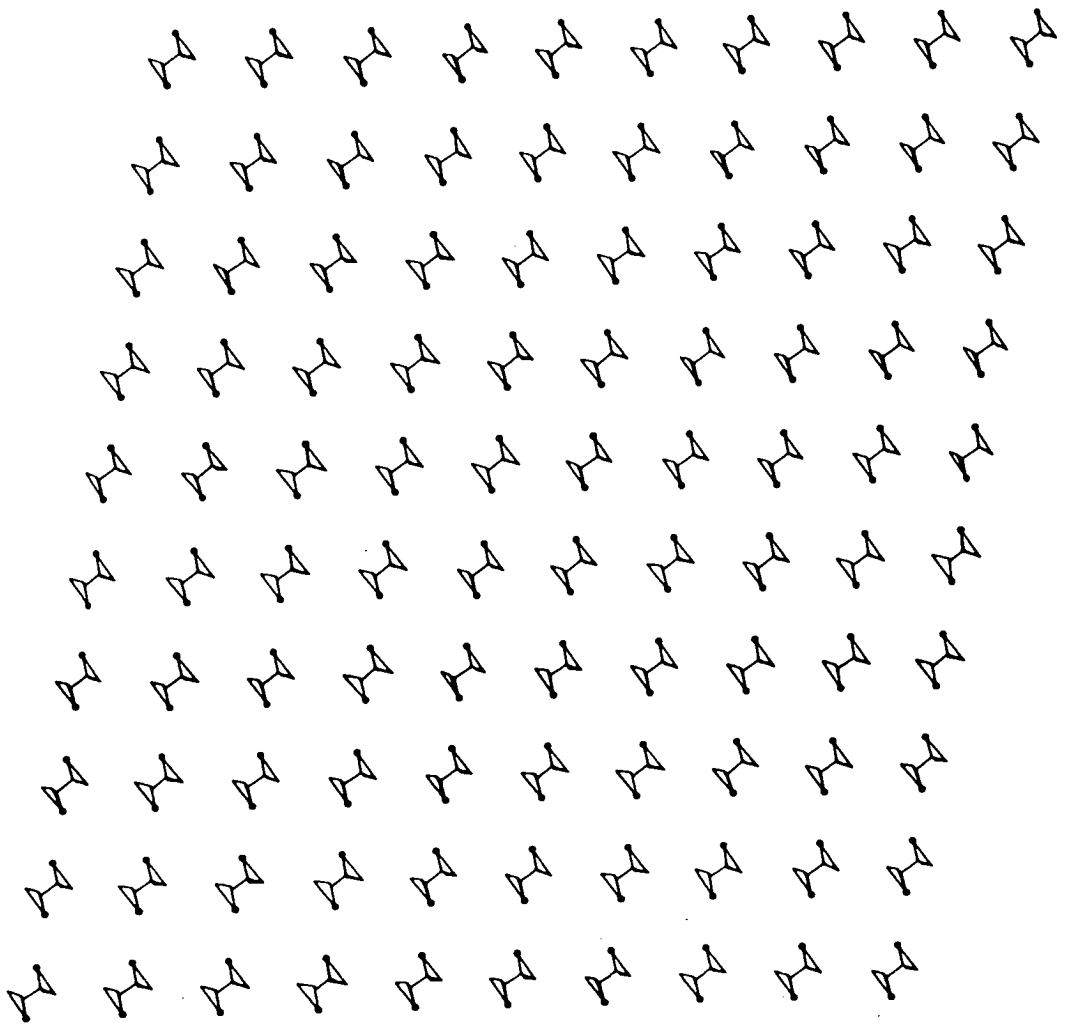

Figure 3.4 One layer of structure obtained after zero stress run.

Thus far all the simulation runs had been at a temperature of 25K. It was noted in §3.1 that it is thermal activation which allows a simulation to search phase space for the structure of minimum free energy. The range of states accessible will obviously increase with temperature and therefore some higher temperature runs were performed. The configuration of fig 3.4 was heated to 90K, still below the experimental transition temperature, and the simulation was run for 3600 timesteps. It was then cooled to 25K once more. During this run half of the molecules rotated to a new orientation. This was monitored by means of the quaternion distribution functions which are shown in fig 3.5. During the run a second peak appeared in $\mathbf{q}_2$ and also, though not as obviously, in $\mathbf{q}_1$ as well. Two cross-sections of the final configuration are shown in fig 3.6 where the molecules of the second layer are at the (0.5,0.5,0.5) positions in a two molecule unit cell. The configuration consists of several grains where the (0,0,0) molecules are in one of two orientations and the (0,5,0,5,0,5) molecules are in the other.

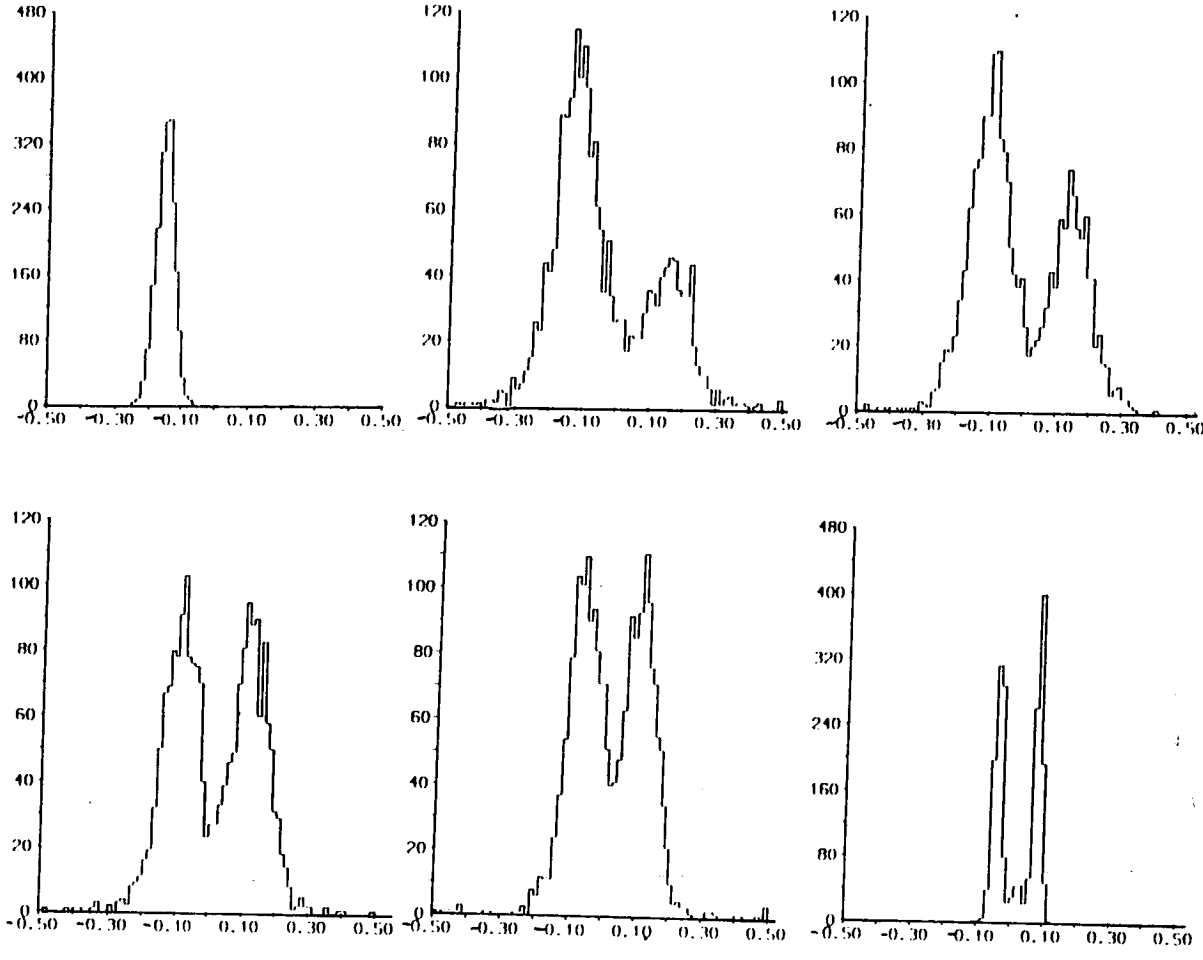

Figure 3.5 Distribution of $\mathbf{q}_2$ *during annealing run.*

It is easily demonstrated using the symmetry properties of quaternions that these two molecular orientations are related by a 180° rotation about the z axis. They are described by quaternions $\mathbf{q}_1=(0.9475,-0.015,-0.164,0.28)$ and $\mathbf{q}_2=(0.9475,0.015,0.164,0.28)$. Define $\mathbf{p}$ to represent a 180° rotation about the z axis, that is $\mathbf{p}=(0,0,0,1)$. The product quaternion $\mathbf{pqp}$ corresponds to the combined application of three rotations. The first is a twofold rotation about z in the molecule reference frame, which is a molecular symmetry operation. This is followed by the rotation $\mathbf{q}$ and a final rotation of 180° about the z axis in the original frame. It is trivial to verify that $\mathbf{pq_1p}=\mathbf{q_2}$ and that $\mathbf{pq_2p}=\mathbf{q_1}$. Thus modulo a molecular symmetry operation the two observed orientations are related by a 180° rotation about the z axis. Because of the translation also involved the actual space

group symmetry operation is a 2_1 axis along (0.25,0.25,z). There is also an **n**-glide perpendicular to z which arises from the inversion symmetry of the molecule in the *trans* conformation. The structure is therefore monoclinic with space group $P2_1/n$ with parameters a=7.132A, b=4.198A, c=7.547A, β=82.35°. It can also be expressed in the customary crystallographic manner as $P2_1/c$.

Although it appears at first glance that fig 3.6 shows many distinct grains, consideration of the boundary conditions reveals that this is not so. Regions of the same orientation on the left and right hand of fig 3.6 are joined by the cyclic condition and the top is joined to the bottom of the next layer. In fact the configuration consists of one continuous crystallite which nevertheless has boundaries with itself. This is a result of the curious topology of the skew cyclic boundary conditions which in this case does not allow the formation of a single unbounded crystal. To see why this is so consider a path through the sample traversed by (100) lattice translations (in the $P2_1/n$ cell). In the numbering of fig 2.2, not only can molecules 1 to 10 be reached in this way, but as 11 is the (010) neighbour of 1, so can 11 to 20 and all of the first layer. Continuing in the (100) direction takes us to 101 and 102, which is displaced from 1 by (0.5,0.5,0.5). In fact every molecule in the sample including the non-equivalent ones can be reached entirely by means of lattice translations, which is clearly inconsistent with the presence of a lattice with a basis. This is the 'topological' constraint on structures mentioned in §3.1. It is, however, easily avoided in this special case.

The 2048 molecules can be divided into two non-intersecting strings which are each closed under lattice translations by partitioning the system into odd and even numbered molecules. All lattice translations are then represented by adding even numbers to the molecule index, or in DAP terminology an even long-vector shift while non-equivalent molecules are reached by odd shifts. It is then possible to form a single crystal of a structure with a two molecule unit cell. There is an obvious extension to n molecules where n is a divisor of the total number in the simulation, in this case 2^m, $m<11$. The restriction remains that the number of molecules in a unit cell must be a divisor of the total. This limitation is quite general and applies to straight as well as skew cyclic boundaries.

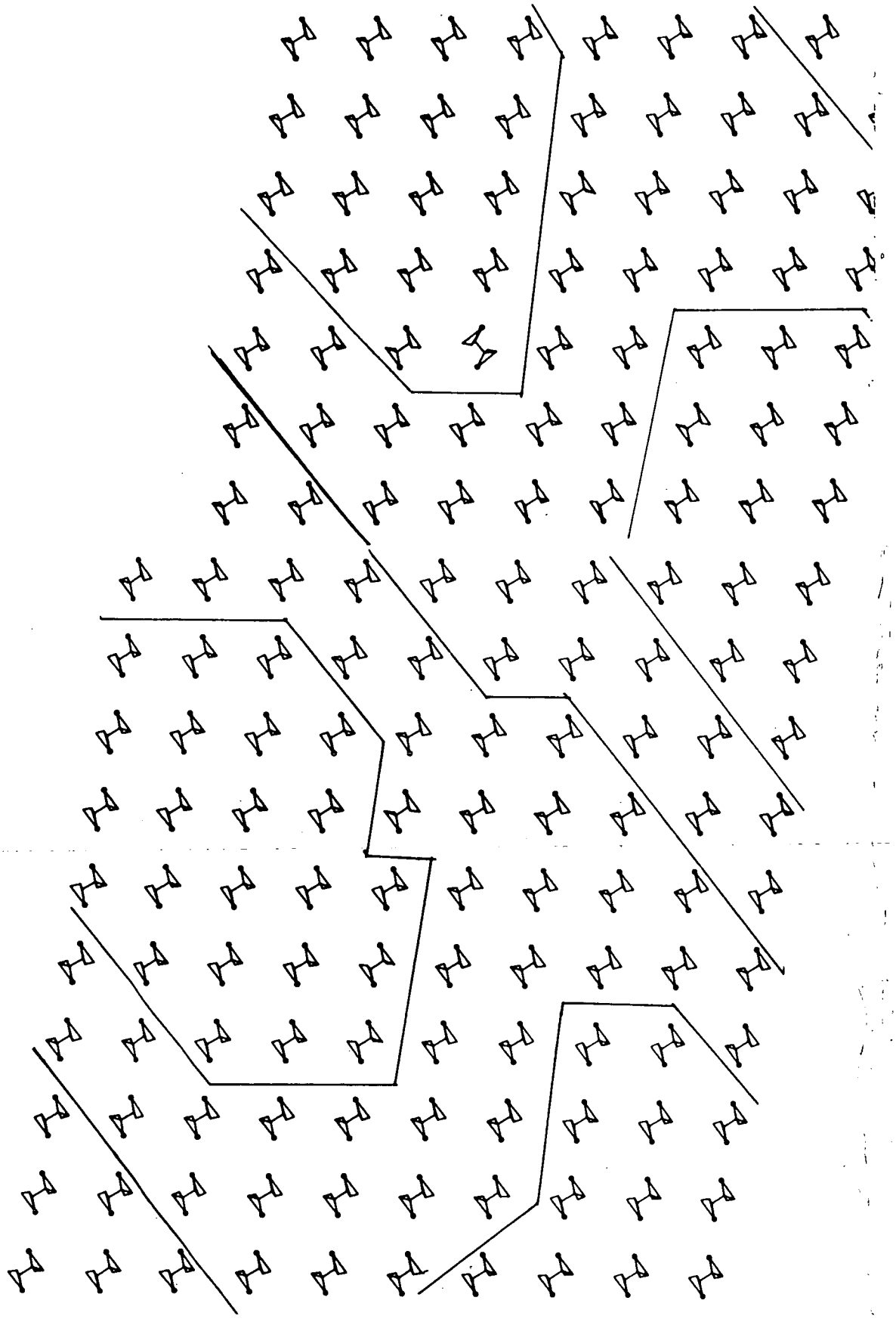

Figure 3.6 The monoclinic structure obtained after 90K run. The upper section is shown as a cyclic continuation of the lower, but is also the layer of 'body centre' molecules at (0.5,0.5,0.5) with respect to the lower.

The new neighbour list of table 3.1 was designed to allow 2 molecules per unit cell and was implemented in the simulation. A configuration consisting of a single crystal of the monoclinic structure was constructed and the simulation run for 1120 timesteps at 25K followed by 2000 timesteps at 90K. No further transformations occurred, which demonstrated that this structure is very stable.

Table 3.1 Neighbour list for a two molecule unit cell.

i	Index	Vector displacement
1	2	(1,0,0)
2	20	(0,1,0)
3	200	(0,0,1)
4	89	(-0.5,-0.5, 0.5)
5	91	(0.5,-0.5, 0.5)
6	109	(-0.5, 0.5, 0.5)
7	111	(0.5, 0.5, 0.5)

In view of the considerations outlined in § 2.2.3 concerning the effect of the small interaction range on the stability of a structure, a few test runs were carried out using a much larger neighbour list. During the previous runs, eight nearest and six next-nearest neighbours were included, which gave molecule centre distances of up to about 7.5A. This meant that atom-atom interactions had an effective cut-off of between 5A and 10A which neglected forces of non-negligible magnitude. The new list contained 32 molecules and was chosen to make the overall interaction more isotropic as well as of longer range. All molecules whose centres were closer than 9.5A were included. This corresponded to an effective atom-atom cut-off of over 7.5A. The simulation was then run for 25ps at 25K followed by a 30ps run at 100K. During these runs no evidence of any structural change was observed. From this it was concluded that the stability of the monoclinic structure is not an artefact of the small neighbour list. It also follows that the smaller list is adequate, and it was used for all the remaining runs.

The desirability of starting from a range of initial configurations has already been discussed. There remains the possibility that there is a more stable structure than the monoclinic one which cannot be reached by the simulation because the potential barrier to the reconstructive transition is too large. It was suggested by Cangeloni and Schettino (1975) that phase III was triclinic with one molecule in the unit cell. Consequently some runs were done with a neighbour list suited to such a structure. Runs were done at various temperatures and an apparently stable structure was produced although evaluation of the internal energies showed it to be metastable with respect to the monoclinic phase. The powder diffraction experiment showed that it was not the correct structure and from this point of view this line of investigation was not pursued. Nevertheless the results show that the potential barriers are too large to allow the simulation to explore phase space exhaustively.

§3.3 High temperature simulation

Some preliminary simulation runs were done at higher temperatures in an attempt to produce a disordered phase. An equilibrated configuration of the monoclinic structure was heated to 140K at which temperature the velocity rescaling was switched off and the simulation was run for a further 2500 timesteps. Although no serious attempt was made to locate the transition temperature closely, the onset of disorder was observed at around 115K. This is to be compared with the value of 108K obtained from specific heat measurements (Aston & Messerly, 1940). One layer of the final configuration is plotted in fig 3.7 and it is clear that a structural change has occurred.

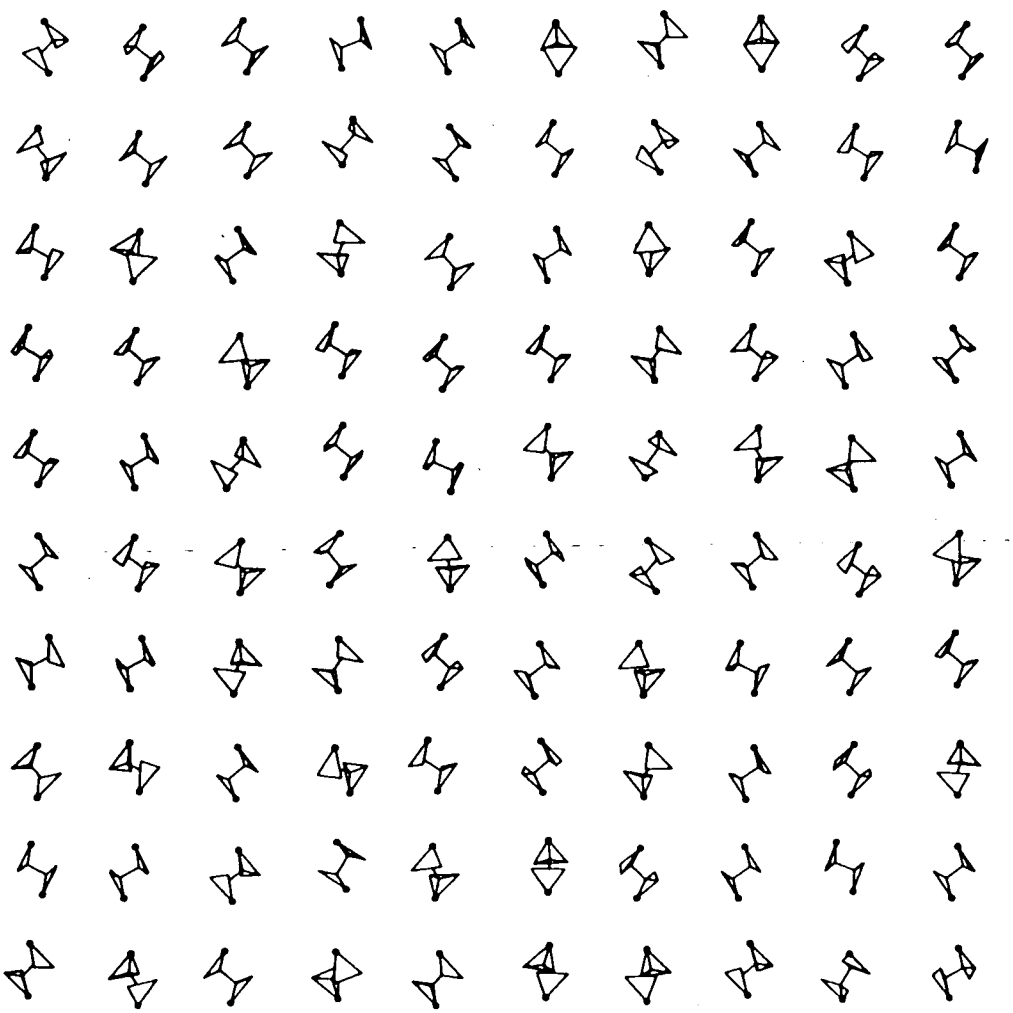

Figure 3.7 The orientationally disordered structure at 140K.

The unit cell angle γ has increased to 90° and the molecules are orientationally disordered. The 'long' molecular axes joining the methyl carbons are all aligned and the disorder takes the form rotation about this axis. The evidence discussed in § 1.3 suggested that the disorder in the plastic phase of real *n*-butane is one dimensional

in nature, in agreement with simulated structure.

It is a non-trivial matter when calculating an orientational distribution function (ODF) from a simulation to separate disorder about one axis from the rest of the thermal motion. The technique which was developed will be described fully in chapter 5. In this case it yielded the result that the disorder axis lies along (0,1,0) to within 0.5°. The ODF plotted in fig 3.8 displays two preferred orientations of approximately equal occupancy at 0° and 180°. There is an extra structural symmetry as the time averaged system is now invariant under a twofold rotation about (0,1,0). This structure therefore has an orthorhombic space group and this is a rather good illustration of why disordered phases are usually of a higher symmetry than their ordered counterparts.

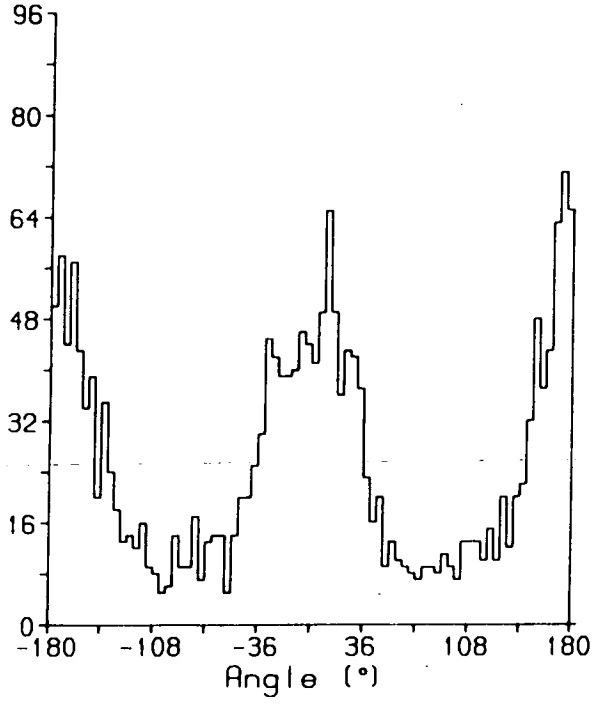

Figure 3.8 The orientation distribution of the structure in fig 3.7.

The disordered configuration was then cooled to 100K in an attempt to reverse the transition and reform the monoclinic structure. However even after prolonged running (80ps) at this temperature there was no evidence of molecular ordering, instead the disorder had frozen in to give a glassy state. This is further evidence that the potential barriers to molecular rotation are very large in this system.

§3.4 Discussion and Conclusions

The foregoing simulation runs have shown that our simple model can indeed produce a phase transition between an ordered low temperature phase and an orientationally disordered phase at high temperature. It was originally intended to search for the structure of minimum internal energy by running the simulation from a range of initial configurations, but due to the difficulties encountered in setting up a physically reasonable structure the search was not as extensive as might have been desired.

The existence of large potential barriers to molecular reordering in this system, which was suspected from the start, was amply confirmed by the metastability of the triclinic and the disordered glassy structures with respect to the lower energy monoclinic structure. It is clear that butane is a rather extreme case in this respect as indicated by the extremely long lived metastable phase II in the real system.

The two structures obtained from the simulation are not in fact those of the real system as they differ from the experimental structures of chapter 4. It might be thought that this results from a failure to find the lowest energy state, but as will be seen in chapter 5 the experimental phase III structure has an energy which is 1% *higher* than that of the monoclinic structure from this simulation. It is apparent from these results that our simple model of n-butane, which includes only short range interatomic forces does show an extremely complex range of behaviour including orientational disorder.

In attempting to elucidate structures from a model, this work has highlighted the constraints associated with periodic boundary conditions which may prevent the system from correctly reproducing the structure of the bulk material. The geometric constraint of the shape of the MD cell was easily overcome by the use of the 'new' MD or zero stress simulation. The topological constraint on the number of molecules in the unit cell can not be so easily circumvented. Instead this number must be chosen to be compatible with the system being simulated. Transitions between structures with different numbers of molecules in the unit cell may therefore be inhibited as a single crystal of the new phase can not form. However in a sufficiently large system a polycrystalline state of the new phase will occur as happened in this case. The fixed list of interacting neighbours did not give rise to serious problems since it can be extended to a large interaction range for short runs. Nevertheless it should be chosen with consideration to the structure of the system.

Finally it should be pointed out that the major structural constraints become progressively less severe as the size of the MD sample increases. With the comparatively large simulations made feasible by supercomputers like the DAP it is possible for the system to break up into crystallites without incurring too great a penalty in defect energy at the boundaries.

Chapter 4

Experimental determination of crystal structure

§4.1 Preamble

There are a number of reasons for embarking on an experimental investigation of the crystal structure of *n*-butane. It was seen in chapter 1 that the nature of the disordered behaviour depends crucially on steric hinderance by short range forces and hence on the molecular environment. Furthermore, as was demonstrated in chapter 3, it is extremely difficult to predict the structure from model potentials using either static or dynamic simulation techniques. Therefore a knowledge of the crystal structure of real butane would allow the simulation to proceed with confidence that the simulation results are relevant to the real system.

It is also desirable to have some experimental data in order to validate the simulation. A simulation is a complex computer program and there is no rigorous manner of checking either whether it is a correct implementation of the model, or indeed if the model appropriately describes the real system. A comparison of simulation results with experimental data is the only way in which the correctness of the simulation can be established.

The work described in this chapter has been submitted as a paper to the journal *Acta Crystallographica*.

The first order nature of the transition is likely to make it difficult to obtain a single crystal of the low temperature phases, as a crystal of phase I would probably become polycrystalline during the transition to phase III. Powder diffraction was therefore used to solve all three phases. Neutrons were used in preference to x-rays in order to give as much information as possible on the positions of the hydrogen atoms.

§4.2 Experimental

The experimental sample of deuterated *n*-butane was obtained from Cambrian Gases and was specified as 98% isotopic purity. It was liquefied in a refrigerator and solidified by pouring the liquid into a mortar in a bath of liquid nitrogen in a dry atmosphere. It was ground to a fine powder and put into a vanadium canister. During this process it was contaminated by nitrogen, whose presence was clearly seen in the data. Temperature was controlled in a helium cryostat and was stable to 0.1K but because the sensor was not in contact with the sample itself the absolute value could have been up to 3K higher.

According to Cangeloni and Schettino (1975) the metastable low temperature phase (II) may be produced by rapid cooling to 77K from the plastic phase (I). A further transition to the stable phase (III) occurs if the sample is maintained between 85K and 90K. To obtain a pure specimen of phase III our sample was left at 90K for 48 hours, which was certainly excessive. It was later heated to 120K and quenched in liquid nitrogen to produce phase II.

The neutron powder diffraction was done using the D1A powder diffractometer at the Institute Laue Langevin at Grenoble (Hewat & Bailey, 1976). The layout of the equipment is shown in fig 4.1. Neutrons from the reactor travelling down the guide tube are reflected and monochromated by a germanium crystal and emerge as a collimated beam targeted on the sample position. They are scattered by the sample under investigation, which is a fine powder, into cones of radiation. The sample is often located within a cryostat or furnace for temperature control. Part of the scattered radiation is intercepted by a bank of 10 He^3 detectors arranged 6° apart on the circumference of a circle centred on the sample. A scan is measured by rotating the detector bank in increments of 0.05° and at each step counting for a period determined by the neutron flux in the incident beam. All of this is controlled by a computer which also stores the output from the counters and later combines it to form a single dataset of scattered intensity as a function of angle, 2θ.

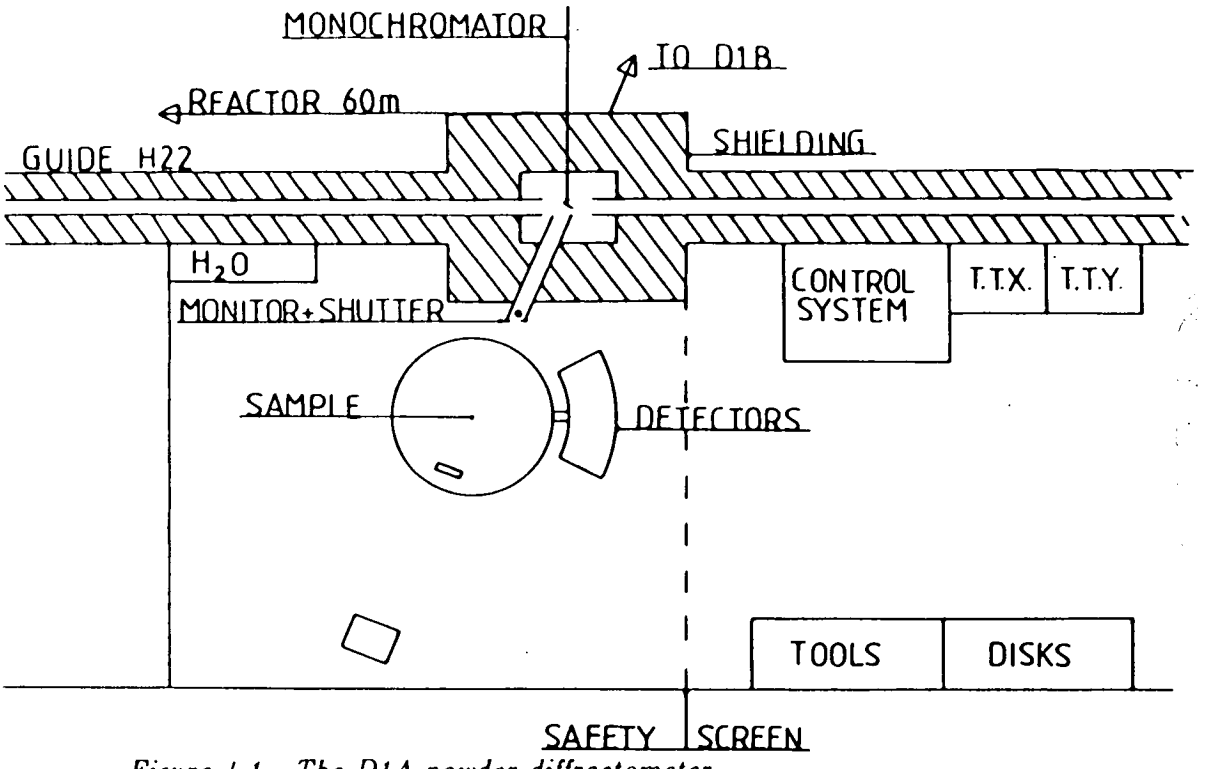

Figure 4.1. The D1A powder diffractometer.

Data was collected at 5K and 90K in phase III, 65K in phase II and 120K in phase I. The suspected contamination with nitrogen was taken into account when choosing temperatures at which measurements were to be made since the extra nitrogen Debye-Scherrer peaks make analysis more difficult. The temperature is especially important for phase II as annealing to phase III takes place above 85K but the nitrogen is crystalline below 63.9K. Because of the possibility of annealing in phase II and of crystallite growth in phase I the data were monitored for any change with time. In both the 120K and the 65K runs the output from counter 10 was compared with that from counter 1 and in both cases there was no change during the four hours which elapsed between the two counters scanning the same points. The sample rod was rotated by hand and further short runs taken at 120K to test for preferred orientation effects. None were found. All the scans had a range of $2\theta = 6°$ to $160°$ in steps of $0.05°$ using a wavelength of 2.980(2)A.

The presence of nitrogen was confirmed by comparing the 5K and 90K scans of phase III. Extra peaks were present in the 5K data at positions corresponding to those expected for the cubic α phase of nitrogen. In all the other scans there was a broad and featureless distribution of fairly low intensity scattering from about $40°$ to $70°$ 2θ from the liquid or dense gas.

All the scans were indexed using the Kohlbeck program (1978). It is a tribute to the recent advances in indexing techniques that we had very little difficulty in

this, while having no previous knowledge of the structures. The systematic absences showed that all three phases are monoclinic with space group $P2_1/c$.

§4.3 Refinement

The data were analysed by the Rietveld profile fitting method using the program EDINP (Pawley, 1980). In order to assess the quality of the fit to the data, all the scans were first fitted by the program ALLHKL (Pawley, 1981). This is a modification of EDINP which refines the intensity of each peak as a separate variable as well as the unit cell, peak shape and background. The R factor thus obtained differs from that of EDINP only because it is not limited by the model structure and is thus the value which the best possible fit of structural parameters would give with EDINP. The quality of fit was assessed by means of the R factor, defined as

$$R(\%) = 100 \sum | I^{obs} - I^{calc} | \; / \sum I^{obs}.$$

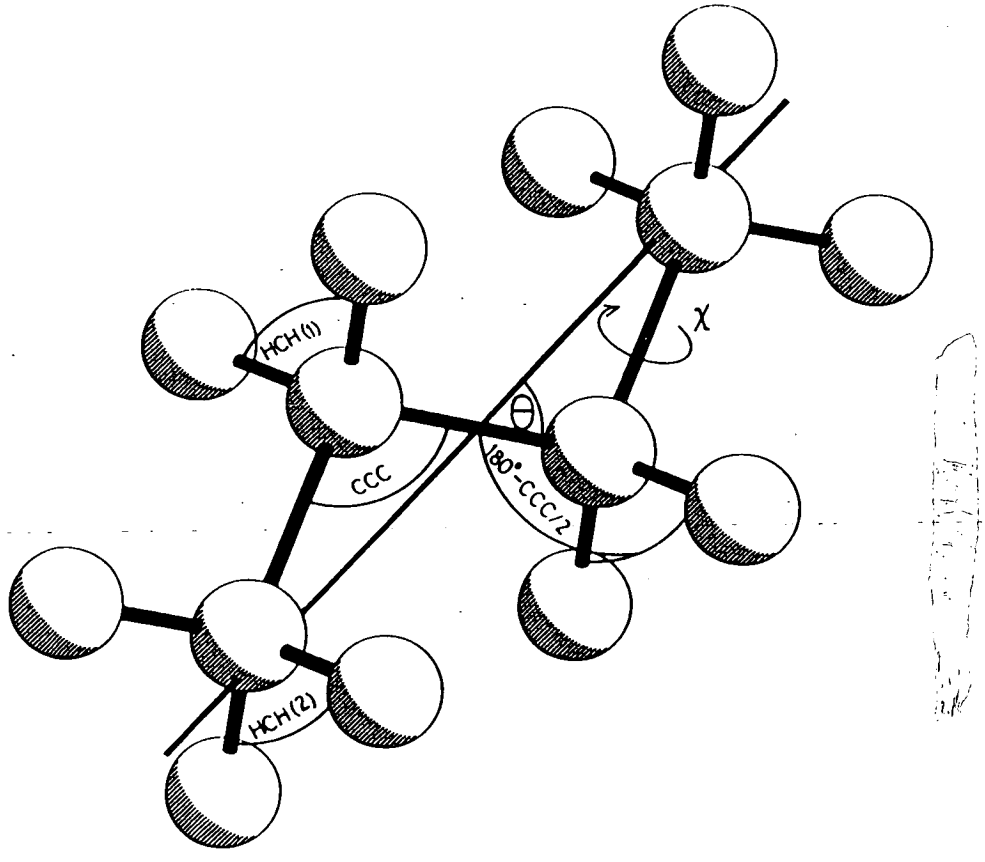

Figure 4.2 N-butane molecule with definitions of refined parameters. Also shown is the definition of the disorder axis for phase I.

The dimensions of the butane molecule in the gas phase have been determined by electron diffraction (Kuchitsu, 1961; Bonham & Bartell, 1959). One possible course of action would be to use this molecular geometry in a constrained refinement. However since the forces experienced by a molecule are very different in the solid from the gas phase we chose to make certain of the molecular structral parameters variables of the refinement. In order to make maximum use of the low

information content of the powder diffraction the technique of constrained refinement was used as implemented in the EDINP program. The constrained parameters for the molecule were the Euler angles for overall rotation, three bond angles, the methyl group dihedral angle and the C-H bond length (see fig 4.2). The Euler angles are as defined in Goldstein (1980) with respect to a reference frame in which the inner two carbons lie on the x axis and the outermost two are at approximately ±(1.2,1.4,0) in units of A. It was found necessary to fix the C-C bond length at the known value of 1.539A because of the high correlation between this and the other parameters. It is a reasonable assumption that bond lengths are less sensitive to the crystal environment and temperature than bond angles. The model molecule was set up in the centrosymmetric *trans* conformation as shown by Raman and infra-red spectroscopy (Cangeloni & Schettino, 1975). Isotropic temperature factors expressed in the customary B units were used throughout, but to take account of the librational and internal modes, the carbon and deuterium atoms had separately refined parameters. The peak shape function used was the three Gaussian form of Howard (1982) in which an 'asymmetry' parameter, P is added to the usual three in order to account for the curvature of the Debye-Scherrer cones. Although the measured scan steps were 0.05° in 2θ the data sets were reduced to a step of 0.1° for the refinements without any apparent loss of definition.

Pawley (1980) has discussed the problem of standard errors in least squares refinement. The usual error contains the factor $1/\sqrt{N}$ which assumes that adjacent points in the scan are statistically independent. (N is the total number of points in the scan.) This is clearly not the case and consequently the errors quoted for structural parameters are calculated by replacing N by N/n where n is the average number of points in the full width at half height of a peak. The final refined values of the peak shape parameters are listed in table 4.5.

Scattering from the contaminant nitrogen was observed in all the data. In the 5K scan extra Debye-Scherrer peaks were present with substantial intensity; the 111 at 54.4° reached over 1800 counts. Fortunately there was no significant overlap with the butane peaks and the contaminant peaks were given zero weight in the refinement. The extra scattering from the liquid in the higher temperature scans was manifest as a very broad low intensity rise in the background. In the case of phase I the background also included a contribution of diffuse scattering increasing with angle as is usual for disordered systems. A backgound function was evaluated by linear interpolation between the values at points distant from the butane peaks and subtracted from the data before fitting.

Phase III

The unit cell of phase III obtained by ALLHKL is clearly not the same as that of the monoclinic structure yielded by the simulation. However when both are expressed in the $P2_1/n$ unit cell a similarity emerges. The dimensions of the experimental unit cell are a=7.17A, b=7.62A, c=4.11A, β=91.8° while those of the simulated cell are a=7.13A, b=7.6A, c=4.2A and γ=82.4° which implies that the molecular packing is similar, though not identical. The molecules of the real crystal must lie almost in the *ab* plane as they do in the simulated system since the *c* axis is so small in both cases. The difference is that in the real system the 2_1 screw axis is along the *c* direction rather than *b*, which means that the body centre molecules are rotated by 180° about *c* with respect to those at the origin of the unit cell. Refinement was started from an initial state with just this molecular orientation and convergence to a fit was rapid.

Table 4.1. *The refined structural parameters in phase III*

		5K	90K
Unit Cell	a(A)	4.110(1)	4.1463(6)
	b(A)	7.621(2)	7.629(1)
	c(A)	8.097(2)	8.169(1)
	β(°)	118.603(6)	118.656(4)
Volume (A^3)		222.7(2)	226.7(1)
Temperature factor (C)		0.4(6)	1.6(4)
Temperature factor (H)		1.1(3)	1.7(3)
Euler angles	ϕ(°)	-127.2(5)	-126.7(4)
	θ(°)	67.3(3)	67.1(3)
	ψ(°)	84.6(2)	84.4(2)
Bond angles	CCC(°)	111.0(7)	110.6(5)
	HCH(1)(°)	106.5(8)	107.1(6)
	HCH(2)(°)	107.5(6)	107.2(4)
Dihedral angle	χ(°)	-1.7(8)	-2.5(5)
C-H bond length(A)		1.087(7)	1.072(6)
R factor (%)(EDINP/ALLHKL)		4.3/3.8	3.6/2.9

The final values of the refined parameters for the 5K and 90K data are presented in table 4.1. The parameters refined were the overall scale, peak shape and flat background, unit cell, temperature factors for C and D atoms and the molecular structure parameters. The value of R obtained from the 5K fit was 4.3% compared with a best possible value from ALLHKL of 3.8%. For the 90K data the values were 3.6% and 2.9% respectively. The 5K structure is presented in fig 4.3 and the atomic co-ordinates in table 4.6.

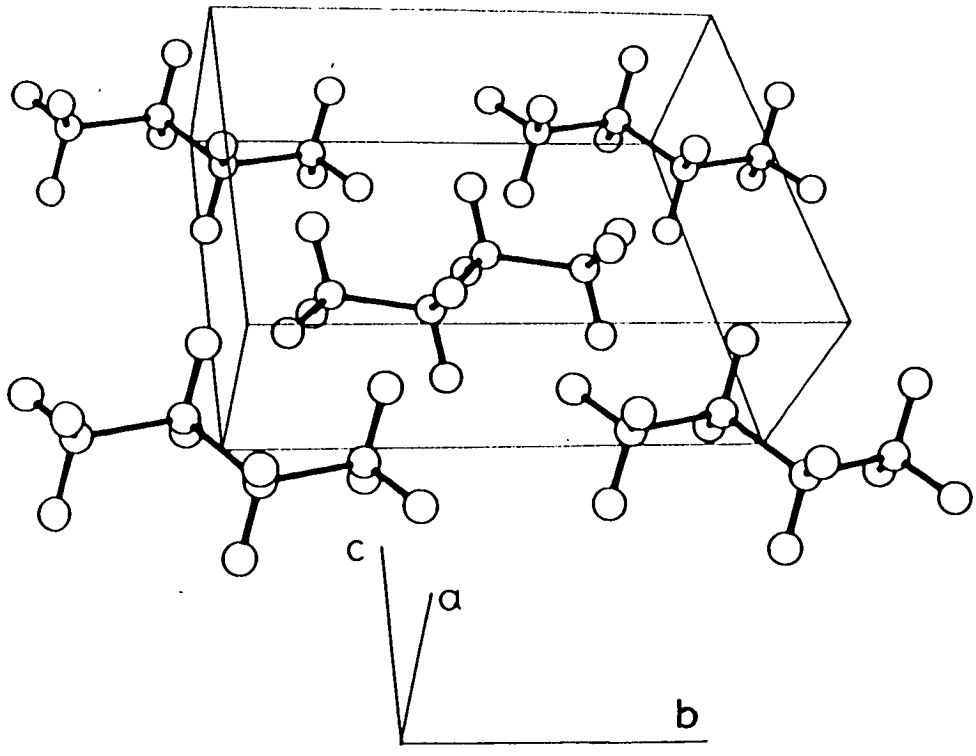

Figure 4.3. Structure of phase III at 5K.

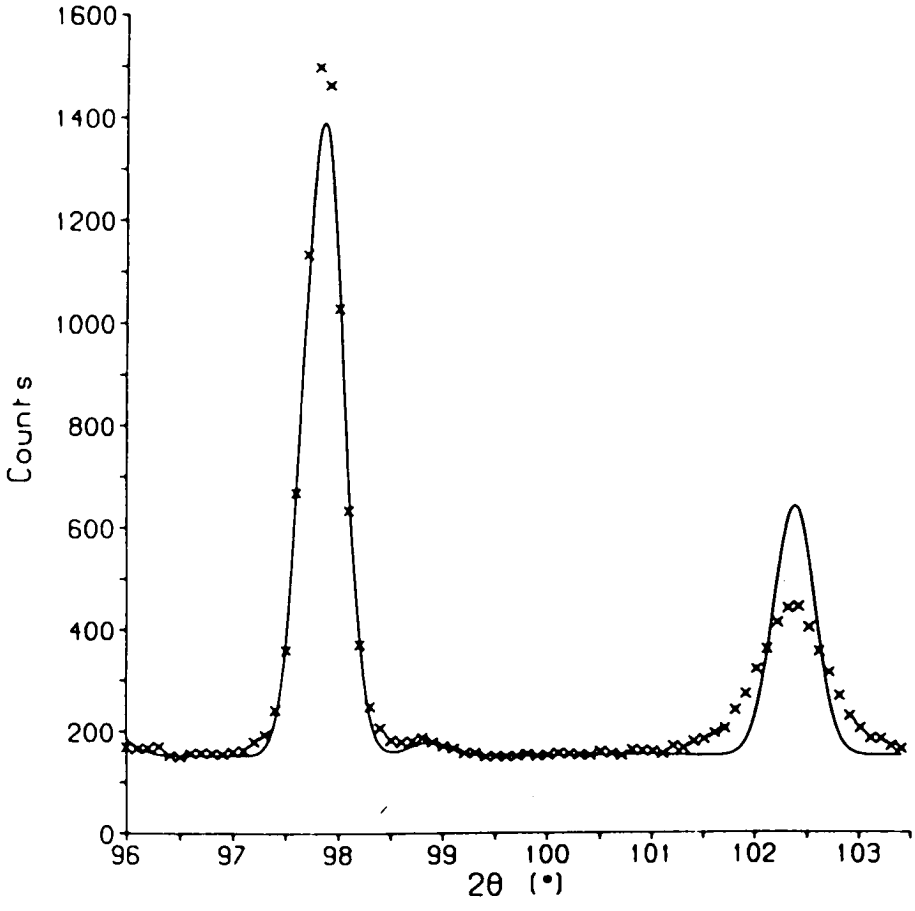

Figure 4.4. A section of the phase II data comparing the broadened 2 2 -1 peak with the 2 0 2. The crosses are the measured intensities and the continuous line is calculated from the final fit of table 4.2.

The starting structure used for the metastable phase refinement was that of 1,2-dichloroethane which was suggested by the similarity in unit cells and molecular structure. Initially all of the structural parameters were allowed to vary during refinement. The R factor decreased to 7.7% compared with 5.4% given by ALLHKL. This scan had the same number of points as the 90K data, consequently the final value of R should not be very different. Closer inspection revealed that the discrepancy was due to about ten peaks which were anomalously broad, and whose shape could not be fitted by the usual peak shape function. These were the 1 1 -1, 1 1 -2, 1 1 -3, 1 1 -4, 2 2 0, 2 2 -1, 2 2 -2, 2 2 -3, 0 1 2, 2 1 0 reflections and possibly also the 3 1 0. The amount of broadening varied from around 20% wider than nearby peaks at $2\theta=60°$ to 100% at 130°. A striking example of this is shown in fig 4.4 where the peak shape function fits the 2 0 2 reflection well the but the 2 2 -1 very poorly. A further fit was done with zero weight assigned to these peaks, except for the 1 1 -1, 2 1 0, 2 2 0 and 3 1 0 which were not sufficiently broad to cause a serious error. Twenty one peaks remained, which proved sufficient to

determine the structure. Using this reduced set the molecule shape parameters were not allowed to vary but were fixed at the values given by the 5K refinement, apart from the methyl group dihedral angle, χ which was thought likely to be structure dependent. Despite this constraint the R factor decreased to 4.2% (cf 3.6% ALLHKL) which is as good a fit as obtained from the 5K and 90K scans. The final values of the unit cell and molecular orientation parameters are given in table 4.2 and the structure in fig 4.5.

Table 4.2. *The refined structural parameters in phases II & I*

		65K (II)	120K (I)
Unit Cell	a(A)	5.708(1)	5.693(1)
	b(A)	5.174(1)	5.508(1)
	c(A)	7.870(2)	8.361(2)
	β(°)	105.98(1)	115.294(5)
Volume (A^3)		223.5(2)	237.0(2)
Temperature factor		1.8(2)	4.4(3)
Euler angles	ϕ(°)	83.4(5)	-144.8(2)
	θ(°)	36.0(4)	76.5(5)
	ψ(°)	-71.8(6)	139.4(2)
Bond angle	HCH(2)(°)	not refined	109.2(2)
Dihedral angle	χ(°)	-1.7(8)	not refined
Axis angle	Θ(°)	n/a	51.3(5)
R factor (%) (EDINP/ALLHKL)		4.2/3.6	3.0/2.7

On comparing the calculated scan with the observed, it was apparent that the anomalous peaks were not only broadened but were also smaller in such a way that the integrated scattering intensity agreed closely with the calculated value (see fig 4.4). This broadening is characteristic of anisotropic thermal diffuse scattering and it is tempting to speculate that it may be an effect of some process of reordering to the stable phase III, but unfortunately crystallographic structural studies can never be conclusive about dynamical phenomena.

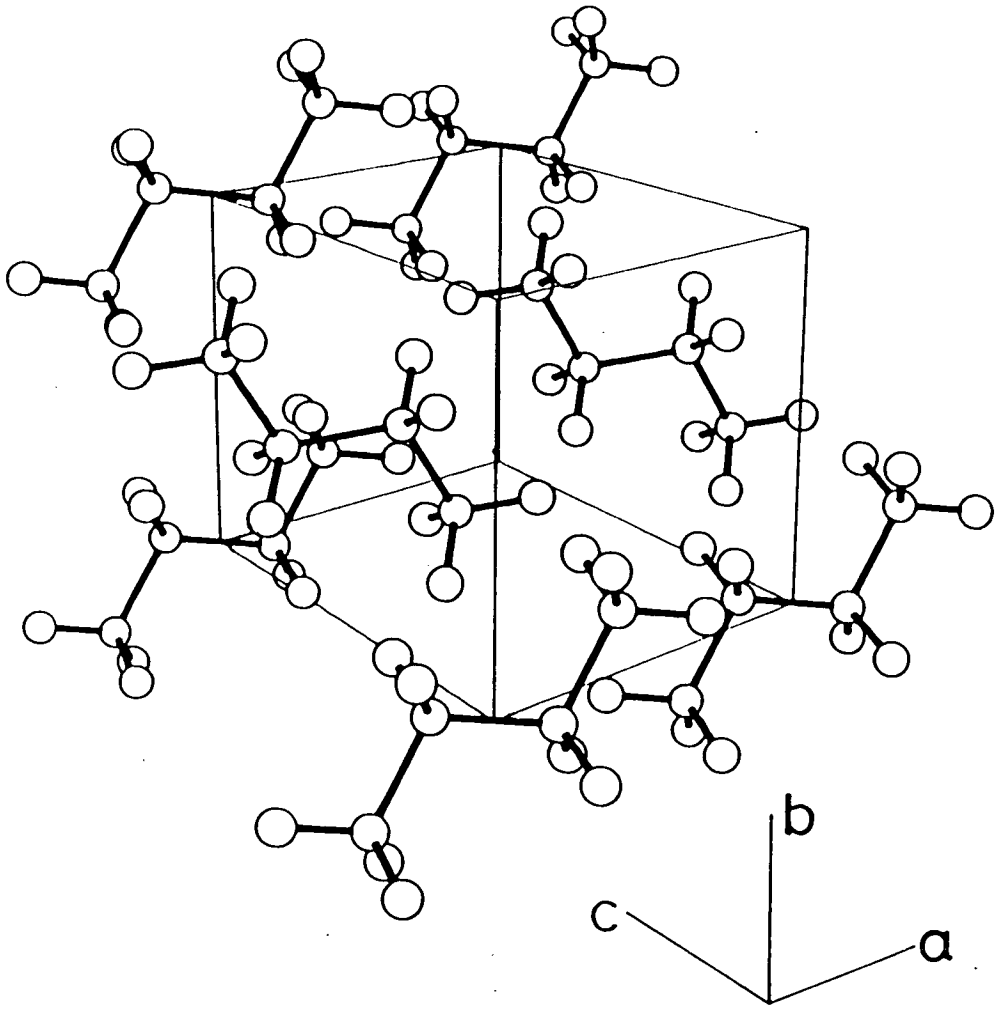

Figure 4.5. Structure of phase II at 65K.

Phase I

The scattering function may be written as the sum of two terms, a coherent (Bragg) term and a diffuse term. In a disordered crystal the second term is often large and only varies slowly with scattering angle. Diffuse scattering was observed as part of the background in phase I of butane and is shown in fig 4.8(d). This background was subtracted from the observed data before fitting and in what follows only Bragg scattering is considered.

The solution of the plastic phase structure involved a number of new features and required a less straightforward method than sufficed for the others. Whereas in the ordered phases the orientational probability distribution of the molecules is a δ function this is certainly not true in the phase I. There are two extreme possibilities to the nature of the disorder. The first is that the distribution is a sum of δ functions, that is the molecules jump between two or more discrete orientations.

The other is that a continuous function of the three quantities specifying the rotation is required. The NMR study of *n*-butane (Hoch, 1980) assumed the first possibility which gave good agreement with experiment and therefore the first refinements tried used this model. It proved easy to modify the EDINP program in order to permit a `multi-site' model in which several molecules were superimposed. The orientation and occupancy at each site could be refined. All the molecules were constrained to have the same centre of mass position, an assumption which disallowed combined rotation/translation jumps, and is justified *a posteriori* by the results obtained using the model.

At this point it is worth considering the limitations of the information in the scan. There are 28 resolved peaks, but the disorder leads to a very large effective temperature factor and hence to the absence of peaks of significant magnitude with 2θ greater than $120°$. Thus the Fourier component of shortest wavelength present is around 1.6A so disordered atom positions closer than some fraction of this, say $1.6/4 \simeq 0.4$A, can not be resolved. A model which has many occupied atomic sites closer than this can not be distinguished from a continuous distribution.

Because the data contained only 28 peaks, it was necessary to limit the number of parameters refined. Since the lower phase results are in agreement as to the molecular shape the values of the corresponding parameters were, with one exception mentioned later, taken from the 5K results. Each independent molecular site required 4 parameters in the refinement; three Euler angles for orientation plus a probability of occupancy. It will be shown that up to 5 partial molecules were needed to fit the data which required 20 parameters to be refined simultaneously. This number is clearly greater than the data can support and leads to the second major assumption of the model; that all the molecules are assumed to be related by a rotation about a single axis. This was suggested by the elongated shape of the molecule and by analogy with 1,2- dichloroethane. Refinements were done with 2 and 3 independent molecules, and the results were consistent with single axis rotation. The final R factors were similar to the `single axis' results. All the following results used a model of one dimensional rotation in which the axis for each molecule was further assumed to lie in the plane of its four carbon atoms. Each molecule therefore required only two additional parameters, giving 13 for five partial molecules. As before the assumptions are justified by the quality of the final fit.

Table 4.3. *Results of 'multi site' model fit of plastic phase data*

	Number of Molecules				
	1	2	3	4	5
R Factor (%)	7.4	5.4	4.5	3.4	3.1
B	11.6(10)	7.9(4)	7.0(4)	5.1(4)	4.4(3)
Euler Angles of molecule 0					
$\phi(^\circ)$	-146.4(6)	-141.2(7)	-144.6(5)	-144.8(2)	-145.3(2)
$\theta(^\circ)$	72(1)	64(1)	74(1)	79(1)	70(2)
$\psi(^\circ)$	141.1(5)	145.7(7)	139.9(5)	138.7(3)	141.3(5)
Axis angle, $\Theta(^\circ)$	-	53.9(14)	55.6(10)	51.3(5)	51.3(4)
Molecular Rotation Angles $\zeta(^\circ)$					
1	-	47(2)	-65(2)	-147(3)	-145(3)
2	-	-	54(1)	-43(2)	-50(3)
3	-	-	-	75(2)	40(4)
4	-	-	-	-	98(4)
Occupancies					
0	1	0.57(3)	0.57(2)	0.50(2)	0.49(2)
1	-	0.43	0.20(2)	0.13(1)	0.13(8)
2	-	-	0.23	0.21(1)	0.12(1)
3	-	-	-	0.16	0.15(2)
4	-	-	-	-	0.11

Trial orientations of the partial molecules for these refinements were obtained from those of phase II by a rotation of the molecule through ζ about the line joining the end carbon atoms. A range of ζ values was tried but only those which gave the best fits are reported. The final values of ζ and the occupancy probabilities are listed in table 4.3 along with the final R factors. The quality of fit increased with the number of molecules and the 'smearing' due to the temperature factor decreased as the disorder was taken into account by the multiple orientations. It is apparent that just one orientation was consistently present with an occupancy of about 0.5 in all cases. None of the occupancies approached zero and the molecules stayed distinct, a clear indication that the 1,2,3 and 4 orientation models were all inadequate. However the R factor of the 5 molecule fit at 3.1% was very close to the best fit value of 2.7%. These results appear to indicate that a discrete model with less than five orientations is not a good representation.

The discrete model is bound to be unsatisfactory in a system undergoing librational motion of large enough amplitude since the locus of atomic positions can not be described by an ellipsoid. This also imposes a limit on the amount of detail that can be determined due to the absence of high angle peaks in the scan. In this case the refinements will not produce well defined orientations, and the temperature factor will be inversely related to the number of molecules. It is apparent from these considerations that a continuous probability distribution is more realistic as well as physically revealing.

Such a distribution can be represented as a function of a single angle with a small number of adjustable parameters. The continuous function was replaced by one evaluated at 32 angles in the range 0 to 2π. In practise this meant refining the occupancies of 32 molecules related by a rotation axis in the plane of the molecule. The overall orientation was again specified by one set of Euler angles.

Refinements were done using two different functional forms,

$$\text{(a)} \qquad P(\zeta) = \Big(1 + \sum_{l=1}^{n} a_l \cos l\zeta \Big)/2\pi$$

and

$$\text{(b)} \qquad P(\zeta) = \Big(1 + ae^{-\zeta^2/\sigma^2} \Big)/N, \qquad N=2\pi+a\sigma\sqrt{(2\pi)}$$

The first is a general form which can represent any (even) function and the purpose of (b) was as a test on the significance of the results obtained using (a). The highest term in the sum, n, determines the level of detail in the fitted function and should be chosen to correspond to the limit of detail in the diffraction data. The component of smallest wavelength present is about 1.6A which corresponds to an arc of $2\pi/5$ for the outermost atoms. Thus a_5 should be the highest coefficient determined by the data.

Refinements were done with values of n ranging from 1 to 6. The coefficients obtained are listed in table 4.4 with the form $P(\zeta)$ plotted for certain n in fig 4.6(a). There is clear convergence as the R factor drops to a minimum of 2.98% compared with a statistical best from ALLHKL of 2.7%. The effect of the limited resolution is manifest in the estimated standard deviations associated with the coefficients, which increase from 9% for l=4 through 48% for l=5 to 97% for l=6. An attempt to include l=7 resulted in a large coefficient, 0.9(8), which gave a form for $P(\zeta)$ with negative values, which is clearly unphysical.

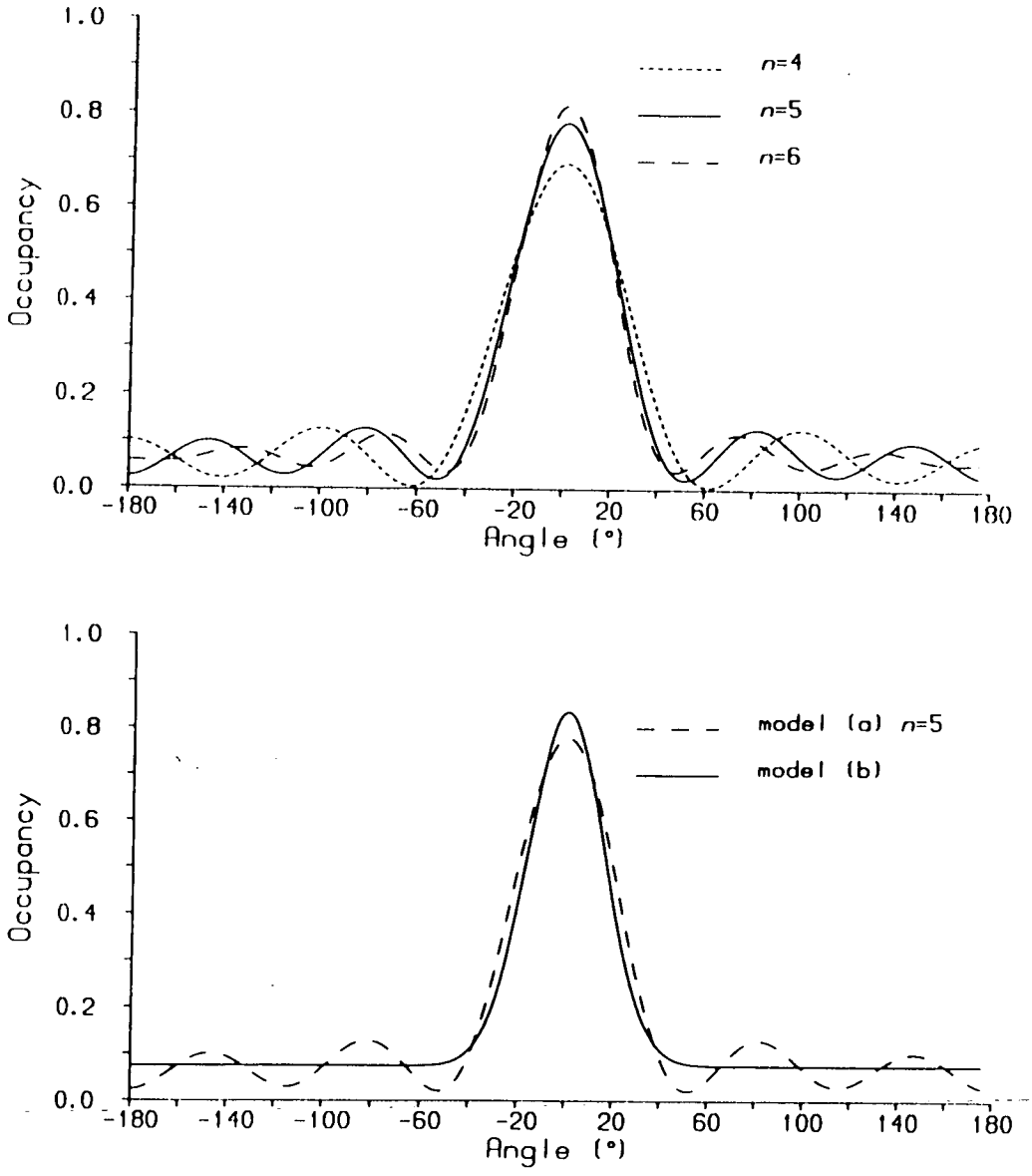

Figure 4.6. Orientational probability distribution, P(ζ). (a) Model a. with n=4, n=5, n=6. (b) Model a. with n=5 and model b.

Table 4.4. *Coefficients of* cos$l\zeta$ *in plastic phase refinement*

n	R Factor (%)	a_1	a_2	a_3	a_4	a_5	a_6
1	5.75	0.240(15)					
2	4.66	0.232(09)	0.127(12)				
3	3.75	0.180(07)	0.141(09)	0.131(11)			
4	3.05	0.175(05)	0.143(07)	0.121(08)	0.095(09)		
5	2.99	0.175(05)	0.145(07)	0.123(08)	0.098(09)	0.079(39)	
6	2.98	0.175(05)	0.146(07)	0.124(08)	0.096(09)	0.081(39)	0.035(34)

These results are consistent with the multi-site model which inspired them. The Euler angles of the $\zeta=0$ molecule (table 2) are close to those of molecule 0 in table 4.3 and the peak in the distribution function at $\zeta=0$ corresponds to the site with

the greatest occupancy.

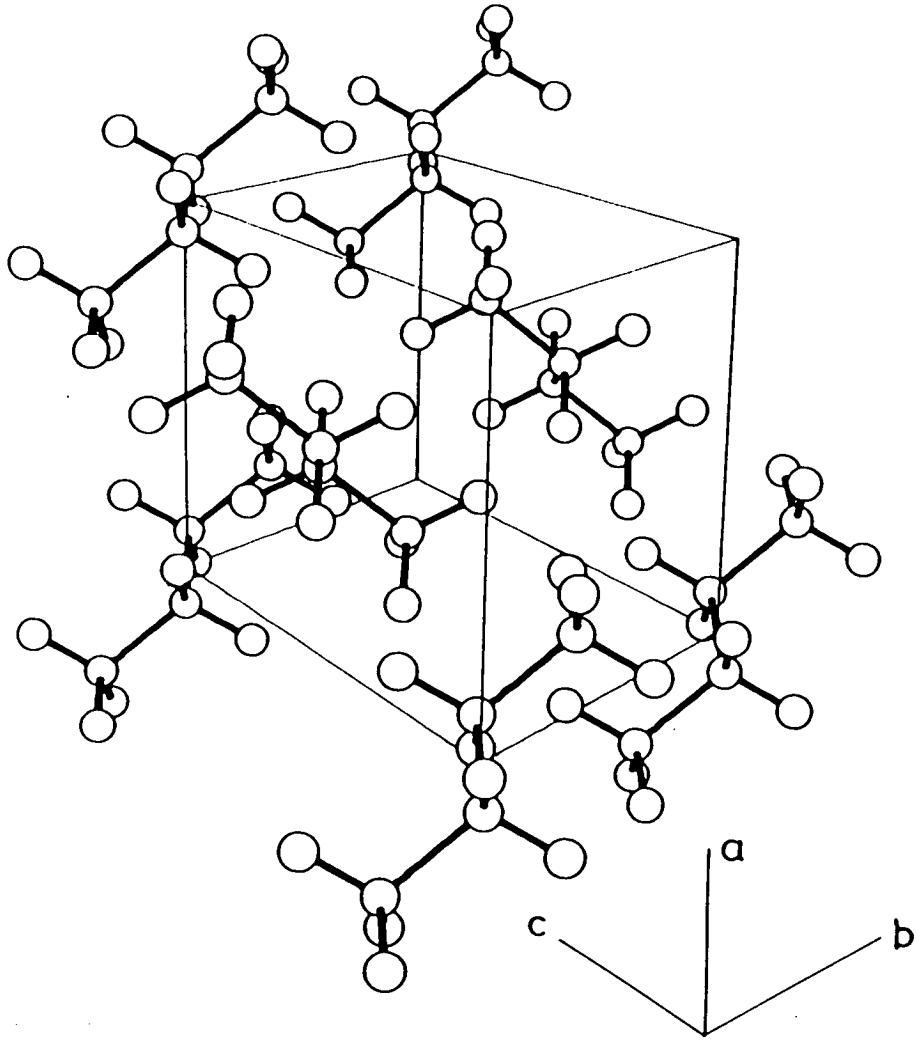

Figure 4.7. Structure of phase I at 120K. All molecules shown are in the $\zeta = 0$ orientation.

In order to try to fit the main features of the distribution with fewer parameters, the functional form (b) was tried. The R factor decreased to 3.00%, which is not significantly different from that given by the n=5 fit of (a). The essential features of $P(\zeta)$ were very similar, a broad central peak with significant occupancy at large angles (see fig 4.6(b)). The final values of the parameters a and σ were 10.3(3) and 16.0(6)° respectively.

The final values of the parameters obtained with form (a) using n=5 are listed in table 4.2. None of the n=4,5,6, or form (b) fits gave significantly different results. Fig 4.7 shows the structure with all the molecules at the ζ=0 orientation. It should be noted that in order to obtain a good fit it was found necessary that the HCH angle of the methyl groups was allowed to vary during all these refinements. The final value is 1.7° greater than given by the 5K fit.

The observed and difference (observed minus calculated) scans and the subtracted background function are plotted in fig 4.8.

It will be observed that the statisical errors in the unit cell parameters are around 5 times smaller than the uncertainty in the neutron wavelength. Therefore there will be a small systematic error (< 0.001) in all the lengths from the latter.

Table 4.5. *Peak shape parameters from all refinements*

	5K(III)	90K(III)	65K(II)	120K(I)
Overall scale	0.201(6)	0.185(4)	0.195(4)	0.0072(1)
Flat background	128(2)	150(1)	151(2)	150.2(7)
Scan zero angle (°)	-0.07(3)	-0.07(2)	-0.05(3)	-0.07(2)
u	0.32(5)	0.22(2)	0.29(3)	0.20(3)
v	-0.51(8)	-0.51(4)	-0.56(6)	-0.49(6)
w	0.43(4)	0.42(2)	0.46(3)	0.42(3)
Asymmetry, P	0.20(6)	0.19(4)	0.13(7)	0.18(4)

§4.4 Discussion

Refinement of phase III yields the molecular dimensions in addition to the crystal structure. The apparent C-H bond length is smaller by 1.5% at 90K than at 5K. This shortening is caused by the `swing arm' effect of rigid body molecular librations, whereby the arc which is the locus of the deuterium position has a centroid closer to the carbon than the true bond length. The magnitude of this effect is probably sufficient to account for the discrepancy between this result, 1.087(7)A, and the values obtained by electron diffraction (Kuchitsu, 1961; Bonham & Bartell 1959) of 1.100(3)A and 1.108(5)A. Since the thermal motion has a much smaller amplitude at 5K than at 90K, the low temperature values of the molecular dimensions are correspondingly more reliable. It is notable that the angle CCC, 111.0(7)°, differs slightly from that obtained in the gas phase, 112.15(15)°, and that χ, the methyl group dihedral angle is non-zero in both low temperature phases. These phenomena can be accounted for by the Van der Waals forces experienced by a molecule in the crystalline environment.

Forms II and I have a very similar unit cell and molecular packing. In both cases the longest dimension of the molecule, the line passing through the outermost carbon atoms, is at almost 90° to that of the symmetry related molecule. This is in contrast to phase III where they are nearly parallel. It is also the same axis about which the molecules disorder in phase I to within 4°. Furthermore the orientation in phase II is very close to that of a molecule orientated at ζ=-105° in phase I. It is clear, therefore, that the transition II -> I is associated with a disordering about this axis. No such simple relationship is apparent between phases III and I and therefore the transition must be reconstructive in character. This is consistent with the observation of Aston and Messerley (1940) that the transition took eight hours to complete after the addition of energy at the transition temperature.

Table 4.6. *Orthogonal atomic co-ordinates in all phases. The other 7 atoms are generated by inversion and the second molecule by the crystal symmetry. Units are A.*

(a) Phase III at 5K

	x	y	z
C	0.1919	0.4856	-0.5652
C	-0.1112	1.9416	-0.1692
H	1.2484	0.3799	-0.7987
H	-0.3520	0.2296	-1.4710
H	0.1851	2.6351	-0.9522
H	-1.1724	2.0897	0.0142
H	0.4196	2.2247	0.7362

(b) Phase III at 90K

	x	y	z
C	0.1943	0.4811	-0.5682
C	-0.1150	1.9366	-0.1751
H	1.2382	0.3793	-0.7881
H	-0.3427	0.2247	-1.4595
H	0.1884	2.6249	-0.9385
H	-1.1631	2.0870	-0.0103
H	0.3918	2.2185	0.7261

(c) Phase II at 65K

	x	y	z
C	0.6147	-0.1091	0.4498
C	1.3748	1.2098	0.6760
H	0.3028	-0.5228	1.4054
H	1.2768	-0.8426	-0.0031
H	2.2276	1.0677	1.3350
H	1.7491	1.6169	-0.2598
H	0.7349	1.9635	1.1276

(d) Phase I at 120K, ζ=0 orientation

	x	y	z
C	0.5448	0.3312	-0.4308
C	1.3854	1.3144	0.4029
H	1.1890	-0.4317	-0.8605
H	0.0864	0.8547	-1.2659
H	2.1474	1.7697	-0.2245
H	0.7445	2.0929	0.8088
H	1.8661	0.7844	1.2212

The results of the refinements of the phase I data must be interpreted with care, giving due weight to information provided by the different models fitted. It may be concluded that:

1) A continuous orientational probability distribution with a general form fits the data as well as the statistics allow. Both calculation and the results of refinement show that $\cos 5\zeta$ is the highest component determined by the data. To establish that the disorder is between discrete sites the number of partial molecules would have to be less than the resolution limit of the data. Since the quality of fit continues to improve beyond this limit such a form is not justified for butane.

2) The detailed form of the distribution $P(\zeta)$ is not well established since there is a negligible difference in the final R factors obtained using significantly different models.

In these models a number of assumptions are made, namely:

1) that all the molecules have the *trans* conformation. This is established by Raman and IR spectroscopic work which shows the existence of a

centrosymmetric structure.

2) that combined rotation/translation jumps do not occur (c.f. $C_{33}H_{68}$). Such jumps are unlikely because of the close packing of molecules in this phase.

3) that the molecules rotate about one axis which lies in the plane of the four C atoms. Refinement of a discrete model with three independent orientations tends to confirm this.

4) that $P(\zeta)$ is an even function. This is simply an expedient to reduce the number of refined parameters so as not to exceed the information content of the data.

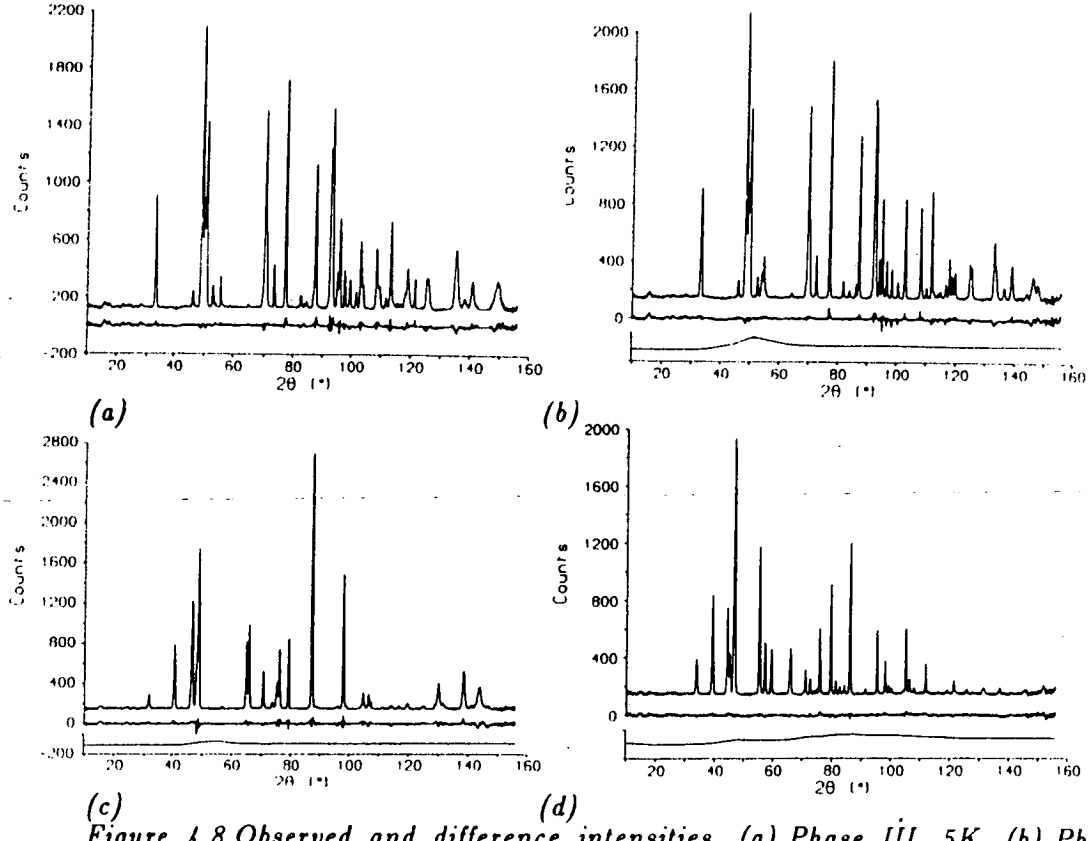

Figure 4.8.Observed and difference intensities. (a) Phase III, 5K. (b) Phase III, 90K. (c) Phase II, 65K. (d) Phase I, 120K, model a. using n=5. The extra curve in (b), (c) and (d) is the background which was subtracted from the observed data. Nitrogen peaks in (a) and the broadened peaks which were not fitted in (c) are not shown.

The refinement is shown to be very sensitive to the deuterium atom mean positions, since the R factor becomes very much worse given a small change in any bond length or angle, especially the methyl group HCH angle. The apparent increase of this angle in phase I can not be accounted for merely by the 'swing arm' effect, which would tend to make the angle appear smaller. It is probably associated

with the complex atomic motion produced by the disorder which is not adequately described by the assumption of isotropic thermal vibration. The sensitivity to atom positions would appear to confirm assumptions 1-3.

On the other hand the almost equally good fits given by model (a) with n=4,5,6 and model (b) show an insensitivity to the detailed form of $P(\zeta)$. It is unlikely, therefore, that assumption 4 is adequately tested. In view of the large error associated with a_6, model (a) with n=5 is clearly the best form of $P(\zeta)$ that the data supports. However it is not possible to assert conclusively that it is correct in detail. All these distributions have certain features in common, the height and width of the central peak and the average occupancy at high angles. These may therefore be accepted with more confidence.

These results show that in phase I the molecules are disordered predominantly around a single axis, which is as found by Hoch (1975). However they are clearly at variance with Hoch's proposed model of 180° reorientations. As NMR measures only one quantity, the proton second moment, it cannot provide sufficient information to distinguish between several models, including that presented here which could equally well account for Hoch's data.

The nature of the disorder in n-butane is clearly different from that of the longer n-paraffins. The latter usually have orthorhombic or hexagonal structures (Ungar 1983) with the rotation axis along a crystal symmetry direction. In contrast the axis in n-butane does not have a unique direction in space but only with respect to the molecule. Indeed the axes of any molecule and its symmetry related neighbour are at nearly 90° to each other. Substances like SF_6 and CBr_4 have plastic phases in which the molecules re-orient between equivalent directions. The butane molecule has no such symmetry equivalents, neither does the disorder introduce a higher mean structural symmetry.

It is interesting however to note the similarities between the structures of n-butane and 1,2-dichloroethane since the molecules of both are of a similar shape. The unit cell, space group and packing of butane in phase II are very close to those of dichloroethane in its only low temperature state, and the orientationally disordered phases are similarly alike (Reed & Lipscomb 1953, Milberg & Lipscomb 1951). Butane, however, has an additional stable phase III. It is the transition from phase III to phase I which causes butane to have a discontinuity in its specific heat and hence a true phase transition, whereas dichloroethane does not.

Finally we note that neither the low temperature monoclinic nor the disordered orthorhombic structures produced by the simulation are those of the corresponding phases of the real system. It may be either that the model molecule or potentials are inaccurate, or as suspected that potential barriers are too high to allow the true structures of the model to be found. This topic will be further explored in the final chapter.

Chapter 5

Simulation of the Three Phases of Butane

§5.1 Preamble

In the previous four chapters a molecular dynamics simulation of a system of *n*-butane molecules was set up. Early results showed that the model undergoes a phase transition from an ordered structure at low temperature to a disordered structure at approximately the same temperature as the real system. However neither of the structures obtained exists in the real system and it remains to explain why the experimental structures were not found. There are two possible reasons for this.

It is clear that the irregular shape of the butane molecule causes enormous potential barriers to the reorganisation of the interlocking molecules. It is therefore quite possible that annealing to the experimental low temperature structure is inhibited by non-ergodic behaviour. The simulated and experimental monoclinic structures are related by a rotation of one of the molecules in the unit cell by 180° about the longest axis and it is between these two orientations that the molecules in the simulation disorder at high temperatures to form the orthorhombic structure of chapter 3. The inability of the simulation to reform an ordered structure on cooling this phase is strong evidence that the potential barriers to rotation are too high to allow such an annealing transition to take place.

On the other hand it might be that the model, either the potential functions or the molecular geometry, does not properly describe the real system. Given a knowledge of the true structures it is possible to test this hypothesis by comparing the internal energies of the low temperature structures. Unfortunately the free energy, necessary to discriminate between the high temperature structures, can not be calculated as the entropy is not easily evaluated from a MD simulation.

For the following runs a change was made to the model. Previously the methyl groups were free to rotate, but for the remaining runs the more realistic potential of equation (2.33) was applied. This gives a frequency for the symmetric methyl torsion, the fastest internal mode, of around 6THz. It is clearly not possible by the criterion of § 2.1.1 to simulate this motion using a timestep of 0.02ps and indeed it was found that the total energy of the system was no longer conserved and that equipartition of energy between the translational and internal/rotational modes was

not achieved. The timestep was therefore decreased to 0.005ps for all of the runs described in this chapter.

What follows is an attempt to simulate the structure of all three phases of *n*-butane. Some possible reasons why these structures were not found in the previous simulation runs will be proposed and tested, but the main area of interest is that outlined in chapter 1, the study of the orientationally disordered phase. A mechanism for the transition from phase II to phase I was postulated in chapter 4, and it is hoped to check this by reproducing the transition in the simulation. If, as will be shown, phase I can indeed be simulated, the dimensionality of the disorder can be studied and an orientational distribution function calculated to compare with the experimental ODF. An analysis of the dynamics of the disordered phase can then proceed by the study of correlation functions and by other techniques.

§5.2 Phases III and II

A configuration corresponding to the experimental structure of phase III was set up and the simulation was run from this with the temperature scaled to 25K. After a period of equilibration without rescaling the structure was examined to see if any change had taken place. The dimensions of the unit cell and the molecular orientations are compared with those of the experimental structure in table 5.1. Although the unit cell lengths had changed slightly the symmetry and molecular packing were unchanged. Thus the essential features of the experimental structure of phase I had been reproduced in the simulation.

Table 5.1. A comparison of the unit cells and molecular orientations of the MD and experimental structures of the two low temperature phases. ε is the angle needed to rotate a molecule in the MD orientation to the experimental one.

	Phase III		*Phase II*	
	MD	*Experimental*	*MD*	*Experimental*
a	4.40(3)	4.110(1)	5.75(9)	5.708(1)
b	7.53(10)	7.621(2)	5.23(3)	5.174(1)
c	8.14(6)	8.097(2)	8.18(8)	7.870(2)
β	120.8(3)	118.603(6)	106.8(10)	105.98(1)
q_1	0.9200	0.9222	0.6557	0.6519
q_2	-0.1384	-0.1115	0.4920	0.4879
q_3	-0.2068	-0.1870	0.4090	0.4242
q_4	0.3028	0.3195	0.4070	0.3900
ε		4.3°		2.6 °

The unit cell dimensions quoted in tables 5.1 and 5.5 were obtained from the simulation by taking an average of the components of the **h** matrix over many timesteps and calculating *a*,*b*,*c* and β from that. Such a procedure is simple to implement but does not yield exactly the same quantities as measured by an experiment. The unit cell dimensions are correctly defined to be the vectors joining the mean positions of the molecular centres of mass rather than the means of the instantaneous vectors (the columns of **h**). There is therefore a systematic error in the result which must, however be smaller than the fluctuations of **h**. A correct calculation of the unit cell dimensions would be a very large computation as it would require the accumulation of a separate average position for each molecule in the simulation. However the exact dimensions of the MD unit cell are not of great interest, neither is it likely on the basis of such a simple model that they will be closer to the experimental values than a few percent. Indeed the values calculated from the simulation differ by up to 5 standard deviations from the experimental values. While these differences are not large in real terms, usually of the order of

1%, they are greater than any systematic error which might arise from the averaging scheme. It is not therefore necessary to do a more accurate calculation and the simple method is quite adequate.

In order to assess the relative stabilities of this structure and the one obtained from the simulation of chapter 3 (which will be henceforth referred to as IV) a comparison of the internal energies was made. This is shown in table 5.2. Phase IV is the more stable of the two, as its energy is lower by 1%, which shows that it did not arise simply from the non-ergodic behaviour, but because it is the most stable structure of the model. It is clear that the model must differ from nature in some small ways since the experimental phase III structure was not exactly at the minimum of the potential energy hypersurface. The difference gives a shift in energy sufficient to alter the balance between phases III and IV.

The main features of the model are the potential functions used, the cut-off radius of the interactions and the molecular shape. All the previous runs used a 6-exp potential with set IV of Williams' parameters (Williams, 1967), however he later developed a more realistic potential which included electric charges (Williams & Starr, 1977) and this is described in §2.2.1 and table 2.3. The new set was implemented and the simulation was run for sufficient time to re-evaluate the internal energies of the two phases. The calculations were done both with the limited list of 14 neighbour molecules and a more extended one with 30 neighbours, and the results are shown in table 5.2. In all cases the experimental phase III has a higher energy than the 'wrong' phase IV, including runs with the extended neighbour list, so the energy shift is not an artefact of the cut-off. Neither is it likely to be due to the potentials since two very different potential functions gave the same result.

Table 5.2. Potential energies of phase III and phase IV (the 'wrong' monoclinic structure of chapter 3) calculated using three different potentials, (1) Williams set IV (1967), (2) set II (1977) with 14 neighbours and (3) set II using 30 neighbours. All are in units of 10^{-16} J.

Potential	Phase III	Phase IV
(1)	-0.969(4)	-0.981(2)
(2)	-1.288(9)	-1.297(14)
(3)	-1.366(3)	-1.374(6)

An alternative possibility is that the shape of the molecule, that is the positions of the masses and interaction centres is sufficiently different from that of real butane to alter the balance between the energies of both phases. It was noted in §2.2.4 that the CCC angle in the model is 1.5° smaller than in the real system and that

the positions of the methyl group hydrogen atoms are therefore in error by up to 0.06A. The discrepancy is small, but the energy difference between the two structures is also small. It is possible that this small difference in angle is responsible for the difference in energies observed. It would be useful to test this hypothesis by modifying the simulation to use the experimental CCC angle, which may be undertaken at some time in the future.

The simulation of the metastable phase II involved the construction of a new list of interacting neighbour molecules because the neighbour list of fig 2.1, if used with the unit cell dimensions of phase II, would give an unacceptably anisotropic interaction cut off. The new neighbour list of table 5.3 was designed to have a minimum cut off of over 7.5A and to support two molecules in the unit cell. For the phase II runs only the first 11 entries were used, so that 22 molecules were included. On starting the simulation from a configuration representative of the experimental structure, the internal energy was highly negative and during a run with the temperature rescaled to 25K, equilibration was rapid. Following a 30ps run with no rescaling when no sign of a structural change was observed the temperature was rescaled to 65K in order to compare the structure with the experimental results measured at that temperature. A comparison of the unit cells and molecular orientation quaternions is presented in table 5.1 and considering the simplicity of the model the similarity is remarkable. The symmetry of the experimental structure is preserved (the angles α and γ are both 90° to within 2 standard deviations). The lengths of the unit cell vectors are within 1-4% of the experimental values although the differences are larger than the uncertainty in the MD values. The molecular orientations are also remarkably similar, as a rotation of only 2.6° will transform one into the other.

Table 5.3. The list of interacting neighbour molecules used for the phase II and phase I simulations.

i	*j*	*k*	*shift*
0	1	0	18
0	0	1	176
1	1	0	20
0	1	1	194
0	-1	1	158
-0.5	-1	0.5	69
0.5	-1	0.5	71
-0.5	0	0.5	87
0.5	0	0.5	89
-0.5	1	0.5	105
0.5	1	0.5	107
1	1	1	196
-1	-1	1	156

§5.3 Analysis of Single Axis Disorder

It has been established by NMR and by the neutron diffraction experiment that in the plastic phase, *n*-butane molecules are disordered about a single axis. A form for the orientation distribution function, $P(\zeta)$ was obtained in chapter 4. It is desirable to be able to establish from the simulation results whether the disorder is one-dimensional in nature and to calculate an ODF. This is not a trivial matter since there will be thermal displacements and librations about all axes in a system at finite temperature and it is therefore necessary to determine whether rotation about one axis is predominant. A method to do this should satisfy three objectives.

1. To characterise the motion and to supply a criterion of whether a single-axis model is valid.
2. If so to find the axis.
3. To calculate the distribution of molecular rotation about that axis while ignoring other motion.

It is first necessary to define a reference orientation and to re-express all molecular orientations with respect to it. The choice of reference is not arbitrary if single-axis rotation is present. If a number of molecules are all related to each other by single-axis rotation then only a reference related to all of them by rotation about the same axis will reveal the nature of the disorder. The method adopted for selecting a reference was to look for a sharp peak where many molecules are found within a narrow range of orientations and to calculate an average quaternion over this small range. The new description of the orientation with respect to the reference is just the quaternion product of the original quaternion and the conjugate to the reference. The triviality of this calculation again shows the superiority of the quaternion description over Euler angles.

If $\mathbf{q}_i=(\cos\alpha_i/2,\ \boldsymbol{l}_i\sin\alpha_i/2)$ denotes the quaternion which expresses the orientation of molecule i with respect to the reference then $\boldsymbol{l}_i$ is the axis about which the rotation by angle α is performed. Let $\boldsymbol{d}_i=\boldsymbol{l}_i\sin\alpha_i/2$ and consider the matrix

$$M = \sum_{i=1}^{N} \begin{pmatrix} \boldsymbol{d}_i^2-d_{ix}^2 & -d_{ix}d_{iy} & -d_{ix}d_{iz} \\ -d_{ix}d_{iy} & \boldsymbol{d}_i^2-d_{iy}^2 & -d_{iy}d_{iz} \\ -d_{ix}d_{iz} & -d_{iy}d_{iz} & \boldsymbol{d}_i^2-d_{iz}^2 \end{pmatrix} \tag{5.1}$$

where the sum is over all molecules. It is symmetric and positive definite and by analogy with the inertia tensor with which it is isomorphic it can be diagonalised by an orthogonal transformation. This takes the form

$$D = R^{-1}MR \tag{5.2}$$

where D is diagonal and R is an orthogonal rotation matrix. Equation (5.2) may be

thought of as a principal axis transformation by analogy with that pertaining to the inertia tensor. The eigenvectors of M which are the columns of R are the principal axes and the eigenvalues, $\lambda_1^2,..,\lambda_3^2$, the diagonal elements of D, are a measure of the degree of disorder about the corresponding axis.

The interpretation of the values of the λ's will be most evident from a consideration of the extreme cases. For isotropic disorder $<d_{ix}^2>=<d_{iy}^2>=<d_{iz}^2>$ and so the eigenvalues are all equal and $\lambda_1=\lambda_2=\lambda_3$. If on the other hand the rotation is purely about the z axis then $<d_{ix}^2>=<d_{iy}^2>=0$, $\lambda_1=\lambda_2$ and $\lambda_3=0$. This is also true of the more general case of disorder about any axis since under the transformation (5.2) the disorder axis is rotated into the direction of one of the cartesian axes which may be chosen to be z. In the real case, predominantly single-axis rotation is superimposed on smaller amplitude libration around all axes. Then the eigenvector which corresponds to the smallest eigenvalue is the principal rotation axis and the ratio of the λ's is a measure of the dimensionality of the disorder.

The formalism may be visualised by means of the ellipsoid defined by the equation $\mathbf{r}.M.\mathbf{r}=1$. The directions of the principal semi-axes are given by the eigenvectors of M and the lengths are just the reciprocals of the λ's. In the isotropic case the λ's are equal and the ellipsoid is a sphere whereas predominantly one-dimensional disorder will give a prolate spheroid becoming increasingly elongated as perfect single-axis disorder is approached.

This analysis satisfies the first two objectives above since it provides a criterion for determining the extent and nature of the disorder and can find the axis in the case of one-dimensional disorder. It therefore remains to calculate the 'component' of the molecular rotation about that axis while disregarding rotation which is not. Let the quaternion describing the individual rotations of the molecules under consideration be $\mathbf{q}_i=(\delta_i,\boldsymbol{d}_i)$ and express this as a product

$$\mathbf{q}_i = \mathbf{q}_{\uparrow}\mathbf{q}_{\rightarrow}. \tag{5.4}$$

If $\mathbf{q}_{\uparrow}$ is a rotation about the disorder axis $\boldsymbol{\Delta}$ by an angle ζ_i and $\mathbf{q}_{\rightarrow}$ represents a rotation perpendicular to $\boldsymbol{\Delta}$ then in some sense ζ_i is the single-axis 'component' of the rotation. Let $c_i=\cos\zeta_i/2$ and $s_i=\sin\zeta_i/2$ so that $\mathbf{q}_{\uparrow}=(c_i,s_i\boldsymbol{\Delta})$. The rotation perpendicular to $\boldsymbol{\Delta}$ may be expressed as $\mathbf{q}_{\rightarrow}=(\mathbf{r}_i.\boldsymbol{\Delta},\mathbf{r}_i\times\boldsymbol{\Delta})$ for some unit vector $\mathbf{r}_i$. The quaternion $\mathbf{q}_i$ may then be re-expressed from (5.4) as

$$\mathbf{q}_i = (c_i\mathbf{r}_i.\boldsymbol{\Delta},\ c_i\boldsymbol{\Delta}\times\mathbf{r}_i+s_i\mathbf{r}_i) \tag{5.5}$$

The required angle of rotation, ζ_i is extracted by taking the dot product of the axis

Δ with $\boldsymbol{d}_i$, the imaginary prime of $\mathbf{q}_i$.

$$\Delta.\boldsymbol{d}_i = c_i\Delta.(\Delta\times\mathbf{r}_i) + s_i\Delta.\mathbf{r}_i = s_i\Delta.\mathbf{r}_i$$

so that

$$\zeta_i = 2\tan^{-1}\left((s_i\Delta.\mathbf{r}_i)/\ (c_i\Delta.\mathbf{r}_i)\right) = 2\tan^{-1}\left((\Delta.\boldsymbol{d}_i)/\delta_i\right) \qquad (5.6)$$

is now expressed entirely in terms of known quantities, the rotation axis and the components of $\mathbf{q}_i$.

The validity of this calculation depends on $\mathbf{q}_\rightarrow$ being a "small" rotation, a condition which is satisfied if the rotation ellipsoid is sufficiently prolate.

The above method was used to calculate fig 3.8 which shows the distribution of ζ_i over the 2048 molecules of a single configuration of the orthorhombic disordered phase. The eigenvalues of M were 1043, 1056 and 35, so that the ellipsoid was a prolate spheroid with a major semi-axis approximately 5.5 times as long as the minor semi-axis. It is thus demonstrated that the disorder of that phase is indeed one dimensional in nature. The rotation axis Δ is very close to the y-axis at (0,0.9999,0.0125) which gives rise to the extra two-fold symmetry.

The vectors $\boldsymbol{d}_i$ used to construct M in (5.1) are the axes of the individual rotations weighted by the sine of half the angle. This is not the only choice and other weighting schemes are possible. Equation (5.1) gives greater weight to large angle rotations which means that the eigenvalues include information on the width of the distribution about the axis as well as the distribution of axes. It is computationally convenient as the vector $\boldsymbol{d}_i$ is just the imaginary prime of the quaternion $\mathbf{q}_i$. On the other hand M could be constructed from the $\boldsymbol{l}_i$'s instead of the $\boldsymbol{d}_i$'s. Such an unweighted scheme has the advantage that the eigenvalues for any set of quaternions are independent of the reference orientation (provided it is on-axis) which is not true in the weighted case. These points should be viewed in the perspective that they only affect the magnitudes of the eigenvalues. The weighting scheme has little effect on the eigenvectors or on the distribution function.

§5.4 The Transition to the Plastic Phase

Instead of setting up a configuration of the plastic phase as was done for phases II and III it was decided to adopt a more ambitious approach and to attempt to simulate a transition to phase I. This might be done by 'heating' the simulated phase III to above the transition temperature. However a careful consideration reveals a serious difficulty. It was found in chapter 4 that the main difference between the true phase III and the monoclinic structure arrived at in chapter 3 is a rotation of half the molecules by 180° about the long axis. On heating the latter structure the molecules just disordered between these two sites to form the orthorhombic disordered structure. It is therefore probable that exactly the same disordered structure would result from heating phase III as the simulated monoclinic structure. This would not contribute any useful result. It is much more likely that a transition to phase I would take place on heating a sample of phase II since the molecular packing and unit cell of phases II is much closer to phase I than that of either phase III or phase IV.

The simulation was therefore run with a configuration of phase II as the initial state for a total of 36000 timesteps of 0.005ps, which corresponds to 180ps of simulated time. The temperature was adjusted by repeatedly rescaling the velocities for several timesteps until the required temperature was reached, when the rescaling was switched off. Four adjustments of the temperature were performed during this run, an initial increase from 65K to 125K and three further times to around 150K. The repeated increases were necessary because the temperature fell during the run while the transition was taking place.

One difference between phases II and I is the unit cell angle β which is 9° larger in phase I than II. It was decided to monitor the progress of the transition by using the instantaneous average of β over the sample. This is trivially obtained from the $\mathbf{h}$ matrix of the zero-stress method (see §2.1.5). It was realised 67ps into the run that any increase in β would make the interaction cut-off less isotropic and the interaction with the (1,1,1) and (-1,-1,1) neighbours would become more important. These were therefore added to the interacting neighbour list of table 5.2 bringing the number of molecules to 26.

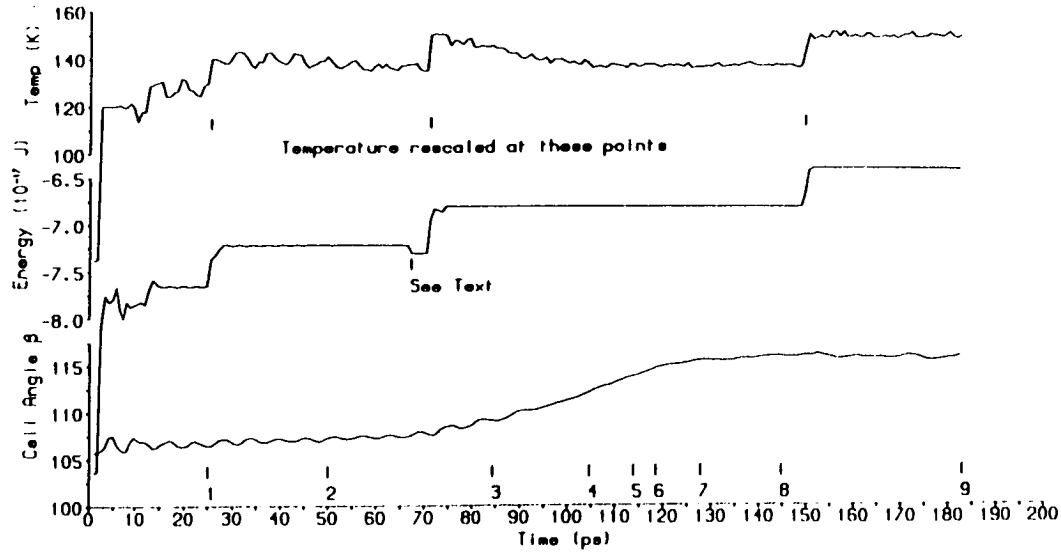

Figure 5.1 Temperature, energy and β throughout the plastic phase run.

The values of the temperature, internal energy and β throughout the run are plotted in fig 5.1. There was a gradual increase of β from 106° which eventually levelled off at slightly over 115°, just the value expected for phase I. This is a good sign that the transition to phase I had indeed been reproduced and is confirmed by analysis of the disorder. Several times during the run the orientation of each molecule in the configuration was stored and later analysed by the method of §5.3 using as a reference orientation that of a molecule in phase II. This gave a different definition of the rotation angle ζ from that of chapter 4 which had ζ=0 at the main lobe of the phase I ODF.

Table 5.4. The eigenvalues of M, λ^2 throughout the plastic phase transition. The numbers correspond to the points marked on fig 5.1.

	(2)	(3)	(4)	(5)	(6)	(7)	(8)	(9)
λ_1^2	146	414	720	899	1000	1112	1189	1107
λ_2^2	99	375	706	888	989	1106	1181	1100
λ_3^2	53	50	25	22	23	17	19	22

Table 5.4 contains the values of λ^2, the eigenvalues of *M* at intervals throughout the run. The onset of orientational disorder is seen as two of the eigenvalues increase markedly. The ODF's at the points corresponding the times marked on fig 5.1 are plotted in fig 5.2. The initial ODF was strongly peaked at ζ=0, showing that most of the molecules were still in their phase II orientations. In fact for point (1) it was not possible to calculate an ODF since the eigenvalues of *M* were nearly equal. As the transition progressed this peak decreased in size as the molecules redistributed themselves to other orientations, where the corresponding peaks grew. The final ODF has a main peak at ζ=-108° plus three subsidiary maxima.

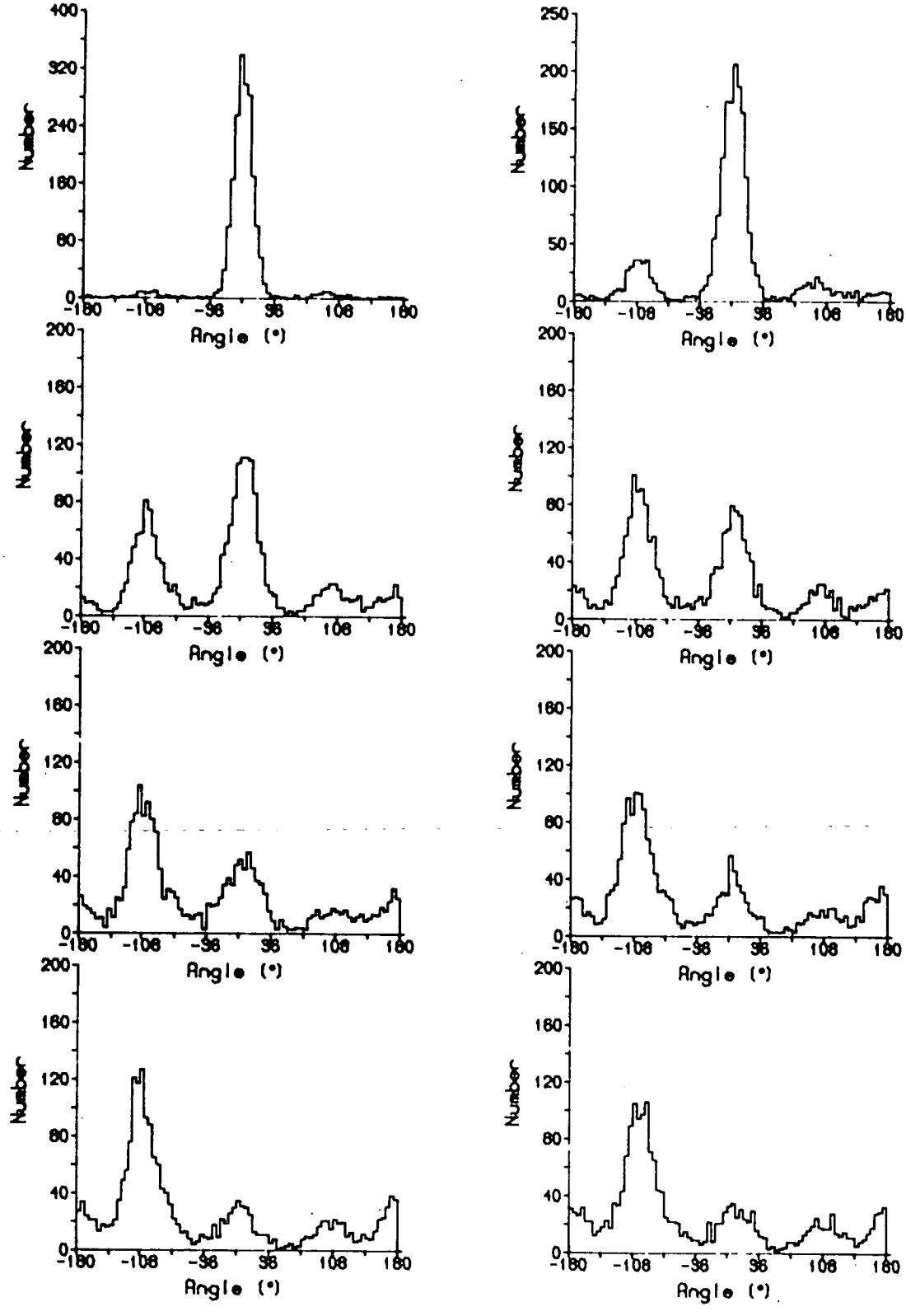

Figure 5.2 Orientational distribution functions throughout the plastic phase run. The graphs show the state at points 2 to 9 on fig 5.1.

Table 5.5. A comparison of the unit cells, molecular orientations and disorder axes of the MD and experimental structures of the plastic phase. ε is the angle needed to rotate a molecule in the MD orientation to the experimental one.

	MD	*Experimental*		*MD*	*Experimental*
a	5.72(2)	5.693(1)	q_1	0.3263	0.3328
b	5.69(2)	5.508(1)	q_2	-0.8885	-0.8898
c	8.63(3)	8.361(2)	q_3	0.2697	0.2789
β	115.6(3)	115.294(5)	q_4	0.1771	0.1402
Δ_1	-0.0319	-0.0371			
Δ_2	0.7269	0.7273	ε		4.3°
Δ_2	0.6860	0.6853			

The unit cell, the quaternion at the centre of the main peak of $P(\zeta)$ and the disorder axis are all compared with their experimental equivalents in table 5.5. All were calculated from a run at 125K in order to be directly comparable to the experiment. As in the case of phases III and II the unit cell lengths are only 1-3% larger than the experimental values and the angle β is well within the quoted uncertainty. The molecular orientation is rotated by 4.3° from the experimental value and the disorder axes are only 0.4° apart. These results show that the simulated phase I has an almost identical structure to that measured experimentally. A single layer of that phase I structure is shown in fig 5.3.

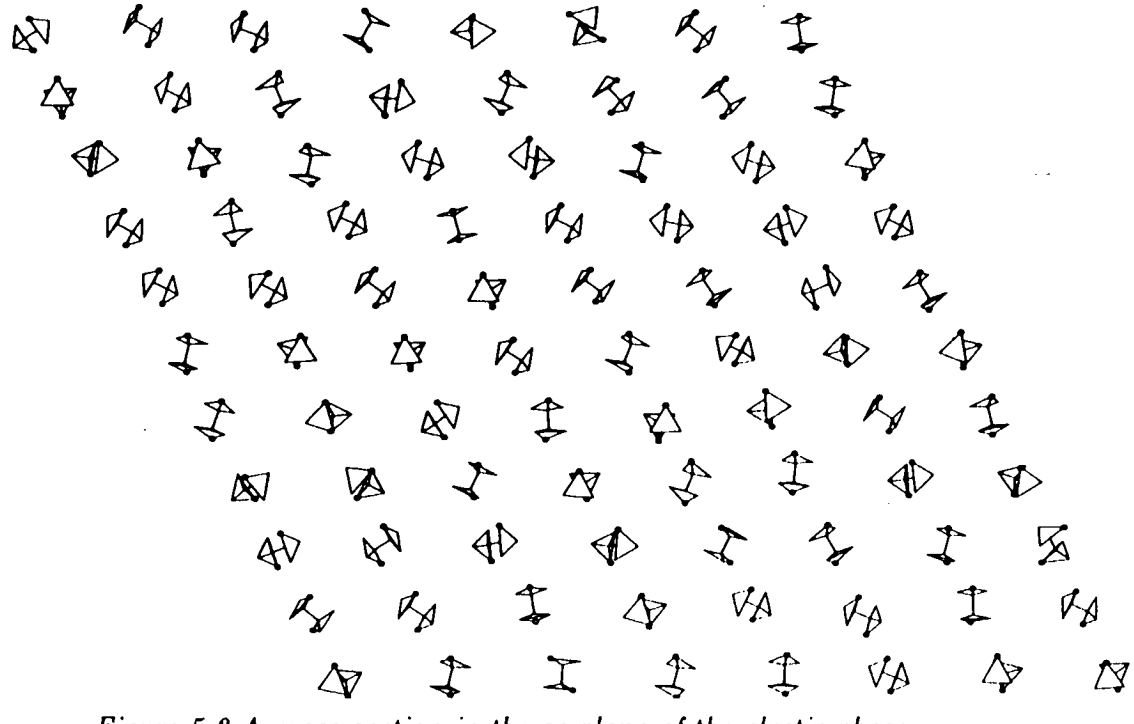

Figure 5.3 A cross-section in the ac plane of the plastic phase.

The ODF's of fig 5.2 were each calculated from a single configuration and the statistics are therefore quite poor. In order to reduce the noise the ODF was

re-calculated as an average over 71 configurations separated by a time increment of 0.16ps. Although these are certainly not statistically independent the total time of 11.4ps is greater than the period of the slowest fluctuations (those of the unit cell), which should eliminate the systematic errors present in a single-configuration calculation.

The new calculation was performed on a run starting from a configuration which had been re-equilibrated at 125K so that the simulated and experimental ODF's pertain to the same temperature. A new reference orientation at the centre of the main peak of the $P(\zeta)$ was used. This effectively re-defined the ζ by a shift of 108° to bring it into agreement with the experimental definition.

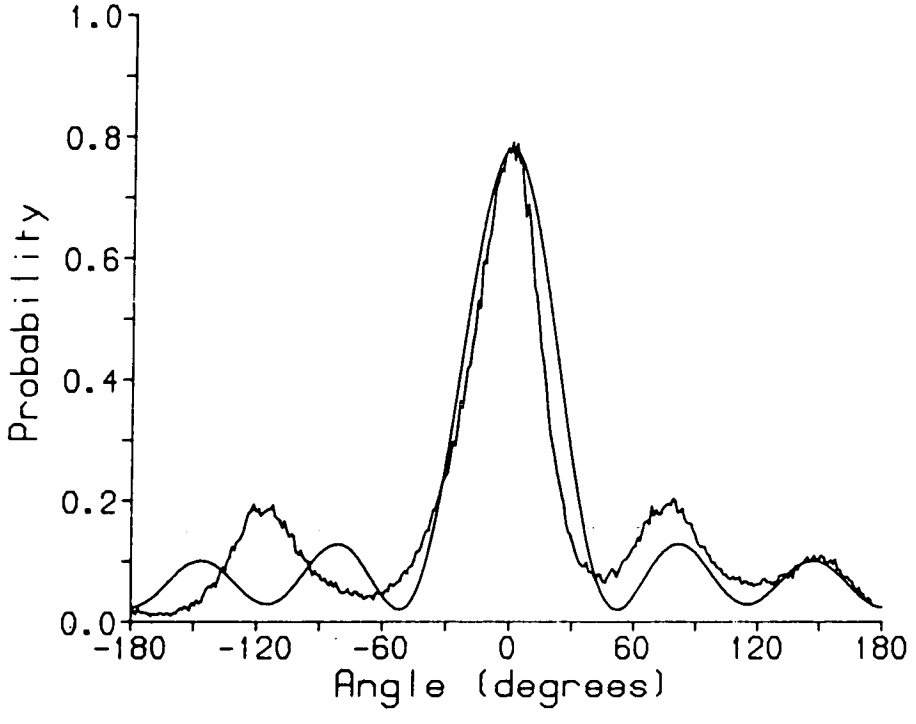

Figure 5.4 Experimental and MD ODF's. The smooth curve is the experimental one.

The eigenvalues of M for this calculation were 37799, 38977 and 1937 giving a ratio $\lambda_3/\lambda_1 \approx 0.23$ and showing that the disorder is strongly single-axis. Both the simulated and experimental ODF's are plotted in fig 5.4 and the resemblance is rather close. The large maximum at $\zeta=0$ is well reproduced as are the two smaller maxima at $\zeta=80°$ and $\zeta=150°$, however instead of the peaks at $\zeta=-80°$ and $\zeta=-150°$ there is a single one at $\zeta=-116°$. It would be wrong though to attribute the discrepancy to a failure of the simulated system to reproduce nature. Recall from chapter 4 that information in the scan was limited by a large Debye-Waller

factor and that this prevented the resolution of atoms closer than 1.6A. To reduce the number of parameters fitted to that limited data it was assumed that $P(\zeta)=P(-\zeta)$ which required that two peaks exist at $\zeta=-80°$ and $\zeta=-150°$. However these are not well resolved and it is likely that a single peak as seen in the MD curve would fit the data just as well. Thus the simulated ODF is the definitive one.

One notable feature about the simulated transition is the length of time required for the process to complete. Even at 140-150K, over 30K above the experimental transition temperature, the transition took around 100ps which is an extremely long time in molecular dynamics terms. It is in marked contrast to the much more rapid *fcc* to *bcc* transition observed in rubidium by Parrinello and Rahman (1980). The latter was a displacive transition which proceeded through a change in the unit cell matrix $\mathbf{h}$ and the consequent collective displacement of all the atoms. No change was required to the scaled atomic co-ordinates $\mathbf{s}_i$ and the transition did not involve the dynamics of the individual atoms at all. The reconstructive plastic transition of *n*-butane is of a quite different nature. The molecular orientations disordered individually and progressively while the unit cell changed to suit the new structure that was developing. This is clearly a far more complex transition and it is only because of the large MD sample size and consequent large fluctuations that it is conceivable to simulate it. Even using the power of the DAP computer which makes a system of 2048 molecules possible the run of fig 5.1 took 132 hours of CPU time.

§5.5 Dynamics

The study of the dynamics of the plastic phase may be conveniently divided into two categories: 'single molecule' quantities which may be calculated from the dynamic co-ordinates of one molecule and averaged over all molecules, and collective properties such as the dynamic scattering factor, $S(\mathbf{Q},\omega)$ which require data relating to more than one molecule. In this section only single molecule results are presented and the important areas of rotation/translation coupling and co-operative dynamics are left to later work.

The linear and angular velocity autocorrelation functions can reveal a great deal of information on the molecular motion and are among the most useful tools in the study of single molecule properties. They are defined as

$$z(t) = \langle \mathbf{v}_i(t_0).\mathbf{v}_i(t_0+t)\rangle / \langle |\mathbf{v}_i|^2 \rangle \text{ and}$$
$$c(t) = \langle \boldsymbol{\omega}_i(t_0).\boldsymbol{\omega}_i(t_0+t)\rangle / \langle |\boldsymbol{\omega}_i|^2 \rangle \qquad (5.7)$$

where the average is over all molecules in the simulation and over a suitable range of initial times t_0. Their spectral densities are just given by the Fourier transforms $Z(\omega)$ and $C(\omega)$, and by the convolution theorem

$$Z(\omega) = \int_{-\infty}^{\infty} z(t)\, \exp(-i\omega t)dt = \langle |\mathbf{v}_i(\omega)|^2 \rangle / \langle |\mathbf{v}_i|^2 \rangle ,$$
$$C(\omega) = \int_{-\infty}^{\infty} c(t)\, \exp(-i\omega t)dt = \langle |\boldsymbol{\omega}_i(\omega)|^2 \rangle / \langle |\boldsymbol{\omega}_i|^2 \rangle \qquad (5.8)$$

where $\mathbf{v}_i(\omega)$ and $\boldsymbol{\omega}_i(\omega)$ are the transforms of the corresponding velocities. Notice that the symbol ω is used in two different senses, as a scalar to represent frequency and as a vector to represent angular velocity. From (5.8) it is clear that $Z(\omega)$ is proportional to the energy spectrum for translational motion. However the corresponding statement, that $C(\omega)$ is proportional to the rotational energy spectrum is only true if the molecule is sufficiently symmetrical that its inertia tensor is isotropic so that $2K=\boldsymbol{\omega}.\mathbf{I}.\boldsymbol{\omega}=I\omega^2$. If that is not true, $C(\omega)$ is biased since rotations about axes with different moments of inertia are given equal weights despite the different energies. Nevertheless $C(\omega)$ is useful as it is non-zero only at regions of the spectrum where there is rotational energy and therefore where rotational states exist.

The values of $Z(0)$ and $C(0)$ are of particular interest since a non-zero value indicates that translational or rotational diffusion is taking place. In fact it is easily shown that the diffusion constant $D=1/6\langle \mathbf{v}^2 \rangle Z(0)$. Similarly a non-zero value of $C(0)$ indicates rotational diffusion and $C(0)/2=\tau$, the rotational correlation time which in a pure diffusion model is the interval between small rotational jumps. However no information is provided on the size of the jumps which may be

reorientations of considerable magnitude.

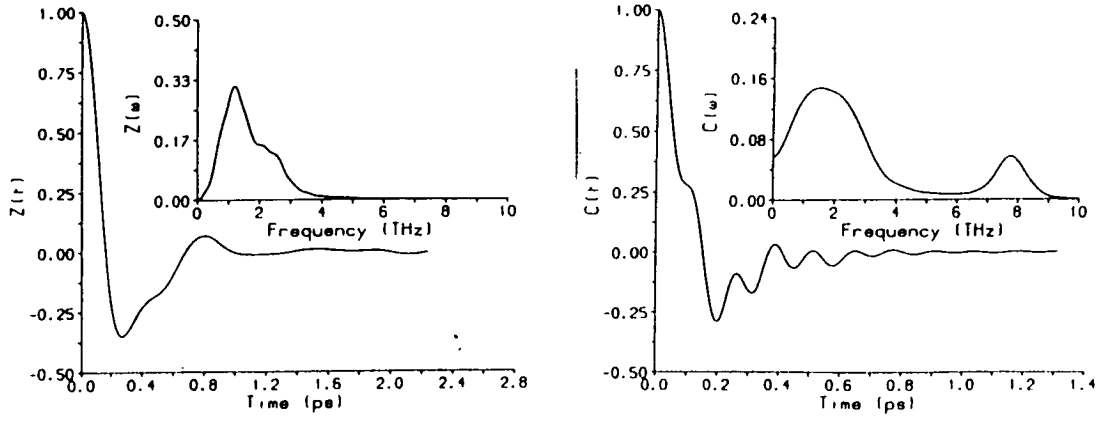

Figure 5.5 Linear and angular velocity autocorrelation functions and their power spectra.

Fig 5.5 shows these quantities calculated during two runs at 125K subsequent to the runs of §5.4. The velocities were recorded every 0.064ps for $z(t)$ using a timestep of 0.002ps. This was found to be inadequate to resolve the fine detail of $c(t)$ which was therefore calculated from a similar run with a smaller timestep of 0.001ps and recording velocities every 0.016ps. The negative value of $z(t)$ at 0.25ps shows a strong 'cage effect' as expected for vibrating systems where the velocities reverse in direction periodically. Two peaks can be distinguished in $Z(\omega)$ which probably correspond to the longitudinal and transverse modes. $Z(0)$ is exactly zero, confirming that there is no linear diffusion. Like $z(t)$, $c(t)$ also goes negative, indicating librational motion, however $C(0)$ is non-zero which means that rotational diffusion does take place. A notable feature of the rotational power spectrum is the optic mode at nearly 8THz which can also be clearly seen in $c(t)$. It will be discussed later in this section.

The correlations calculated above do not discriminate by the direction of the velocities and hence do not reveal anything about the dimensionality of the disorder in *n*-butane. The autocorrelation of the components of $\boldsymbol{\omega}$ parallel and perpendicular to the disorder axis $\boldsymbol{\Delta}$

$$c_{\uparrow}(t) = \langle(\boldsymbol{\omega}_i(t_0).\boldsymbol{\Delta})(\boldsymbol{\omega}_i(t_0+t).\boldsymbol{\Delta})\rangle \,/\langle|\boldsymbol{\omega}_i.\boldsymbol{\Delta}|^2\rangle$$
$$c_{\rightarrow}(t) = \langle(\boldsymbol{\omega}_i(t_0)\times\boldsymbol{\Delta})(\boldsymbol{\omega}_i(t_0+t)\times\boldsymbol{\Delta})\rangle \,/\langle|\boldsymbol{\omega}_i\times\boldsymbol{\Delta}|^2\rangle \qquad (5.9)$$

and their power spectra $C_{\uparrow}(\omega)$, $C_{\rightarrow}(\omega)$ are more useful. These quantities were calculated from exactly the same data as used for $C(\omega)$ and are plotted in fig 5.6. There is a striking difference between the motions parallel and perpendicular to the disorder axis. $C_{\uparrow}(0)$ is large while $C_{\rightarrow}(0)$ is almost zero, clearly demonstrating that the rotational diffusion takes place almost entirely about the disorder axis. By

contrast rotational motion about the other axes is overwhelmingly librational in character as shown by the large negative value of $c_{\rightarrow}(0.2)$ and the near zero value of $C_{\rightarrow}(0)$.

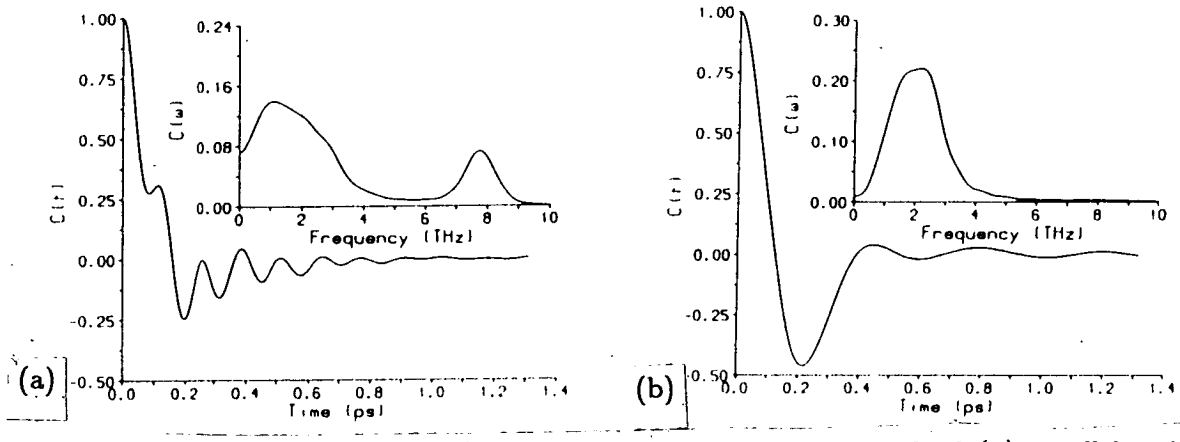

Figure 5.6 Angular velocity autocorrelation functions resolved (a) parallel and (b) perpendicular to the disorder axis.

From the value of $C_{\uparrow}(0)$ the rotational correlation time and diffusion constant for diffusion around Δ may be evaluated,

$$\tau = C_{\uparrow}(0)/2 = 0.0363\text{ps and}$$

$$D_r = 1/3\langle|\omega.\Delta|^2\rangle\tau = 0.0716\ \text{rad}^2\text{ps}^{-1}.$$

Both of these quantities are experimentally accessible, the correlation time from Raman linewidths and the diffusion constant from quasi-elastic incoherent neutron scattering. No measurements have been made on butane but the value of D_r is rather close to that of 1,2-dichloroethane at 227K of 0.08 (Leadbetter and Turnbull, 1977). Also of interest are the components of the mean square angular velocities which are $\langle|\omega.\Delta|^2\rangle$=5.92 and $\langle|\omega\times\Delta|^2\rangle$=1.70. Their ratio is 3.5, seven times that expected for isotropic motion.

These correlation functions therefore show that in the plastic phase the molecules of *n*-butane librate about the disorder axis, presumably around the four maxima in the ODF, and also undergo reorientations between these maxima.

Although it is small, $C_{\rightarrow}(0)$ is not quite zero which would appear to show that there is some rotational diffusion about the short molecular axes. Before drawing any such conclusion we should examine the possibility that it is due to some computational effect. Similarly unexpected non-zero intercepts in $Z(\omega)$ were found by Bounds *et al* (1980) and McDonald *et al* (1982) which were accounted for by truncation errors and noise. However the statistics in this case are greatly superior to either of those studies, which considered only 108 molecules compared to our

2048. The exact zero of $Z(\omega)$ (fig 5.5) and the complete cancellation of the 8THz peak from $C_{\rightarrow}(\omega)$ show that no such statistical limitations apply here. It is possible that the non-zero value may be a residual effect of the splitting of c into $c_{\uparrow}$ and $c_{\rightarrow}$ associated with the non-commutativity of rotations in three dimensions.

We now return to the high frequency rotational mode observed in $C(\omega)$. It must involve the rotation of the methyl groups as at nearly 8THz the frequency is too high for it to be due to a lattice mode. It is significant that the peak only appears in the angular velocity component along the disorder axis and that there is no detectable perpendicular component which one would expected in a methyl twist mode. Since these groups rotate around C-C bonds at an angle of only 20° to the molecular rotation axis their motion will couple to the molecular rotation about that axis. The antisymmetric methyl twist mode has a frequency of 6THz, and the shift to 8THz must be due to the intermolecular forces in the crystal environment.

The presence of such a high frequency mode must cast doubt on the inclusion in the simulation of the two degrees of freedom of the methyl groups. The usual justification for constraining any degrees of freedom and adopting a rigid or semi-rigid body model is that certain internal modes are well separated in frequency from the lattice modes and do not interact strongly with them. The first criterion certainly applies to the 8THz mode. Furthermore the peak in $C(\omega)$ is rather narrow so that the mode is fairly harmonic as seen in fig 5.5 which shows that the interaction with the lattice modes is weak. Finally, the high frequency means that this mode would not be populated in a real quantum system. The energy quantum of a harmonic oscillator at 8THz is $h\nu$=770K so that at 150K the system would have a 99.5% probability of being in the ground state. Thus the methyl mode does not appear to be an essential part of the system's dynamics and in any case is not excited in a real crystal of *n*-butane. The same does not however apply to the third internal degree of freedom, the twist about the central C-C bond. At around 3THz it cannot be distinguished from the lattice modes and it must therefore play a part in the rotational dynamics. Its inclusion in the simulation is therefore justified.

One feature of $Z(\omega)$ that deserves comment is the form of $Z(\omega)$ as $\omega \rightarrow 0$. $Z(\omega)$ is proportional to the density of states which in an ordered system goes as ω^2 for small ω. However previous simulations of the orientationally disordered phases of SF_6, bicyclo-octane and CBr_4 (Dove & Pawley, 1983; Neusy *et al*, 1984; Dove, 1986) all found that $Z(\omega)$ was linear in ω. Dove (1986) has suggested that this linear behaviour is characteristic of orientationally disordered systems and results from a coupling of the disorder to the acoustic phonons. The form in the present

simulation can be seen to be parabolic from fig 5.5 which may well be connected with the low dimensionality of the disorder in n-butane.

§5.6 Summary and Conclusions

The work described in this thesis was initiated with two major aims. The first was to study a molecular system in which the internal deformation of the molecule plays a part in the dynamics of an orientationally disordered phase, and *n*-butane was chosen as a typical example. This study was to be conducted mainly by molecular dynamics simulations implemented on the ICL DAP computer. A neutron powder diffraction experiment was also performed to find the crystal structure of deuterated *n*-butane. The outcome was very successful and the structures of all three solid phases were solved. In addition the disorder in the plastic phase was shown to be single-axis and the orientational distribution function about this axis was measured. This provided valuable data with which to validate the simulation and the model. The other aim was to develop the techniques and experience needed for MD simulations of large, low symmetry and flexible molecules.

To implement a simulation of a system of many molecules requires a large number of similar calculations to be performed, one for each molecule. The basic model must therefore be simple so that its dynamics can be efficiently calculated. Thus a classical model is required with the molecule represented by a collection of massive point atoms whose interactions are defined by pair potentials of a simple analytic form. These potentials are rather crude approximations to nature as they ignore many-body terms, anisotropic effects and residual electric charges. We stated in §2.2.1 that this simple model nevertheless captures the essential features of the statics and dynamics of all but the smallest molecules in the solid state. The success of the simulation in reproducing the experimental structures of all three phases of *n*-butane amply justifies that statement. Indeed the only serious disagreement, the stability of the low temperature phase found in chapter 3 over the experimental phase III is likely to be due to the over-simplified geometry of the model molecule rather than the potentials. The inclusion in the model of the internal rotation about the central C-C bond was justified by the failure to distinguish any separate mode attributable to it, although there is some doubt as to the value of the degrees of freedom corresponding to rotation of the methyl groups.

As well as the crystallographic structure of phase I, the simulation has reproduced the nature of the orientational disorder, and shows the molecules to be disordered about a single axis. The calculated form of the orientation distribution function is not inconsistent with the experimental one but contains more detail than the limited information in the experimental curve. Until a better experiment is performed the MD form is therefore the definitive one. The transition from phase II

to phase I was also demonstrated and shown to be a reconstructive phase transition involving the progressive disordering of molecules about the long axis with a consequent change in the unit cell.

However considerably more has been achieved than the mere duplication of the rather limited experimental data. New results on the phase transition and on the statics and dynamics of the disordered phase have been revealed. A quantitative measure of the dimensionality of the disorder was given, which proved that it is about a single axis with a ratio of the principal axes of the disorder ellipsoid of over 4 to 1. It was also shown that the component of the mean square angular velocity along the disorder axis is 7 times that along either of the perpendicular axes. The dynamics was studied using various autocorrelation functions, which showed that the molecular motion consists mainly of libration around the disorder axis centred on four preferred orientations with rotational jumps between them. The values of the rotational correlation time and the diffusion constant, direct measurements of the disordering process, were calculated.

To implement the simulation it was necessary to develop some new techniques and to extend some existing ones. One of the novel features of this simulation is the use of generalised co-ordinates to model a molecule with internal degrees of freedom. This saved a great deal of storage compared with the alternative method of constrained dynamics. The equations of motion are therefore more complicated than usual and their solution involved the inversion of a matrix every timestep. The use of generalised co-ordinates did however cause another problem. Both the low symmetry of the molecule and the presence of internal motion lead to force terms which depend on the generalised velocities. All of the more common simulation algorithms are designed for forces which depend only on distance and can not be consistently used when there is velocity dependence. The solution was to modify the Beeman algorithm by the addition of a velocity predictor term and this was found to work well.

The use of quaternions to represent molecular orientations is by now well established. However their advantages are not confined to usually stated ones of the absence of singularities and special cases in the equations of motion. Molecular symmetry operations are elegantly represented and the property of combining rotations by quaternion multiplication proved its utility many times, both in the simulation and in the analysis of the results.

Also very popular now is the zero stress MD algorithm of Parrinello and Rahman. Its effect of removing stress from the MD sample was clearly

demonstrated in chapter 3. Two small modifications were made to the algorithm. Firstly the **h** matrix represented a unit cell rather than the whole MD cell. Secondly the cell had only 6 degrees of freedom rather than the 9 of the original paper. This considerably simplified the analysis by preventing rotation of the whole MD cell and therefore keeping the orientation of the sample fixed with respect to cartesian axes.

The butane simulation was considerably larger than most having 2048 molecules compared with the more usual 108 or so. The use of computing resources in this way requires some justification. It was demonstrated in chapter 3 that it is possible for a system of this size to break up into crystallites to form a structure with a crystallographic unit cell which is not commensurate with the unit cell. Thus a large system can to some extent avoid the constraints which are otherwise imposed by the periodic boundary conditions. It is unlikely that the monoclinic phase of chapter 3 would have been found were the system much smaller. Another advantage of large systems is that the maximum fluctuation in (say) molecular displacements increases with size making more probable such 'rare' events such as a cage of molecules all moving apart simultaneously. This is just the kind of process which allows molecular reorientation to occur in, for example SF_6 and it probably helped to initiate the transition from phase II to phase I. Yet another advantage of a large system is apparent when calculating dispersion curves using the dynamic scattering factor, $S(\mathbf{Q},\omega)$. The number of allowed wavevectors increases with system size and in the typical 3^3 system there are only three points between the origin and the zone boundary which is certainly not sufficient.

There has certainly been progress towards the second aim stated in the introduction, to develop the techniques and experience of large scale simulations of flexible molecules in the solid state. Given a large enough computer the same techniques as used here could be directly implemented in a simulation of biphenyl to investigate its incommensurate behaviour. Even more simply, the program could be trivially modified to simulate other molecules similar in shape to *n*-butane. Two obvious examples are 1,2 dichloroethane and succinonitrile ($(CH_2CN)_2$). The comparison of butane with dichloroethane has been noted previously; both have very similar plastic phases, but rather more experimental data is available for the latter. On the other hand succinonitrile has a cubic orientationally disordered phase, quite unlike butane. It is especially interesting because the disordered phase is a mixture of molecules in the *trans* and *gauche* conformations and the G<->T isomerism is important to the dynamics.

Although much has been achieved it is clear that there is a great deal more work to be done on the plastic phase of *n*-butane. The previous work has left many questions unanswered and revealed many new ones.

For example, it is not certain whether or not the small non-zero value of $C_{\rightarrow}(0)$ means that rotational jumps about the short molecular axes do occur or whether it is merely an artefact of the calculation. This should certainly be investigated more thoroughly.

The reason for the stability of the 'wrong' monoclinic phase at low temperatures is not known. The hypothesis that it is due to the use of tetrahedral bond angles should be checked.

There is more which could be known about the orientational distribution function, for example its temperature dependence. The nmr results showed a decrease in the proton second moment as the temperature increased, which might be accounted for by a redistribution of molecules into the smaller maxima of the ODF. A calculation of the time average rotational potential would also be useful since if the barrier heights between minima were known jump rates could be calculated. Any deviation between the calculated and observed (from the MD) rates must be due to co-operative effects involving more than one molecule.

Many thermodynamic quantities could be fairly easily calculated, such as elastic constants, thermal expansion *etc.* The investigation of the dynamics has barely started and rotation/translation coupling and co-operative phenomena were not looked at at all. The study of these phenomena is a prime target for future simulations.

It is also hoped that this study, when published, will stimulate experimental work on *n*-butane, which at the moment is marked mainly by its absence. One phenomenon revealed by the powder diffraction experiment which certainly requires explanation is the anomalous broadening of certain Debye-Scherrer peaks in the scan of phase II.

It would be useful to know the orientation distribution function in more detail. A single crystal diffraction experiment would help here if it is possible to grow a crystal. Also all the information on the disorder contained in the diffuse scattering was discarded in the solution of the structure, and this might be investigated.

Furthermore the simulation of the plastic phase yielded values for two quantities τ and D_r which describe the rate of molecular reorientation. Both are accessible to experiment using Raman scattering and the relatively new method of quasi-elastic incoherent neutron scattering and an experimental determination of these quantities would be valuable.

It was remarked in the introduction that MD simulations can provide the models by which experimental data may be interpreted. It would therefore be a priority of any future simulation to calculate the dynamic scattering factor, $S(\mathbf{Q},\omega)$ and to suggest useful experiments. Furthermore, with high energy resolution instruments, quasi-elastic neutron scattering can explore phenomena on the same picosecond timescale as molecular dynamics simulations and a fruitful cross-fertilization could result.

The method of molecular dynamics simulation has many applications, only a fraction of which have been mentioned and the prospect is that still more will be found in the future. It is certain that it will contribute much more to the study of condensed molecular systems and to the plastic phase in particular. Complex phase transitions may be simulated using large systems and the zero-stress algorithm. The techniques for doing so are already available and we only await the arrival of tomorrow's even more powerful computers.

References

Alder B. J. & Wainwright T. E. (1959) *J. Chem. Phys.* **31** 459-466
Andersen H. C. (1980) *J. Chem. Phys.* **72**, 2384-93
Aronsson R., Jonsson B., Knape H. E. G., Lunden A., Nilsson L., Sjoblom C. A. & Torell L. M. (1984) *Journal de Physique* **41**,C6-35
Aston J. G. & Messerly G. H. (1940)*J Am Chem Soc* **62**, 1917-1923
Beeman D. (1976) *J. Comput. Phys.* **20**, 130
Berendsen H. J. C. & van Gunsteren W. F. (1983) in *Proc NATO ASI on Superionic Conductors*, Plenum Press
Bol'shutkin D. N., Gason V. M., Prokhvatilov A. I. & Erenburg J. (1971) *Structural Chem.* **12**, 313
Bonham R. A. & Bartell L. S. (1959). *J. Amer. Chem. Soc.* **81**, 3491-3496
Born M. & Huang K. (1954) *Dynamical Theory of Crystal Lattices* (Oxford)
Bounds D. G, Klein M. L. & Patey G. N. (1980) *J. Chem. Phys.* **72**, 5348-56
Bruce A. D. & Cowley R. A. (1981) *Structural Phase Transitions* (Taylor & Francis, London)
Buckingham R. A. (1938) *Proc. Roy. Soc.* **A168**, 264
Cailleau H. (1984) in *Incommensurate Phases in Dielectrics* (ed Blinc & Levanyuk), North holland.
Cangeloni M. L. & Schettino V. (1975) *Mol Cryst Liq Cryst* **31**, 219-231
Carter G. F. & Templeton D. H. (1953) *Acta. Cryst.* **6**, 805
Cochran W. & Cowley R. A. (1967) *Handbuch der Physik* **25-2a**, 59
Cochran W. & Pawley G. S. (1964) *Proc. Roy. Soc.* A**240**, 1
Cole R. H. & Havriliak S. (1951) *Disc. Faraday Soc.* **23**, 31
Cowley R. A. (1965) *Phil. Mag.* **11**, 673
Della Valle R. G. & Pawley G. S. (1984) *Acta Cryst* **A40**, 297
Dickey J. M. & Paskin A. (1969) *Phys. Rev.* **3**, 1407-18
Dixon M. & Gillan M. J. (1978) *J. Phys.* **C11**, L165
Dolling G. & Powell B. M. & Sears V. F. (1979) *Mol. Phys.* **37**(6), 1859-83
Dolling G. & Powell B. M. (1970) *Proc. Roy. Soc.* A**319**, 209
Dove M. T. & Pawley G. S. (1983) *J. Phys.* **C16**, 5969-83
Dove M. T. & Pawley G. S. (1984) *J. Phys.* **C17**, 6581-99
Dove M. T. (1986) To be published in *J. Phys. C*
Du Val P. (1964), *Homographies, Quaternions and Rotations* (Oxford Mathematical Monograph)
Dunning W. J. (1979) in *The Plastically Crystalline State* ed J. N. Sherwood (Wiley)
Durig J. R. & Compton D. A. C. (1979) *J. Phys. Chem.* **83**, 265-268
Evans D. J. (1977) *Mol. Phys.* **34**, 317-325
Ewen B. & Strobl B. R. (1980). *Faraday. Discuss. Chem. Soc.* **69**, 19-31
Ewen B. & Richter D. (1978) *J. Chem. Phys.* **69**, 2954
Ewen B., Fischer E. W., Piesczek W. & Strobl G. (1974) *J. Chem. Phys.* **61**, 5265
Finbak C. & Hassel O. (1937) *Z. Phys. Chem.* **B36**, 301
Fincham D. (1985) in *Information Quarterly for Computer Simulation of Condensed Phases.* No 17.
Goldstein H. (1959) *Classical Mechanics* p143ff (Addison-Wesley, Reading, Mass)
Hansen J. P. & McDonald I. (1976) *Theory of Simple Liquids.* (Academic Press)
Harada I., Takeuchi H., Sakakibara M., Matsuura H. & Shimanouchi T. (1977) *Bull. Chem. Soc. Jpn.* **50**(1), 102-110
Hewat A W & Bailey I (1976) *Nucl. Instrum. & Methods* **137**, 463-71
Hewat A. W., Taylor J. C., Gaune-Escard M., Bros J. P., Szczepaniak W. & Bogacz A. (1984) *J. Phys* **C17**, 4587
Hoch M. J. R. (1976) *J Chem Phys* **65**, 2522-2526
Hockney R. W. & Eastwood J. W. *Computer Simulation Using Particles* (McGraw-Hill) pp100ff.
Howard C. J. (1982). *J. Appl. Cryst.* **15**, 615-620
Impey R. W., Klein M. L. & McDonald I. R. (1984) *J. Phys.* **C17**, 3941
Impey R. W., Klein M. L. & McDonald I. R. (1985) *J. Chem. Phys.* **82**, 4690

James H. M. & Keenan T. A. (1959) *J. Chem. Phys.* **31**, 12
Kitaigorodsky A. I. & Mirskaya K. V. (1972)*Materials Res. Bull.* **7**, 1271
Klein M. L. & Weis J. J. (1977) *J. Chem. Phys.* **67**, 217-224
Kohlbeck F., Hoerl E. M. (1978). *J. Appl. Cryst.* **11**, 60-61
Kuchitsu K. (1961). *Bull. Chem. Soc. Japan.* **32**, 748-769
Leadbetter A. J. Lechner R. E. (1979) in *The Plastically Crystalline State*, ed Sherwood J. N. (Wiley)
Leadbetter A. J., & Turnbull A. (1977) *J. C. S. Farad. Trans. II* **73**, 1788-1804
Lebowitz J. L., Percus J. K. & Verlet L. (1967) *Phys. Rev.* **153**(1), 250-254
Lennard-Jones J. E. (1924) *Proc. Roy. Soc.* **A106**,463
Levesque D. & Verlet L. (1970) *Phys. Rev.* **A2**, 2514
Levesque D., Verlet L. & Kurkijarvi J. (1973) *Phys. Rev.* **A7**, 1690
Luty F. (1981) in *Defects in Insulating Crystals* ed Turkevich & Shvarts (Springer-Verlag, Berlin) 69-89
Lynden-Bell R. M., McDonald I. R. & Klein M. L. (1983) *Mol. Phys.* **48**, 1093
McDonald I.R., Bounds D.G. & Klein M.L. (1982) *Mol. Phys.* **45**, 521-542
Metropolis N., Rosenbluth A. W., Rosenbluth M. N., Teller A. H. & Teller E. (1953) J. Chem. Phys. **21**, 1087
Milberg M. E. & Lipscomb W. N. (1951) *Acta Cryst* **4**, 369-373
Mones A. H. & Post B. (1952)*J. Chem. Phys.* **20**, 755
More M., Lefvebre J. & Fouret R. (1977) *Acta. Cryst.* **B33**, 3862
Murthy C. S., Singer K., Klein M. L. & McDonald I. R. (1980) *Mol. Phys.* **41**, 1387-89
Musso G. F. & Magnasco V., (1984) *Mol. Phys.* **53**, 615-630
Neusy E., Nose S. & Klein M. L. (1983) *Mol. Phys.* **52** 269-279
Nose S. & Klein M. L. (1983) *Mol. Phys.* **50**, 1055-76
Nose S. (1984) *Mol. Phys.* **52**, 255-268
Parrinello M. & Rahman A. (1980) *Phys. Rev. Lett.* **45**, 1196-99
Parrinello M. & Rahman A. (1981) *J. Appl. Phys.* **52**, 7182-90
Pawley G. S. (1980). *J. Appl. Cryst.* **13**, 630-633
Pawley G. S. (1981). *J. Appl. Cryst.* **14**, 357-361
Pawley G. S. (1981) *Mol Phys* **43**, 1321-30
Pawley G. S. & Thomas G. W. (1982) *J. Comput. Phys.* **47**, 165-178
Pitzer K. S. (1940) *J Amer Chem Soc* **62**, 331-335
Polion A. & Grimsditch M. (1984) *Phys. Rev. Lett.* **52**, 1312
Rahman A. (1964) *Phys. Rev.* **A136**, 405
Ramdas S. & Thomas J. M. (1977) *Chemical Physics of Solids and their Surfaces* **7**, 31-58; The Chemical Society, London.
Reed T. B. & Lipscomb W. N. (1953) *Acta Cryst* **6**, 45-48
Ryckaert J. P. & Bellemans A., (1975) *Chem. Phys. Lett.* **30**, 123-125
Scott R. A. & Scheraga H. A., (1966) *J. Chem. Phys.* **44**, 3054-3069
Simon F. & von Simson C. (1924) *Z. Physik* **21**, 168
Strobl G., Ewen B., Fischer E. W. & Piesczek W. (1974) *J. Chem. Phys.* **61**, 5257
Timmermans J. (1935) *Bull. Soc. Chim. Belge.* **44**, 17
Timmermans J. (1938) *J. Chim. Phys* **35**, 331
Ungar G. (1983). *J. Phys. Chem.* **87**, 689-695
Verlet L. (1967) *Phys. Rev.* **159**, 98
Verlet L. (1967) *Phys. Rev.* **163**, 201
Weis J. J & Klein M. L. (1975) *J. Chem. Phys.* **63**, 2869-73
Williams D. E. & Starr T. L. (1977) *Computers and Chemistry* **1**, 173-177
Williams D. E. (1967) *J. Chem. Phys.* **47**, 4680
Yamamoto T. (1985) *J. Chem. Phys* **82**, 3790-3794
Zerbi G., Magni R., Gussoni M., Moritz K. H., Bigotto A. & Dirlikov S. (1981) *J. Chem. Phys.* **75**, 3175

Butane simulation Host Program

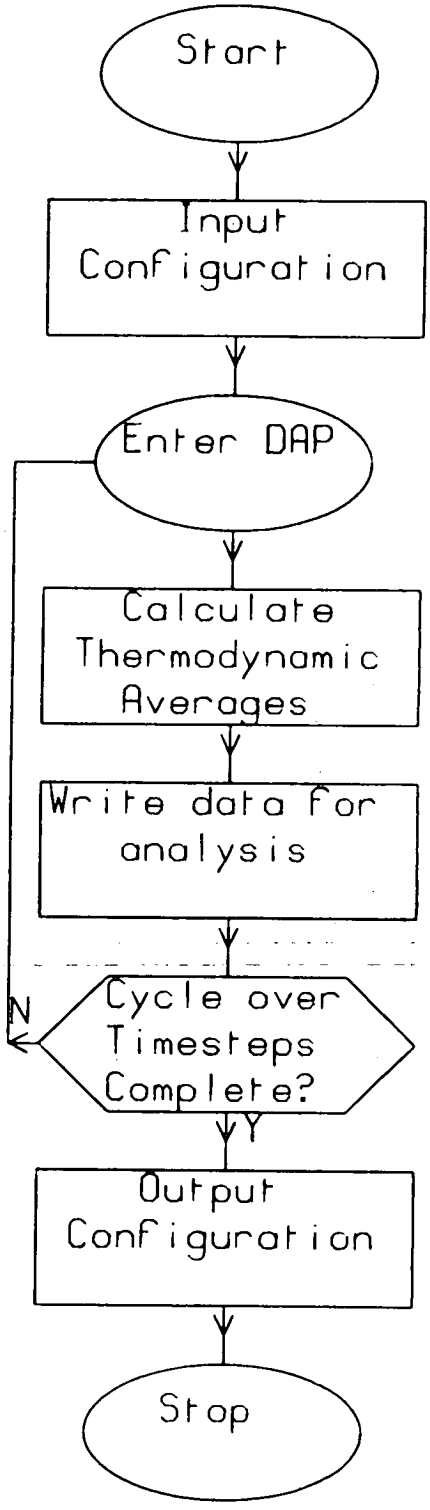

Butane Simulation DAP Program

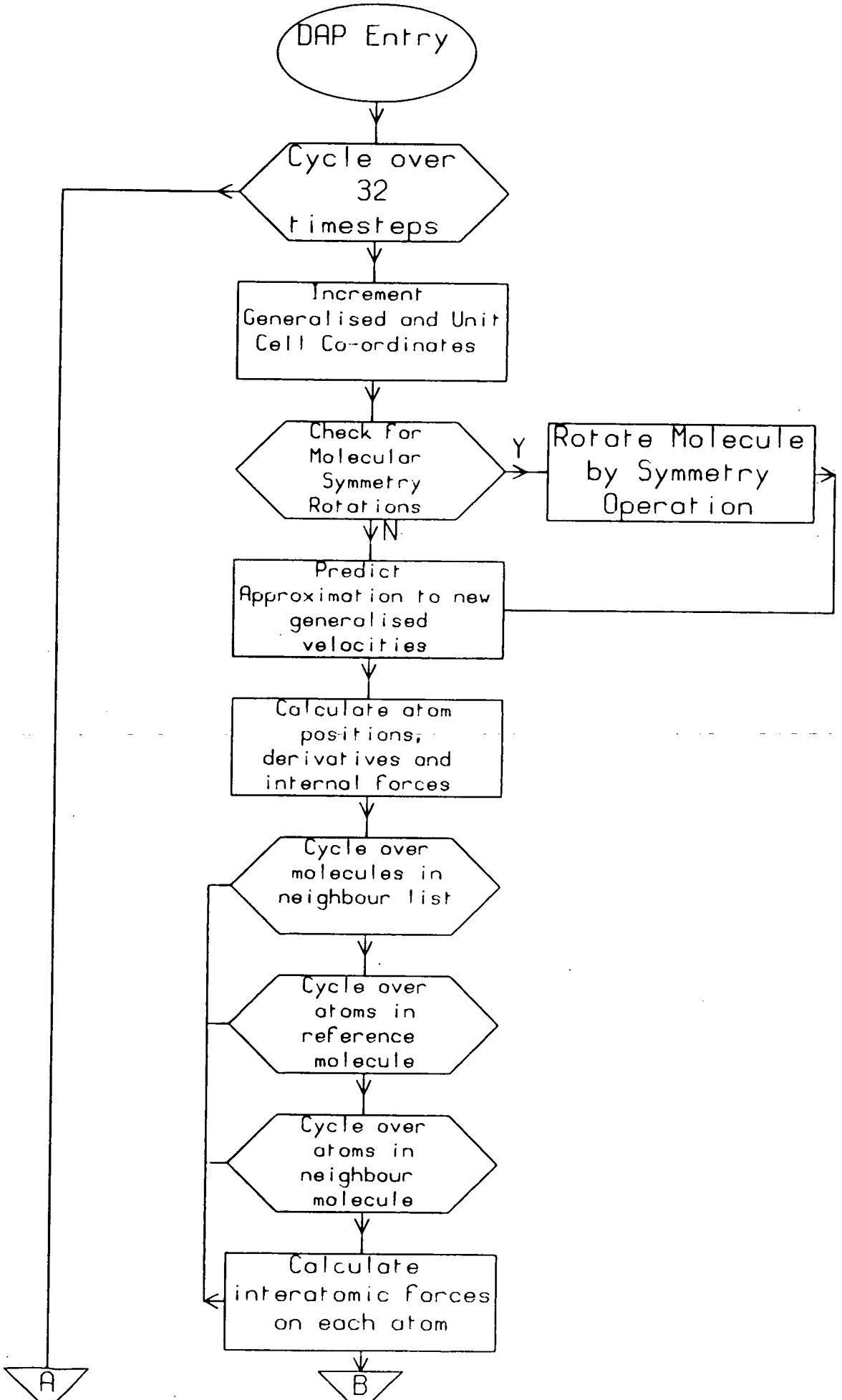

Butane Simulation DAP Program

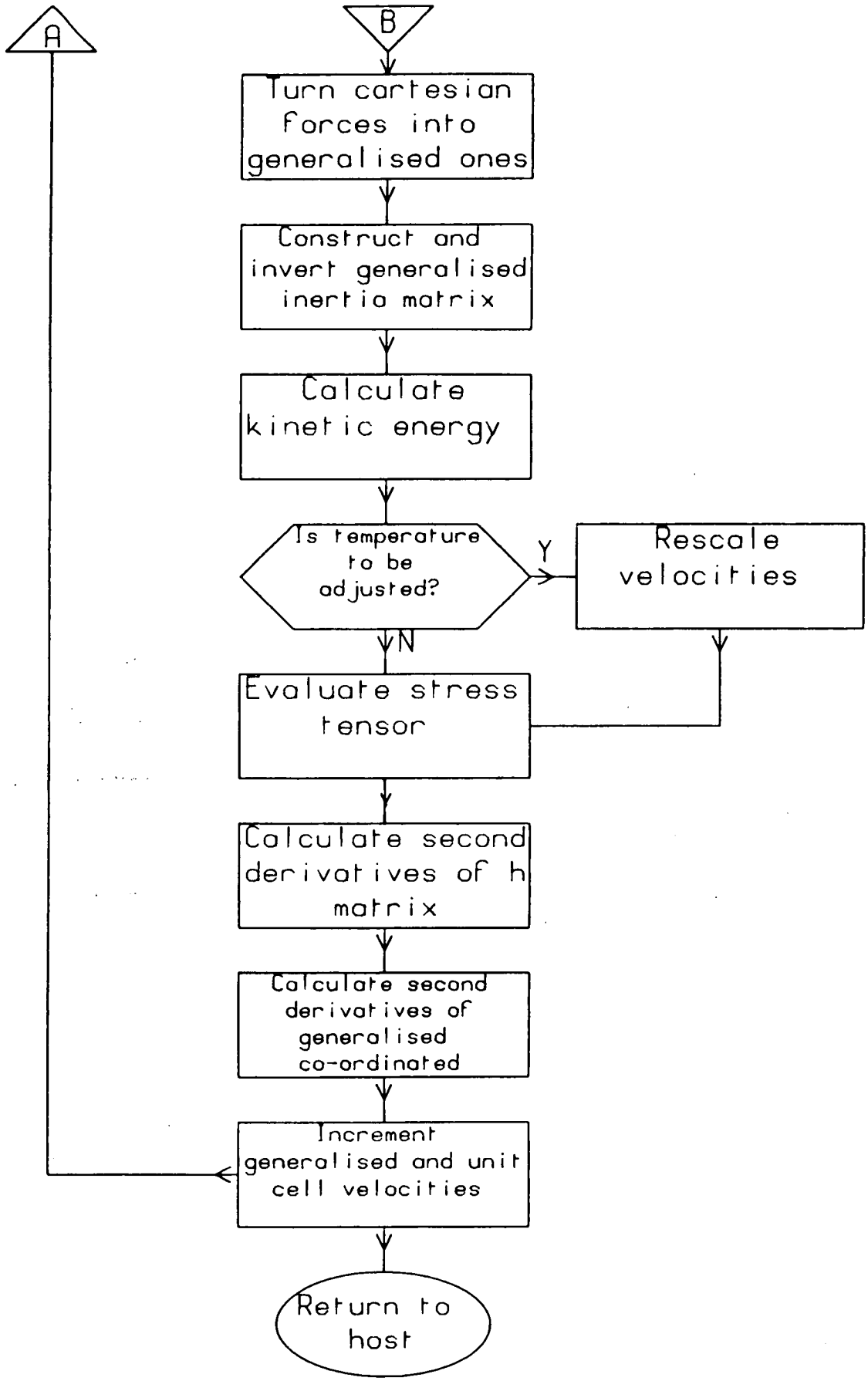

Physica 131B (1985) 256–266
North-Holland, Amsterdam

MOLECULAR DYNAMICS SIMULATION OF SOLID *n*-BUTANE

Keith REFSON
Dept. of Physics, University of Edinburgh, Mayfield Road, Edinburgh EH9 3JZ, UK

A molecular dynamics simulation of the low temperature phases of crystalline *n*-butane as implemented on the ICL DAP computer in Edinburgh is reported. Results obtained using a fixed MD cell are compared with a zero-stress calculation, clearly showing the constraints imposed on any structure by the fixed cell. Further constraints due to the skew cyclic nature of the boundary conditions, the number of molecules in a unit cell and the neighbour list are considered, leading to the conclusion that even at zero stress the boundary conditions must be tailored to the system.

Two phases were obtained below the transition at 108 K. One was triclinic and metastable. The stable structure is monoclinic with space group $P2_1/c$ with two molecules in the unit cell. It is not clear however, that this is the correct structure of a real butane crystal.

A simulation at high temperatures gives an orientationally disordered state, in qualitative agreement with experiment.

1. Introduction

N-butane is one of a class of molecular crystals which has an orientationally disordered phase below the melting point. It is solid at temperatures less than 135 K and undergoes a first order phase transition at 108 K [1]. Raman, IR [2, 3] and NMR [4] experiments show that between 108 K and 135 K the molecules become orientationally disordered.

The molecule may exist in two conformations; *trans*, where all four carbon atoms lie in a plane and *gauche* where one ethyl group is rotated by 120° about the central C–C bond. In the solid state all molecules are in the trans form.

Many molecules whose orientationally disordered forms have been studied are either very small (e.g., HF or methane) and/or have a high degree of symmetry (e.g., adamantane or SF_6) [5]. Butane has rather low symmetry and is over twice as long along the line joining the two methyl groups as in any other direction. It is to be expected that the shape of the molecule will be important in determining the nature of the disorder. In a closely packed crystal of non-spherical molecules, the rotation of any molecule will be obstructed by its neighbours and this may lead to anisotropic disorder. For example the longer *n*-alkanes such as $C_{33}H_{68}$ [6] have phases in which the molecules become disordered about the long axis. In fact NMR studies [4] show that in the high temperature phase butane makes rotational jumps of 180° about its long axis.

However, the crystal structure of butane has never been determined experimentally. The only information available is about the symmetry and is obtained from Raman and IR spectroscopy [2]. This suggests that below the transition at 108 K there are two possible structures, a stable one which is triclinic with one molecule per unit cell, and a long-lived metastable phase which is monoclinic with two molecules per unit cell.

Molecular Dynamics (MD) simulation has been used on liquids for some time, but has only recently emerged as a useful method of studying the microscopic behaviour of matter in the solid state. The present paper describes a MD simulation of the low temperature structure of *n*-butane. Since the properties of the molecular motion depend on the packing of molecules, it is important that a plausible model structure is used. As the actual structure is not known experimentally, a model must be obtained from the simulation before an investigation of the disordered phase can proceed. This paper concentrates on a number of factors which restrict

the formation of the structure which would be stable were there no artificial constraints. Also included are some preliminary results obtained from a study of the plastic phase.

All the calculations were carried out on the ICL DAP (Distributed Array Processor) computers at Edinburgh. In summary the DAP is a massively parallel computer. It consists of 4096 very simple computers called processing elements (PE's) which perform operations in parallel under control of a Master Control Unit (MCU). Each PE has 4096 bits of data on which it operates. These are connected in a 64×64 array such that each PE Can access the data of its four neighbouring PE's. By carrying out 4096 operations simultaneously the effective computational power achievable for certain calculations is of the order of a CRAY-1 at 10% of the cost. The use of the DAP for MD has been previously described by Pawley and Dove [7].

2. Description of simulation

The n-butane molecule has 4 carbon and 10 hydrogen atoms. The bond lengths in this model are 0.153 nm (C–C) and 0.108 nm (C–H) [8] and all the bond angles are tetrahedral. Each molecule has 9 degrees of freedom; three translational, three rotational and three internal rotations about the C–C bonds. The equations of motion are formulated in generalised co-ordinates $q_k (k = 1, \ldots, 9)$.

Defining $\boldsymbol{r}'_{ij} = \partial \boldsymbol{r}_i / \partial q_j$ and $\boldsymbol{r}''_{ijk} = \partial^2 \boldsymbol{r}_i / \partial q_j \partial q_k$ it can be shown that

$$\sum_i \left(\boldsymbol{F}_i - m_i \sum_{k,l} \boldsymbol{r}''_{ikl} \dot{q}_k \dot{q}_l \right) \cdot \boldsymbol{r}'_{ij} = \sum_k M_{jk} \ddot{q}_k ,$$

where

$$M_{jk} = \sum_i m_i \boldsymbol{r}'_{ij} \cdot \boldsymbol{r}'_{ik}$$

is a generalised inertia matrix.

The index i runs over all atoms in the molecule and j, k run over the generalised co-ordinates. The accelerations $\ddot{q}_k$ may be determined from the cartesian forces on the atoms $\boldsymbol{F}_i$ after inverting M_{jk}. This is in general a 9×9 matrix whose entries are a function of the internal, rotational and translational co-ordinates of the molecule, and is different for each independent molecule. Thus the storage required is $9 \times 9 \times 2048$ (molecules) $\times 4$ (bytes in a word) $\approx$ 663 kbytes which is far too much for a practical simulation. However, if three of the generalised co-ordinates are the centre-of-mass positions of each molecule then the centre-of-mass motions decouple from the internal ones and may be treated separately. M_{jk} is then reducible to a 6×6 matrix. Furthermore, as it is symmetric by definition, only 21 entries need be stored for every molecule which is a more reasonable number.

Because the DAP deals with 4096 calculations in parallel, it is natural to simulate just this number of molecules. However, since butane is a large molecule with 14 atoms and 9 generalised co-ordinates, the amount of store required to implement 4096 molecules is around 4 Mbytes, twice as much as the DAP actually possesses. For this reason the information relating to a single molecule is distributed between 2 processing elements. Therefore the simulation consists of only 2048 molecules.

It should be noted that the accelerations depend on the set of generalised velocities $\{\dot{q}_k\}$. This must be considered when choosing an integration algorithm since many common ones assume that the forces depend only on the position co-ordinates. The one used in this simulation is a modified form of the Beeman algorithm [9]. Its simplest form consists of three steps:

1) $q(t + \delta t) = q(t) + \dot{q}(t)\delta t + \{4\ddot{q}(t) - \ddot{q}(t - \delta t)\}\delta t^2/6$;

2) calculate $\ddot{q}(t + \delta t)$ as a function of $\{q(t + \delta t)\}$;

3) $\dot{q}(t + \delta t) = \dot{q}(t) + \{2\ddot{q}(t + \delta t) + 5\ddot{q}(t) - \ddot{q}(t - \delta t)\}\delta t/6$.

The velocities $\{\dot{q}_k(t + \delta t)\}$ are not available at step 2 so in this form the algorithm is inadequate. To deal with this an extra step must be

inserted between 1) and 2) to calculate an approximation to the velocities at time $t + \delta t$,

1b) $\dot{q}'(t+\delta t) = \dot{q}(t) + \{3\ddot{q}(t) - \ddot{q}(t-\delta t)\}\delta t/2$;

2) calculate $\ddot{q}(t+\delta t)$ as a function of $\{q(t+\delta t)\}$ and $\{\dot{q}'(t+\delta t)\}$.

Initially it was thought that steps (1b) to (3) should be repeated until the $\{\dot{q}'\}$ and $\{\dot{q}\}$ converge, but it was found that a single iteration sufficed.

Velocity dependent forces also arise when implementing the zero-stress algorithm of Parrinello and Rahman [10]. The above integration scheme allows a direct implementation of the equations as given in their paper, avoiding the need to reformulate them in order to eliminate the velocity dependent term.

The rotational degrees of freedom are represented by quaternions since they give a singularity-free description of molecular orientations. They were first used by Evans [11] and the equations required to relate these to angular velocities and accelerations are given by Pawley [12].

The interatomic forces, $\boldsymbol{F}_i$, are represented by a 6-exp potential with set IV of Williams' parameters [8]. The model also includes a torque about the centre C–C bond only, from the calculations done by Scott and Sheraga [13] and as used in Ryckaert and Bellemans' simulation of liquid *n*-butane [14]. The rotational potential of the end CH_3 groups is small in comparison with intermolecular forces so this rotation is assumed to be free.

The fixed number of PE's (4096) on the DAP gives rise to difficulty in implementing a lattice with periodic boundary conditions in three or more dimensions, though in 1D and 2D it is trivial. The butane simulation has either 1024 or 2048 unit cells, each containing 2 or 1 molecules respectively. However, neither 1024 or 2048 is a perfect cube, so it is obviously impossible to construct a cubic MD cell. Pawley and Thomas have shown [15] how a parallelopiped shaped MD cell may be set up using skew cyclic boundary conditions. This uses a "long vector" shift where the PE's are considered to be joined in a one-dimensional cyclic chain. Consider the case of 1024 unit cells. The side of the MD cell should be approximately $\sqrt[3]{1024} \approx 10$. If the "chain" of molecules is considered to lie in the x direction, then the cyclic image of the neighbour molecule in the y direction is the 10th neighbour along x. Thus the first 100 molecules form a 10×10 lattice, one plane of the 3D structure. In the simplest case one would expect to find the nearest neighbour in the z direction 10^2 along the chain. So if i, j, k are the relative x, y, z indices of the neighbour molecule then the displacement along the chain is $i + 10j + 100k$. However, in the case of the two molecule unit cell, there are neighbours at $(0.5, 0.5, 0.5)$ to be included, so the $(0, 0, 0.5)$ plane contains molecules 101 to 191. Fig. 1 shows the arrangement of 2048 PE's into a three-dimensional MD cell. For general (including half integral) k the index formula is $i + 10j + 192[k] + 101(k - [k])$ where $[k]$ is the integer part of k. To calculate (say) the distance between all 2048 molecules and their respective $(0.5, 0.5, 0.5)$ neighbours it is only necessary to subtract (in parallel) the position vectors, stored in a 64×64 matrix from the same matrix shifted as a long vector by 101. In this way the three-dimensional problem may be implemented using shifts in one dimension. This gives rise to a MD cell with edge vectors $(10, -1, 0)$, $(0.5, -9.5, 0.5)$ and $(7, -6, 11)$. Note that this does not put any constraint on the *shape* of the MD cell, but only on how its images join onto it.

For the initial runs the shape of the MD cell was fixed so that the simulation was run at constant strain. This proved to be inadequate and in order to reproduce the solid phases, the zero stress method of Parrinello and Rahman [10] was subsequently incorporated into the program.

In a MD simulation the computation time is directly related to the number of atom–atom interactions considered, which should therefore be as small as possible. In the case of a liquid, a cut-off radius is usually defined beyond which any residual interactions are ignored. However in most solids, atoms or molecules are confined to fixed sites and only move away from these by

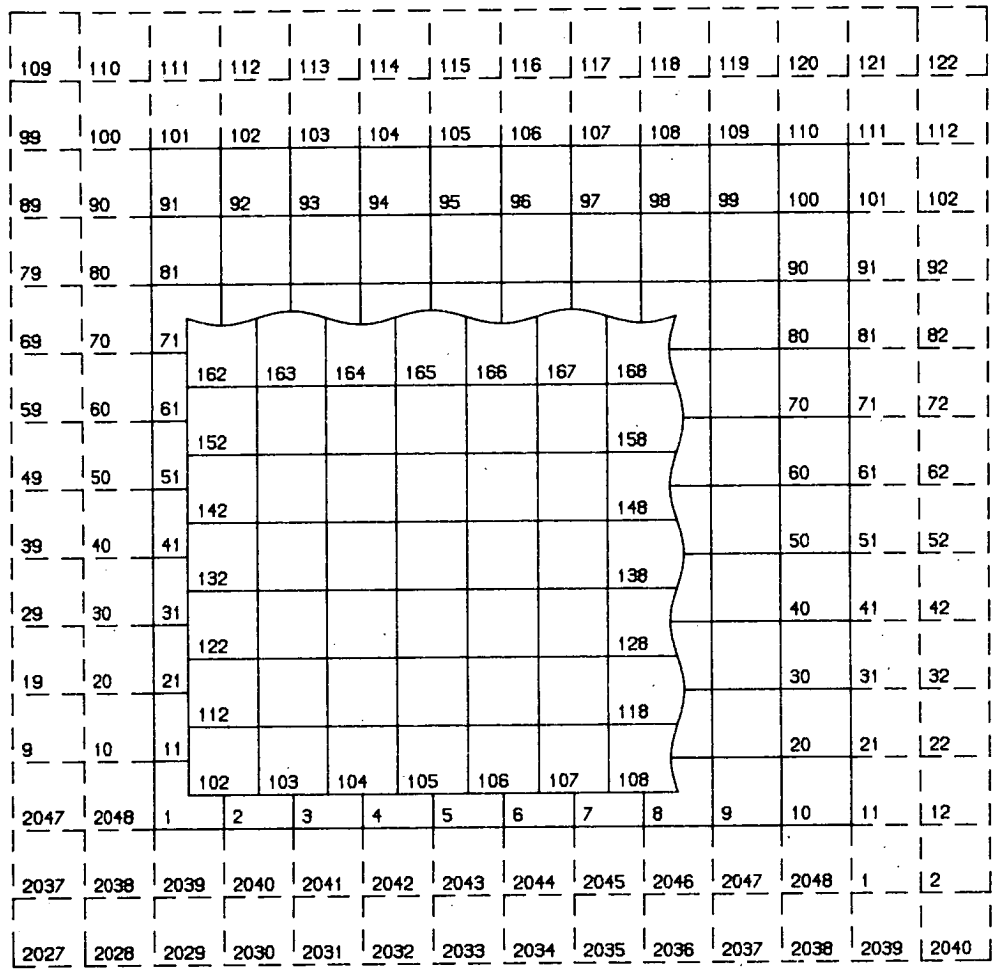

Fig. 1. Arrangement of 2048 PE's into a 3D lattice. Inset is the (0, 0, 0.5) layer.

small displacements. Thus it is more convenient to define a list of 'neighbour' molecules with which each molecule interacts, which remains fixed during the simulation run. However, the number and placing of such molecules is obviously structure dependent and the arrangement chosen will tend to favour certain structures at the expense of others with a different symmetry. This means that the 'true' structure (i.e., that calculated with a large interaction range) may not be stable in the restricted case and phase transitions between different structures may be inhibited. For example if the true structure of a crystal was fcc, with 12 nearest neighbours, but the simulation considered only 8, then it is impossible to form the fcc structure. Instead it would be likely to give a bcc structure which requires only 8 neighbours. One way round this problem is to run the simulation with a large number of neighbours for an initial run. This is time consuming since run time is directly proportional to the number of neighbour interactions, but once the structure has been established the number may be reduced to be consistent with its symmetry.

The MD program was written in such a way that changing the list of interacting neighbours was very easy. Most of the runs described below considered 14 neighbour molecules although for certain special runs more were used.

Since in any simulation the number of pair interactions calculated is restricted there will be an error in the pressure or stress. An equivalent cut-off radius may be calculated and the residual parts of the interaction integrated to give a correction to the stress. This we call a 'distant stress' term and its magnitude (typically of the order of 500 kbar) is a significant correction to the pressure.

3. Low temperature simulation

In the first instance the shape of the MD cell was fixed and the simulation was run for the equivalent of 72 ps and 25 K from an ordered initial state with a timestep of 0.02 ps. Fig. 2 shows one layer of the final configuration. It is apparent that two different structures are present; in fact there is a third which differs from

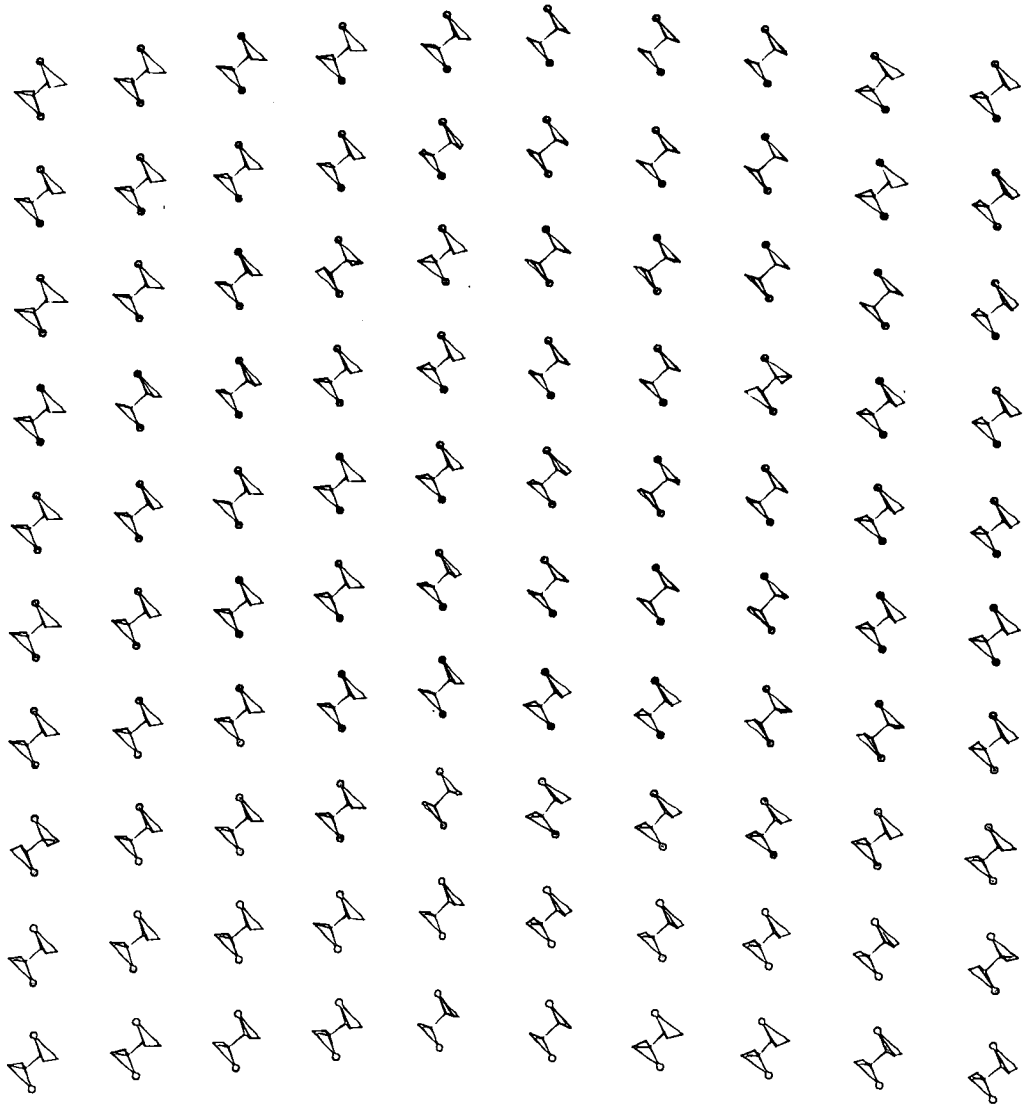

Fig. 2. One layer of configuration at 25 K with a fixed MD cell. In this schematic molecule the atoms lie at the vertices of the tetrahedra but the hydrogens of the CH_3 groups (indicated by dots) are not shown.

one of these in the direction of the unit cell vector out of the plane of the diagram. One of these is marked by an obtuse angle and the other two by an acute one. The presence of both of these phases allows the y displacement to return to where it started on satisfying the cyclic condition in the x direction. Conversely, their presence is required in order that the sample fits the MD cell. Thus the possible structures are constrained by the fixed shape MD cell.

However, the algorithm introduced in 1981 by Parrinello and Rahman [10] allows a solution to this problem. It enables the MD cell shape and size to fluctuate in response to stress in the sample, effectively giving a simulation at zero stress. This was implemented and the simulation run for 41 ps from the state at the end of the first run. Fig. 3 shows the potential energy during this run and fig. 4 the same layer of the final state. The sample had become a single crystal and the potential energy of the new structure was 3% lower. The structure was triclinic, but with two angles very close to 90°. The rapidity of the transformation indicated that all but one of the previous structures were unstable, confirming that the others were indeed artifacts of the fixed boundary conditions.

Since the simulation had been conducted entirely at low temperatures (25 K) the structure obtained could be metastable, reflecting the starting configuration. To test this possibility, further runs were carried out at 90 K (below the transition temperature) in the hope that the higher kinetic energy available would allow the molecules to find a true minimum of free energy. Over a simulated period of 70 ps half the molecules rotated to a new orientation, related to that of its (0.5, 0.5, 0.5) neighbour by a 2_1 screw axis. Thus the structure became truly monoclinic with two molecules per unit cell. Fig. 5 shows the structure obtained and includes regions of both molecular orientations. Although several grain boundaries are present it is interesting to note that when the cyclic condition is applied there is only one crystallite! In fact it was impossible to form a single, unbounded crystal for the following reason.

The condition for an unbounded crystal is that each molecule on a lattice site should be identical. Because of the skew cyclic boundary condition, *any* molecule can be reached from any other by a translation in the (1, 0, 0) direction. This includes the non-equivalent molecule at (0.5, 0.5, 0.5). But a path along a lattice translation which joins two inequivalent regions must pass through a grain boundary. This particular constraint is peculiar to the skew cyclic conditions required on the DAP, although *all* cyclic

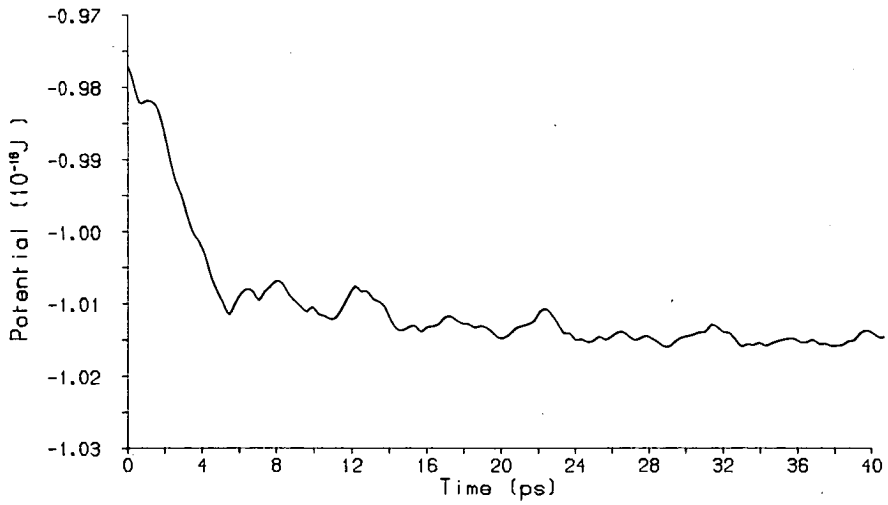

Fig. 3. Potential during zero stress run.

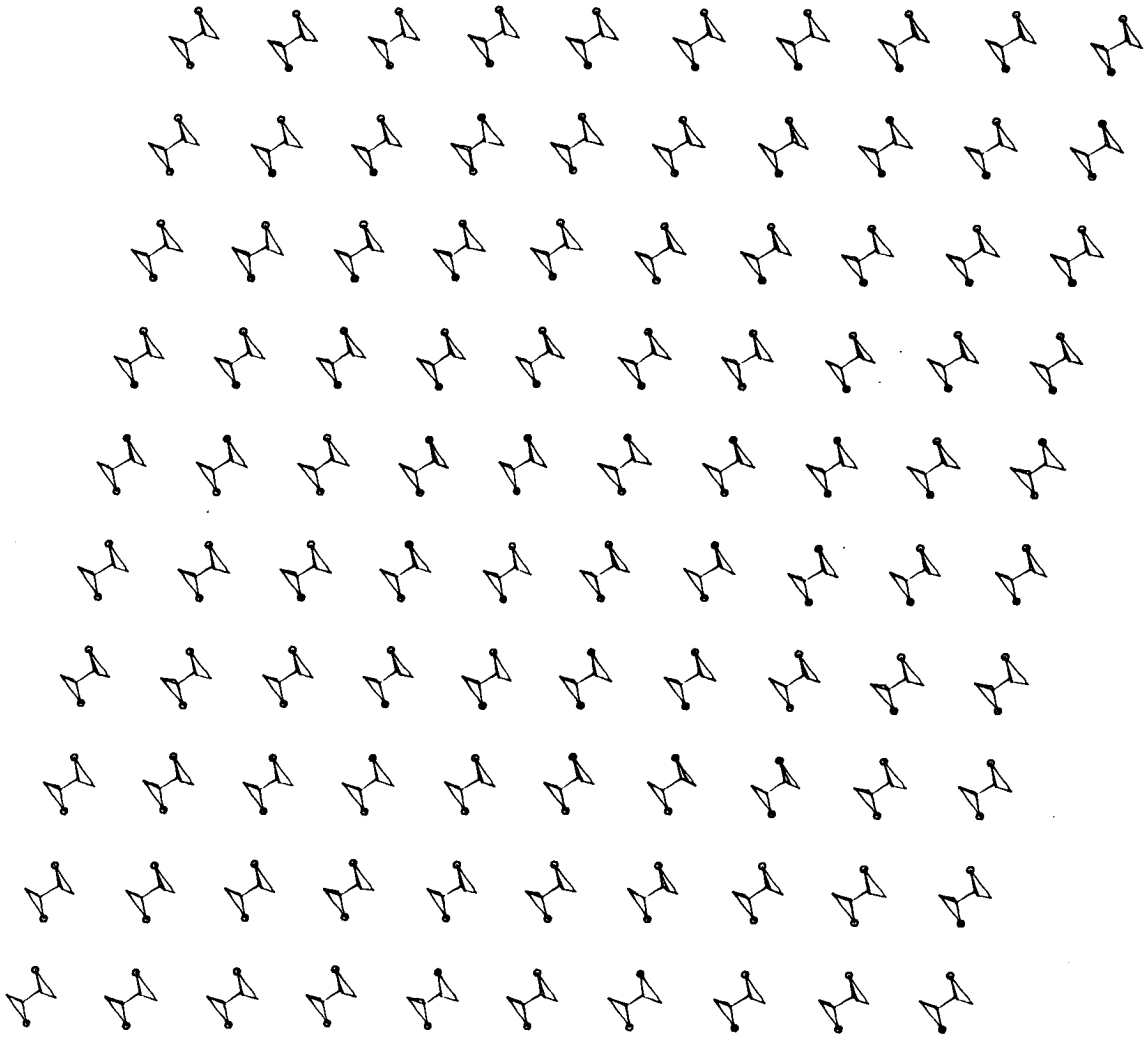

Fig. 4. One layer of configuration at 25 K with zero stress.

boundary conditions may impose some constraint by frustrating the formation of a crystallite.

A fairly simple modification sufficed to overcome the difficulty in this case. Instead of having one 1-dimensional chain, the coordinates are stored on two interleaved vectors of 1024 elements each. Equivalent molecules are confined to alternating elements, 'odd' or 'even'. This allows an unbounded single crystal with a two molecule basis. A configuration of a single crystal of the monoclinic phase was set up and run to see if it was stable. No transformations occurred.

In view of the considerations outlined above concerning the effect of the small interaction range on the stability of a structure, a few test runs were carried out using a much larger neighbour list. During the previous runs, eight nearest and six next-nearest neighbours were included, which gave molecule centre distances of up to about 7.5 Å. This meant that atom–atom interactions had an effective cut-off of between 5 Å and 10 Å which neglected forces of non-negligible magnitude. The new list considered 32 molecules and was chosen to make the overall interaction more isotropic as well as of longer

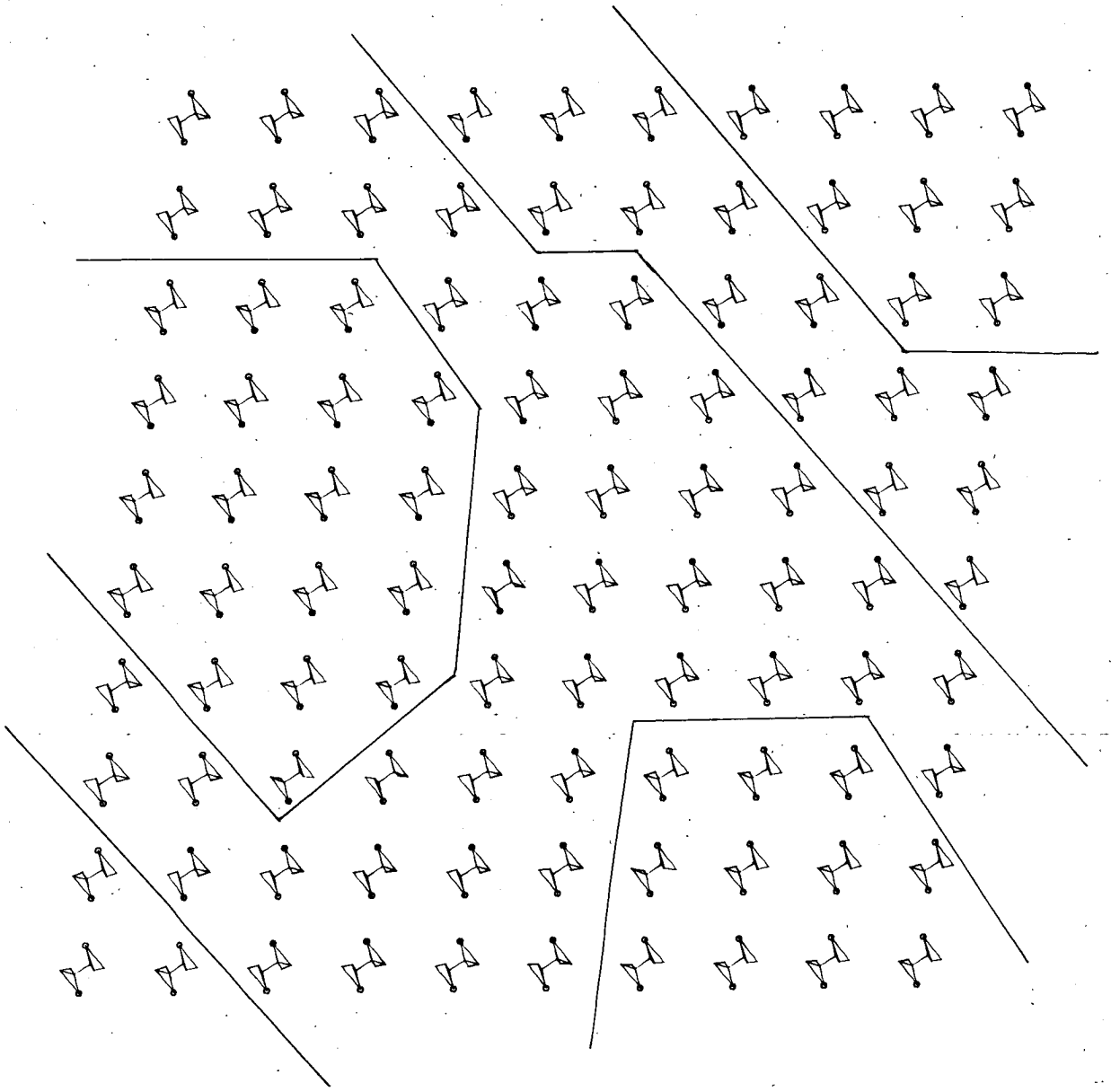

Fig. 5. Structure after equilibrating at 90 K showing domain structure.

range. All molecules whose centres were closer than 9.5 Å were included. This corresponded to an effective atom–atom cut–off of over 7.5 Å. The simulation was then run for 25 ps at 25 K followed by a 30 ps run at 100 K. During this run no evidence of any structural change was observed. From this it was concluded that in spite of its deficiencies the smaller list was adequate, and it was used for all the remaining runs.

The simulation was then run at 140 K, well above the plastic transition temperature of real *n*-butane and cooled in the hope that it would reform a crystalline structure. This, of course, would be very good evidence that the structure

so formed was truly stable. When the sample was cooled the disorder froze in and even after prolonged running (80 ps) at just below the expected transition temperature there was only slight evidence of one orientation becoming predominant. Thus the simulated transition does not appear to be reversible on presently attainable MD time scales.

The structural symmetry information available, relating to solid *n*-butane consists of studies of raman and IR spectra [2, 3] and an as yet unsolved neutron power diffraction spectrum. Unfortunately there appears to be a conflict with the simulation results. The raman data shows three optic modes, indicating a single molecule unit cell and attempts to fit a monoclinic structure to the neutron diffraction pattern have failed. Consequently, it was decided to start the simulation from an entirely new initial state with interactions conducive to a one molecule unit cell in an attempt to find such a structure. At the time of writing this has not been completed.

4. Simulation of the disordered phase

As has been previously mentioned, the simu-

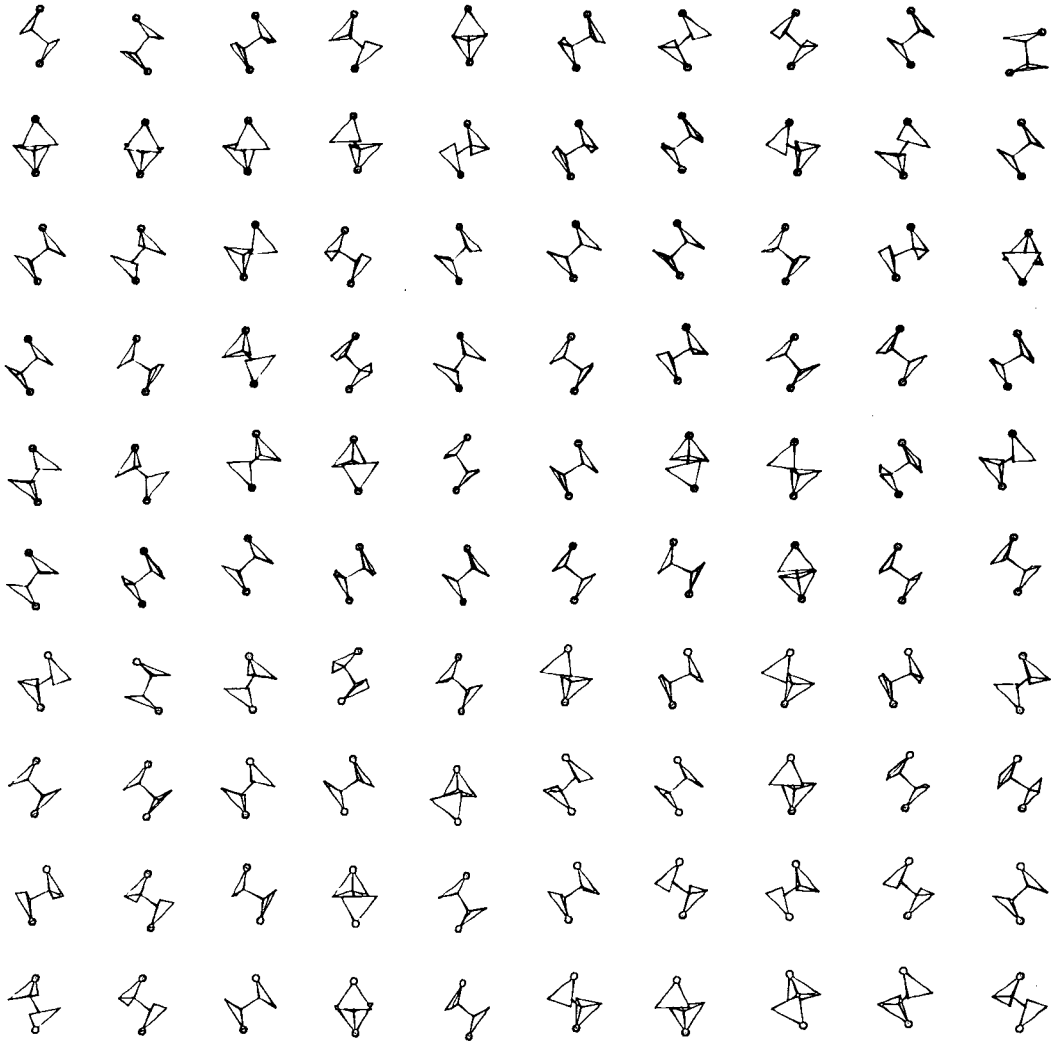

Fig. 6. Structure at 140 K in the plastic phase.

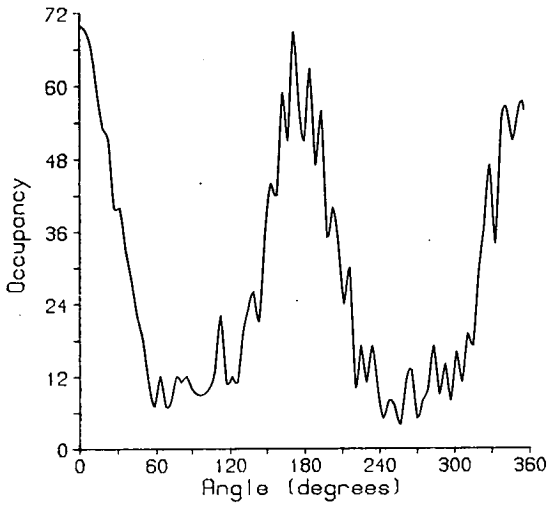

Fig. 7. Distribution of molecule orientations about the long axis.

lation has been run for some time at 140 K. Although no serious attempt was made to locate the transition temperature closely, the onset of disorder was observed at around 115 K. This is to be compared with the value of 108 K obtained from specific heat measurements [1]. An example of the state obtained is shown in fig. 6 showing that the in-plane cell angle has become 90° and that the structure is orthorhombic. It can be seen that there is disorder present, which takes the form of rotation about the long axis of the molecules and that there are two preferred orientations separated by 180°. This is confirmed by the angle distribution of molecules about the long axis (fig. 7) which shows two maxima at 0° and 180° and is in agreement with the NMR studies [4] which also suggest that long axis flips of 180° are taking place. The evidence strongly suggests that there is a double well potential for long axis rotation.

5. Conclusions

It may be concluded that with currently available computer power there are a number of factors which may prevent the formation of the structure of lowest free energy in a MD study. Some of these are easily circumvented, although others give rise to more serious problems.

1) The structure may be sensitive to the details of the potential function which in general is not well known. There is no reason to suspect that this is the case in butane, where the predominant forces are of the short range Van der Waals type.

2) The need for periodic boundary conditions imposes constraints on the possible structures and the choice of these may stabilize a structure which would not be that of lowest free energy. However if the conditions are chosen with sufficient care and variations are tried, this need not be a serious limitation. In particular, carefully selected skew cyclic conditions do not add a further constraint. This also becomes less important with the larger systems possible on the DAP since sizeable crystallites of different orientations may grow, giving a polycrystalline sample.

3) The small number of neighbour interactions necessitated by time limitations discriminates between different structures and the list of interacting molecules must be chosen with reference to some experimental data or theoretical model. It is desirable to perform relatively short simulation runs using a much larger interaction range in order to investigate the effects of the cut-off. In this particular case these effects do not appear to be significant.

4) The existence of long lived metastable states may limit the usefulness and validity of MD results, which are done on time scales of the order of a few hundred picoseconds at most. This is of particular importance to order–disorder transitions such as that in butane, where the disorder may freeze in to form a glass.

It has been suggested that in the absence of an experimental structure, static lattice energy calculations may provide a better means of finding the true stable structure. However the mechanisms which impose a real limit on the usefulness of MD pose similar problems to the static technique, in particular the existence of many metastable minima. A MD simulation can cross most, but not all, potential barriers whereas a static one can not. Thus the static calculation

needs to be started from many more initial configurations to obtain the same result, although the saving in computer time may offset this. In addition, a static calculation can not possibly reproduce the structure of the high temperature phase as it minimises potential energy rather than free energy.

The simulation is successful in predicting a first order phase transition to a disordered phase, very close to the temperature at which the real system undergoes such a transition. Furthermore, the nature of the disorder is in agreement with experimental results.

Acknowledgements

Acknowledgements are due to the SERC for funding the DAP computers on which this work was done, to the Carnegie Trust for the Universites of Scotland for financial support and to Dr G.S. Pawley for helpful discussions and advice.

References

[1] J.G. Aston and G.H. Messerly, J. Am. Chem. Soc. 62 (1940) 1917.
[2] M.L. Cangeloni and V. Schettino, Mol. Cryst. Liq. Cryst. 31 (1975) 219.
[3] I. Hadara, H. Takeuchi, M. Sakakibara, H. Matsuura and T. Shimanouchi, Bull. Chem. Soc. Jpn. 50 (1977) 102.
[4] M.J.R. Hoch, J. Chem. Phys. 65 (1976) 2522.
[5] The Plastically Crystalline State, J.N. Sherwood, ed. (Wiley, New York, 1979).
[6] B. Ewen and B.R. Strobl, Faraday Discuss. Chem. Soc. 69 (1980) 19.
[7] G.S. Pawley and M.T. Dove, Helv. Physica Acta 56 (1983) 583.
[8] D.E. Williams, J. Chem. Phys. 47 (1967) 4680.
[9] D. Beeman, J. Comput. Phys. 20 (1976) 130.
[10] M. Parrinello and A. Rahman, J. Appl. Phys. 52 (1981) 7182.
[11] D.J. Evans, Mol. Phys. 34 (1977) 317.
[12] G.S. Pawley, Mol. Phys. 43 (1981) 1321.
[13] R.A. Scott and H.A. Scheraga, J. Chem. Phys. 44 (1966) 3054.
[14] J.P. Ryckaert and A. Bellemans, Chem. Phys. Lett. 30 (1975) 123.
[15] G.S. Pawley and G.W. Thomas, J. Comp. Phys. 47 (1982) 165.

MOLECULAR DYNAMICS SIMULATIONS ON A PARALLEL COMPUTER, PLASTIC CRYSTALS AND RELATED SYSTEMS

by G.S. PAWLEY, A.M. BRASS, M.T. DOVE and K. REFSON

Department of Physics, University of Edinburgh,
James Clerk Maxwell Building,
Mayfield Road, Edinburgh EH9 3JZ, U.K.

ABSTRACT

Four molecular dynamics projects concerning dynamic molecular disorder are discussed, all having in common the fact that they are being done on a computer which is an array of parallel processors. The computer architecture is ideal for these systems as the molecules do not undergo translational diffusion.

The first system is SF_6 both in the plastic phase and below, where two phase transitions have been identified. In the plastic phase orientational disorder is apparent, the molecules arranging themselves so as to minimise the effect of the frustration between the nearest neighbour attraction and the next-nearest neighbour repulsion. The phase transitions represent the compromises enforced by this frustration as the temperature is lowered. A time correlation analysis shows that it is unlikely that phonon-like modes can exist in the plastic phase.

The second system is naphthalene very near to melting, where the predominant molecular reorientation is about the axis of greatest inertia. This is contrasted with experimental results which suggest that the reorientation about the axis of least inertia is associated with melting, the other reorientations not being catastrophic for the crystallinity of the system. Arguments are presented that the system does not have a plastic phase just below the melting point.

The third system is butane, where the molecule itself has internal degrees of freedom which are incorporated in the model. A number of crystal phases have been discovered, most of which must be metastable. On warming the stable triclinic phase to a temperature above the plastic transition in the real system, the model system takes on an orthorhombic structure where the symmetry is a time average.

The last system discussed is an invented two-dimensional system of molecules we call quaternane, as they have four atoms arranged in a chain. Each molecule has two internal degrees of freedom both of which carry a double-well potential. The system develops domain walls when warmed from a low-temperature crystal phase, and it is apparent that the structure within the walls shows smectic liquid-crystal-like behaviour. This model could well prove to be a starting point for liquid-crystal simulations at the atomic level.

RESUME

On discute ici quatre études de dynamique moléculaire sur les systèmes désordonnés qui ont été faites avec une calculatrice constituée d'un ensemble de processeurs parallèles. Cette architecture est idéale pour de tels systèmes dans lesquels les molécules ne subissent pas de diffusion par translation.

Le premier système est SF_6 en phase plastique et en-deçà, où deux transitions de phase ont été identifiées. En phase plastique, le désordre orientationnel se voit clairement, les molécules se plaçant de manière à minimiser l'effet de frustration entre l'attraction par le plus proche voisin et la répulsion par le second voisin. Les transitions de phase représentent les compromis imposés par cette frustration quand on abaisse la température. L'analyse des temps de corrélation montre que l'existence de modes de type phonon est peu probable en phase plastique.

Le second système est le naphtalène près de son point de fusion. La réorientation moléculaire prédominante se fait autour de l'axe de plus grande inertie. Contrairement aux résultats expérimentaux, qui suggèrent qu'une réorientation autour de l'axe de moindre inertie est associée à la fusion, les autres réorientations n'ayant guère d'influence sur l'état du système. On montre que le système ne présente vraisemblablement pas de phase plastique avant sa fusion.

Le troisième système est le butane, où la molécule possède des degrés internes de liberté incorporés dans le modèle. On propose l'existence de diverses phases cristallines, dont la plupart doivent être métastables. Au-dessus de la température de transition vers la phase plastique, la phase triclinique se transforme en une phase orthorhombique dont la symétrie est une moyenne temporelle.

Le dernier système discuté est un système imaginaire bidimensionnel de molécules que nous appelons "quaternane" car il possède quatre atomes disposés en chaine. Chaque molécule à deux degrés internes de liberté, qui présentent chacun un double puits de potentiel. Ce système forme des parois de domaine quand il est chauffé à partir de la phase cristalline de basse température, et il est apparent que la structure interne de la paroi a un comportement de cristal liquide smectique. Ce système pourrait être le point de départ de simulations de cristaux liquides au niveau atomique.

Introduction

It is our intention to give a brief overview of the molecular dynamics (MD) work in which we are currently engaged in the hope that our readers will be able to appreciate the range of problems that can now be realistically studied beyond the few that we will cover. All these problems are well suited to the two ICL DAP computers in our department. Each DAP (1) is an array of 4096 interconnected processing elements (PEs) which work in lock-step, each PE simultaneously performing the same operation on its own individual data set. Where a computational problem maps easily onto the architecture of this computer it is usually possible to run the computer very close to its full efficiency (about 60 Mflops). It should be appreciated that the DAP computer was designed ten years ago and that much larger machines will be developed in the very near future. When this happens we will be able to move on from the small systems of a few thousand molecules to much larger systems composed of more complex molecules.

The properties of the systems we shall investigate often appear to depend at least as much on the size of the system as on the potential function in use. In all our examples the crystal potential is assumed to be the sum over atom-atom interactions between non-bonded atoms, these interactions being either of Lennard-Jones (6-12) or Buckingham (6-exp) form. None of the systems here considered involve Coulombic interactions of sufficient significance to be included – strong Coulomb forces are not a common feature of plastic crystals and so the interactions used are relatively short range. Nevertheless longrange order becomes established in these systems through the many-body interactions, counteracted of course by the disordering

effect of temperature which is properly modelled through molecular dynamics.

Modelling of phase transitions is central to this work, and for success a large system is mandatory. Most of our simulations are performed at zero stress, this being achieved either in the time-stepping algorithm [2] or by occasional readjustment [3,4]. The discovery of a simulated phase transition can best be made, as we shall see, when the MD system is sufficiently large that separate crystallites of the new phase can grow in such away that their differing orientations alleviate the strains which accompany any change of structure. A limited number of transitions however can be discovered with small systems in which the structures of both phases agree with the cyclic boundary condition imposed on the MD cell – these are particular rather than general transitions and could well be driven by the finite size effects.

Molecular dynamics

The ideas involved in this technique are very simple and well understood. If the potential for a configuration of molecules is known then all the interaction forces can be calculated for that moment in time. Knowing the molecular masses and moments of inertia the appropriate accelerations can be calculated, whereupon the known positions and velocities of the molecules can be moved on by a small time step using Newton's laws, giving a new configuration. As this is repeated a great many times a highly probable trajectory in configuration space is described, and this can be analysed for any desired property of the system.

The algorithm used here for time-stepping is that developed by Beeman [5] for systems which are governed by potential functions having large localised gradients. These occur in the repulsive part of the 6-12 or 6-exp potential and could cause problems with higher-order algorithms using configurations from a number of previous time steps. We have found the Beeman algorithm most satisfactory for controlling all the molecular coordinates involved. Molecular rotational motion is best described in MD systems by quaternions [6,7] as the algorithms based thereon have no singularity problems. A random molecular orientation has three degrees of freedom whereas the quaternion description needs four mathematically equivalent coordinates [6]. In a MD time step all four quaternions are stepped together and the unwanted degree of freedom is removed by a normalisation of the quaternion coordinates. The formalism is ideal for plastic crystal simulations as the symmetry properties of the quaternions can be used to discover the occurrence of molecular reorientations [8].

There is a certain class of plastic crystal where the molecules have internal degrees of freedom which may play an important role in the solid state phase transitions. Understanding how to model the internal motion in MD is of further importance as the whole field of liquid crystal simulations at the microscopic level will need this technique. Moreover an internal degree of freedom with a double-well potential may well be essential for certain incommensurate molecular systems, and for this reason we include the 2-D study which concludes this article.

There are two ways of controlling internal motion in MD. The most obvious method, which we use [9], requires the introduction of generalised coordinates equal in number to the degrees of freedom involved. This requires the inversion of a matrix which becomes uncomfortably large for molecules more complex than butane (see later), and requires a predictor/corrector procedure. The other method [10] involves the use of atomic coordinates, and as these vary they are constrained in a manner similar to the Lagrange method.

Sulphur hexafluoride

Sulphur hexafluoride is a molecule of octahedral symmetry that exists in an orientationally disordered condensed phase over the wide temperature range of 96-223 K. Fuller details of our simulations of this system have been discussed elsewhere [3, 11-13] and we describe here only the most relevant features of the calculation. The intermolecular potential was modelled using a 6-centre 6-12 potential, the centres corresponding to the fluorine atoms. As the structure of the plastic phase is body-centred cubic only nearest neighbour (nn) and next-nearest neighbour (nnn) interactions were considered. This model is as simple as possible in order to retain only the important features, yet is of sufficient complexity to reproduce the overall behaviour of the real SF_6 crystal.

Initial calculations [11,12] of the single molecule S-F bond orientational distribution function have shown that at 150 K the average orientation of the SF_6 molecules is such that the S-F bonds are preferentially aligned along the cubic unit cell axes, with a root-mean-square librational amplitude of 17°. This result is in good agreement with the results of a neutron powder diffraction experiment [13]. The orientational motions of two nnn molecules have been studied as functions of time, showing that the molecules librate about this orientation, with the molecules occasionally flipping to a new but symmetrically equivalent orientation with a flipping rate of 0.1-0.2 THz. Orientational disorder is more clearly demonstrated in the calculations of distribution functions for relative orientations of neighbouring molecules. One such distribution function [12] which is shown in Figure 1 as a contour plot, defines the distribution of the relative orientations of the two closest S-F bonds of two nnn SF_6 molecules. The two

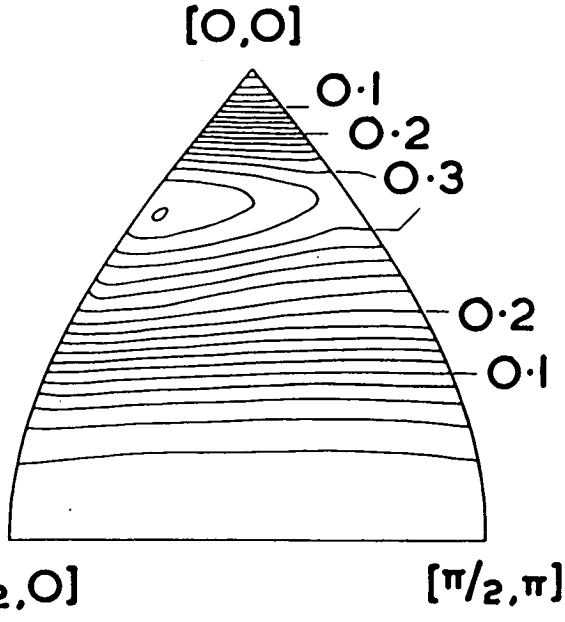

Fig. 1. – Linear contour plot of the distribution of the relative orientations of the two closest S-F bonds of two nnn (next-nearest neighbour) SF_6 molecules.

parameters α and β are defined by using the polar coordinates (θ_i, ϕ_i) and (θ_j, ϕ_j) that describe the orientations of the relevant S-F bonds of the i-th and j-th nnn molecules with respect to the vector between them :

$$\alpha = |\theta_i + \theta_j|$$

$$\beta = |\phi_i - \phi_j| \cdot$$

It is clear from Figure 1 that the orientations of nnn molecules are correlated, suggesting the existence of steric repulsion between the closest fluorine atoms which lie on average along the cube directions.

In Figure 2 the intermolecular potential of two SF_6 molecules with relative orientations corresponding to those of the nn and nnn molecules in an ordered bcc lattice is given as a function of intermolecular distance. The arrows indicate the distances between the nn and nnn positions in the simulated crystal at 150 K and zero pressure. It can be seen that the nn interactions in the crystal are attractive, providing the primary cohesion in the crystal, whereas the nnn interactions are indeed repulsive. Thus there exists a competition or frustration of interactions, with the nn interactions favouring orientational order and the nnn interactions acting to oppose this order. This frustation results in a dynamic orientational disorder, as manifested in the pair distribution function in Figure 2, and this frustration is the key to an understanding of the orientational disorder in SF_6.

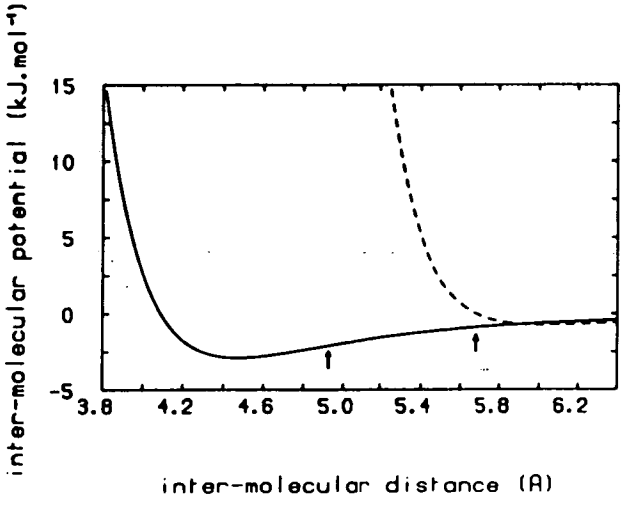

Fig. 2. — The intermolecular potential (as used) of two SF_6 molecules with relative orientations corresponding to those of nn and nnn in the time-averaged bcc structure. The arrows indicate the respective equilibrium S-S distances.

At low temperatures, when the system no longer has enough kinetic energy to balance the competing interactions dynamically, the crystal undergoes a phase transition which involves the ordering of molecular orientations. The MD simulation at 25 K showed the formation of a crystalline phase (3), and a section through the MD configuration is shown in Figure 3(a). Because the crystal structure forming was triclinic, a considerable internal strain built up in the MD sample which was only relieved by the growth of crystallites. The fact that the same structure formed in these crystallites in different orientations was taken as a guarantee that the most stable phase had been found.

Electron diffraction measurements (14) on very thin samples at 80 K show an intermediate phase, and

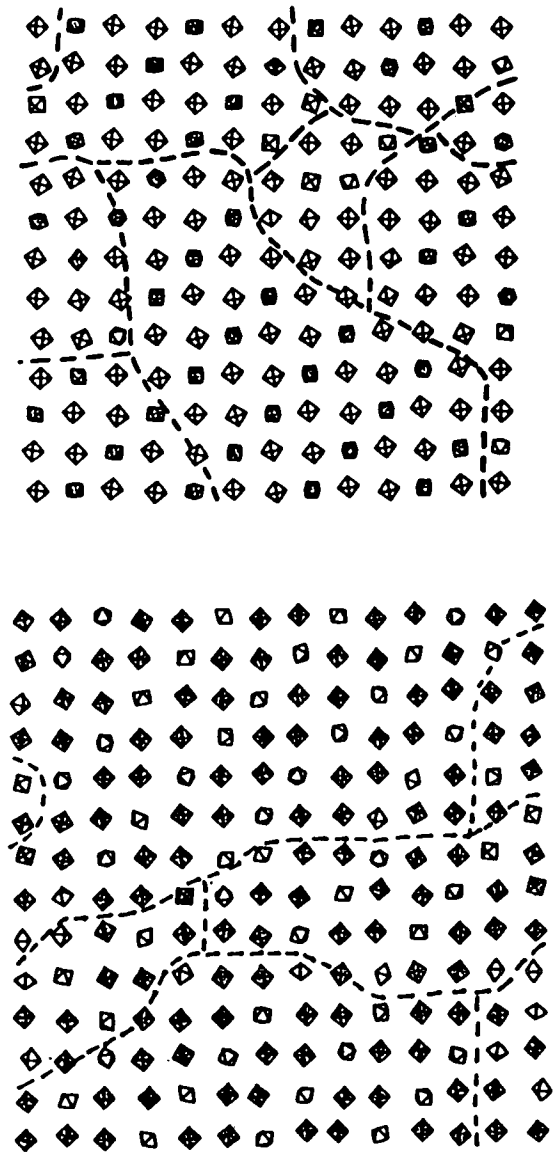

Fig. 3. — Sections through the SF_6 MD cell for (a) the 25 K triclinic phase and (b) the 80 K trigonal partially plastic phase. In both case the crystallites are outlined by dashed lines. In (a) the molecules which are stippled are those positioned in an orientation quite different from the bcc orientation, and these become disordered in the intermediate phase (b) where they are represented unstippled.

so a MD simulation was done at that temperature (15). An intermediate phase was found, as shown in Figure 3 (b), in which two molecules out of three order in a trigonal honeycomb fashion while the third resides in the honeycomb channels orientationally disordered. This is exactly as found by electron diffraction, and so it is most surprising that this phase has not been found as yet by neutron scattering from bulk samples (16). Thus although the actual behaviour of SF_6 in the solid state is not yet known it is clear that our elementary simulations yield a complexity which may well exist in nature.

As well as providing information concerning static structures and time averaged properties, molecular dynamics can be used to provide much information on the single molecule and collective dynamics of orientationally disordered crystals. Previous calculations of phonon densities of states for SF_6 (11) have shown that there are no well defined optic (librational) modes, and

that the acoustic modes are strongly coupled to the orientational disorder. More recently we have been calculating $S(Q,\omega)$ in order to compare with and attempt to explain some neutron inelastic scattering results [13], but here we focus our attention on the form of the Fourier transforms of $S(Q,\omega)$, given as $F(Q,t)$. Representative calculations of $F(Q,t)$ for longitudinal and transverse modes of SF_6 at 115 K are shown in Figure 4. In a crystal with only weak anharmonicities this function should be oscillatory and only slowly decaying, but in the present case the amplitude of $F(Q,t)$ generally decreases to below the noise level in less than 1 psec. This defines a very short lifetime for the excitations and implies a frequency "width" of an acoustic mode of greater than 1 THz ! This explains why experimentally no well defined excitations corresponding to either acoustic or optic modes are observable, and provides striking evidence for the coupling between the acoustic modes and the orientational disorder.

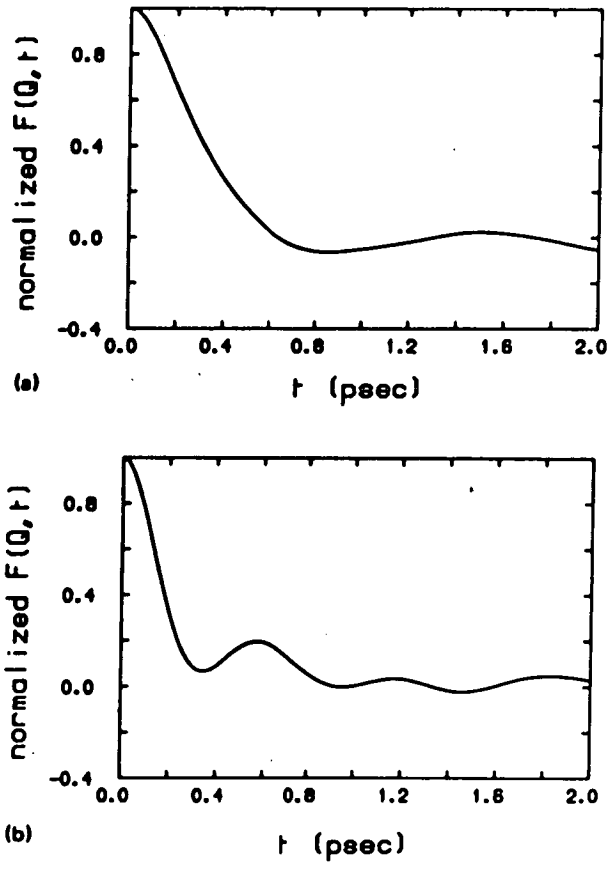

Fig. 4. — Representative calculations of $F(Q,t)$ for (a) transverse and (b) longitudinal modes of SF_6 at 115 K for (a) $Q \doteq (0, 0, 3.3)$ and (b) $Q \doteq (0.3, -4, 0)$.

Naphthalene near melting

One question addressed here is whether a molecular solid goes into a plastic phase just before it melts [17]. To answer this for naphthalene we present a MD simulation involving 4096 molecules interacting through an 18-centre 6-exp potential [18]. Molecular reorientations have been monitored as a function of temperature as shown in Figure 5. The orientation rate increases very

NB $\doteq$ means 'approximately equal to'.

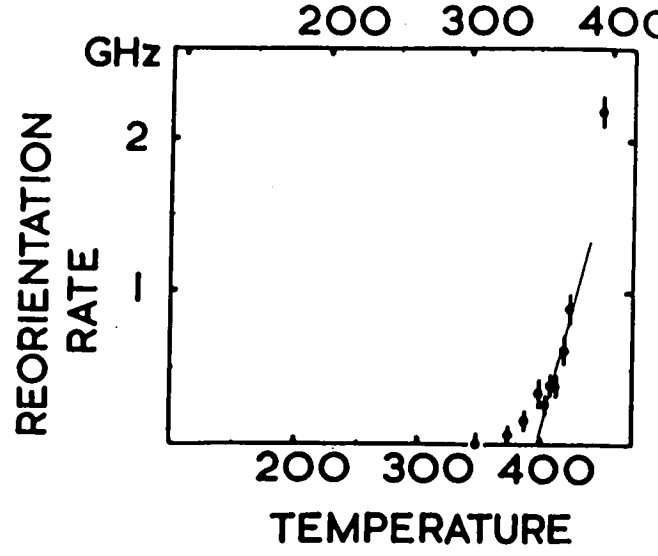

Fig. 5. — Variation of the reorientation rate of naphthalene molecules about the axis of greatest inertia, as a function of temperature. Errors are estimated assuming events to be independent. The upper temperature scale is achieved after a small scaling of the simulation. The hand-drawn straight line gives an estimate of the melting temperature.

rapidly near 400 K which can be taken as the MD melting point. Although this is somewhat higher than the actual melting point of 353 K, all the results can be scaled to give this value for the MD melting point.

Reorientation occurs almost entirely about the axis of greatest inertia (see Fig. 6). In this reorientation the molecule sweeps out a smaller volume than it would by reorienting about the axis of least inertia. Arguments based on lattice dynamical measurements favour the latter reorientation as being the ultimate cause of melting [19], and this motion does take place in MD at higher temperatures. At lower temperatures reorientation is about the axis of greatest inertia, and we therefore deduce that this motion can take place without any catastrophic effect.

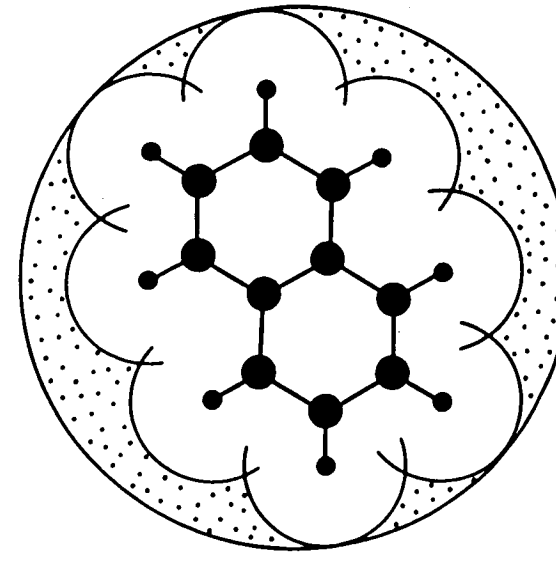

Fig. 6. — A molecule of naphthalene, $C_{10}H_{18}$, drawn with circles of radius 1.5 Å about each hydrogen to indicate range of interaction. The stippled area gives an indication of the region which must be vacated for the molecule to be able to reorient in the plane of the diagram.

It is well known from NMR work that these reorientations occur well below the melting point [20], but can the system then be described as plastic ? We believe the answer is no, after analysing our MD results as follows. A record is kept of all reorientations which take place on neighbour sites following the reorientation of a chosen molecule, and this record is then analysed to see if the neighbour reorientation is correlated or not. For naphthalene the individual reorientations are quite random, whereas a similar test for SF_6 shows a very high correlation. This could well be a way of distinguishing in MD between crystalline naphtahalene and plastic crystalline SF_6.

Butane — internal coordinates

Normal-butane is a 4-carbon saturated hydrocarbon chain, C_4H_{10}. It is not a rigid molecule as it can twist about any of the three C-C bonds giving three extra degrees of freedom which are included in the MD model. It can exist in at least three solid phases, two at low temperatures (<108 K) which are truly crystalline and one plastic or disordered phase [21]. These two low-temperature phases may coexist, but only one can be truly stable. The structures of all three phases are as yet unknown, but we hope to make progress in elucidating their structures through neutron powder diffraction.

The simulations consist of 2048 molecules interacting via a 6-exp potential. Each PE of the DAP contains details of half a molecule, there being insufficient storage space for a sample of 4096 molecules. Storage is at a premium in this work because for each molecule at each time-step a 6 x 6 symmetric matrix has to be inverted in order to treat the internal motion properly. The search for the most stable structure was hampered by the frustration effects introduced by the cyclic boundary conditions since any structure consistent with them was able to form a single crystal and was thus favoured.

In an early calculation the MD cell was kept fixed and the simulation was run for the equivalent of 72 ps at 25 K from an ordered initial configuration with randomised displacements. Figure 7 shows one layer of the final configuration where two different structures are present — in fact there is a third which differs in the direction out of the plane of the diagram. The line of molecules from one side of the diagram to the other suffers a sudden change in direction at the boundary between the two structures and this is clearly necessary to satisfy the cyclic boundary condition.

In a later calculation the shear-relieving algorithm of Parrinello and Rahman [2] was used, and the structure of the left side of Figure 7 grew until it formed a single crystal MD sample. There were no problems for this structure to fit any cyclic conditions as it was triclinic with one molecule in the unit cell. The unit cell was found to have two angles very close to 90°, but there was no symmetry which would support a monoclinic structure. Clearly the structure on the right of Figure 7 was metastable and had been stabilised by the cyclic condition.

Since the simulation had been conducted entirely at low temperature (25 K) the structure obtained could itself be metastable, reflecting the starting conditions. To test this, further runs were done at 90 K (still in the low-temperature phase for real n-butane) in the hope that the higher kinetic energy available would allow the molecules to find a true free-energy minimum. Over a simulated period of 70 ps half the molecules rotated 180° about their long axes (methyl-group to methyl-group) giving rise to a screw-diad symmetry relationship with certain neighbours. In this case, because of the skew-cyclic boundary conditions [22] it was impossible for the system to form a single monoclinic crystal. On setting up the boundary conditions similar to that of the naphthalene simulation [18] a true single crystal was achieved.

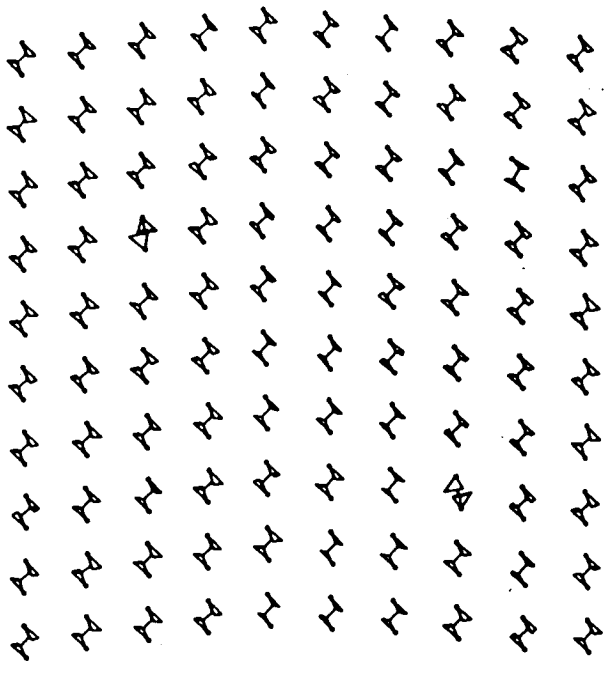

Fig. 7. — A layer through the simulated structure of butane at 25 K. The large dots on the ends of each molecule represent methyl groups, and these are placed on one of the corners of the tetrahedra at either end of the central C-C bond, these tetrahedra representing the bonds from these C atoms. The right side and the left side of this figure contain different structures.

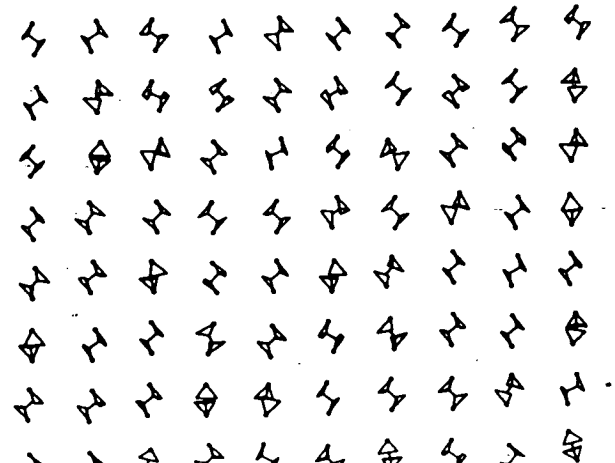

Fig. 8. — The sample of Figure 7 warmed to 140 K, where the molecules become disordered about the long axis and the structure becomes orthorhombic.

At the time of writing it appears that the lowest phase is characterised by an ordering of the twisting angles for the methyl groups so that the overall length

of the long molecular axis is as short as possible. These angles must suffer disorder at a temperature well below the plastic transition.

To investigate the plastic phase one of the MD configurations was "warmed up" and a transition was observed at roughly 115 K. This is to be compared with the experimental value of 108 K obtained from specific heat measurements [23]. A configuration section at 140 K is shown in Figure 8. The in-plane unit cell angle has become 90° and an orthorhombic Immm structure has developed. Of course the symmetry elements are only valid in the time average as in the course of time the molecules reorient through 180° about their long axes, in agreement with NMR studies [24]. A histogram of the angular positions of the molecules about this long axis is given in Figure 9 which strongly suggests that there is a double-well potential for long axis rotation.

We hope that these simulation studies will help in the further interpretation of actual experiments and may lead to a correct structure determination of the various phases. The complexity achieved with our simple model is consistent with the fact that such a simple compound has not yet given up its structural secrets.

"Quaternane" — a two-dimensional model

The complex phenomena associated with a double-well potential are sometimes expected to include incommensurate structure transitions. Simulation of three-dimensional incommensurates must require an order of magnitude more molecules than we can manage on our DAPs, and so as an exercise we have performed a two-dimensional simulation. 4096 molecules make a respectable configuration for this work, though it is not expected that a two-dimensional system would display true incommensurate behaviour even at the thermodynamic limit [25].

For this model we chose a four atom molecule — shall we say "quaternane" — as shown in Figure 10. Potential minima with respect to the variables θ_1 and θ_2 occur symmetrically about $\theta = 0$ at an angle which

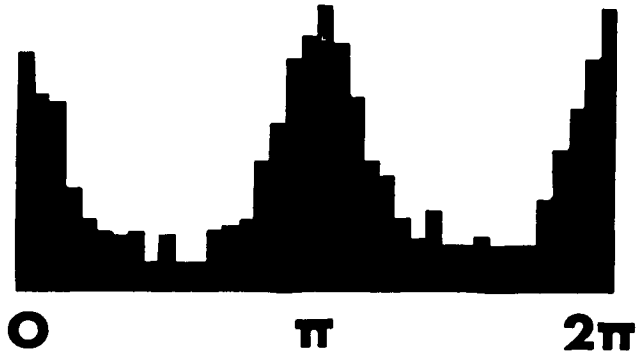

Fig. 9. — Histogram of the angular positions of the molecules about the long axis at 140 K, showing two peaks at 0° and 180°, consistent with an orthorhombic structure.

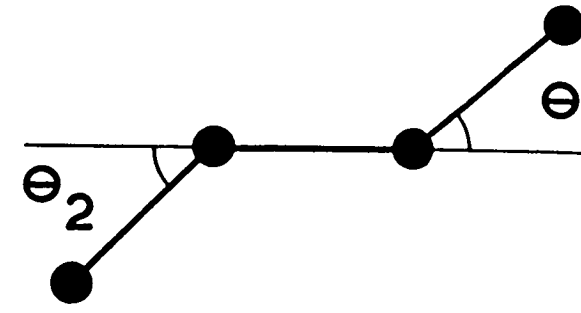

Fig. 10. — The molecule of 'quaternane', showing the two internal degrees of freedom.

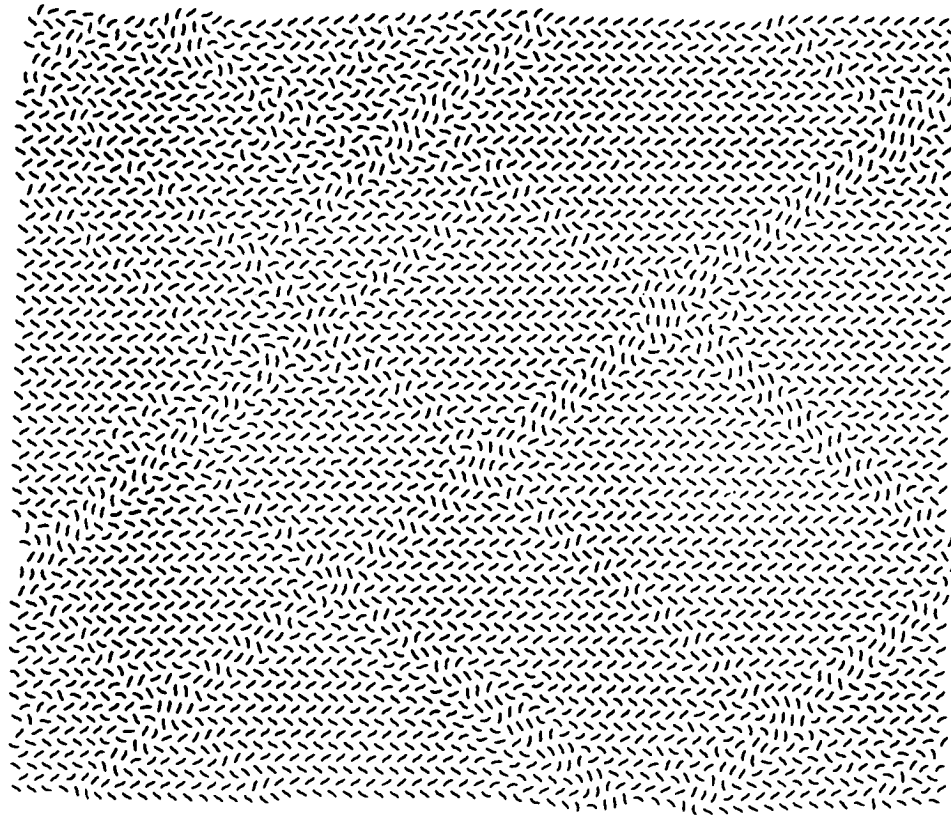

Fig. 11. — A configuration of the two-dimensional structure of quaternane at 5 K, showing the build-up of domain walls.

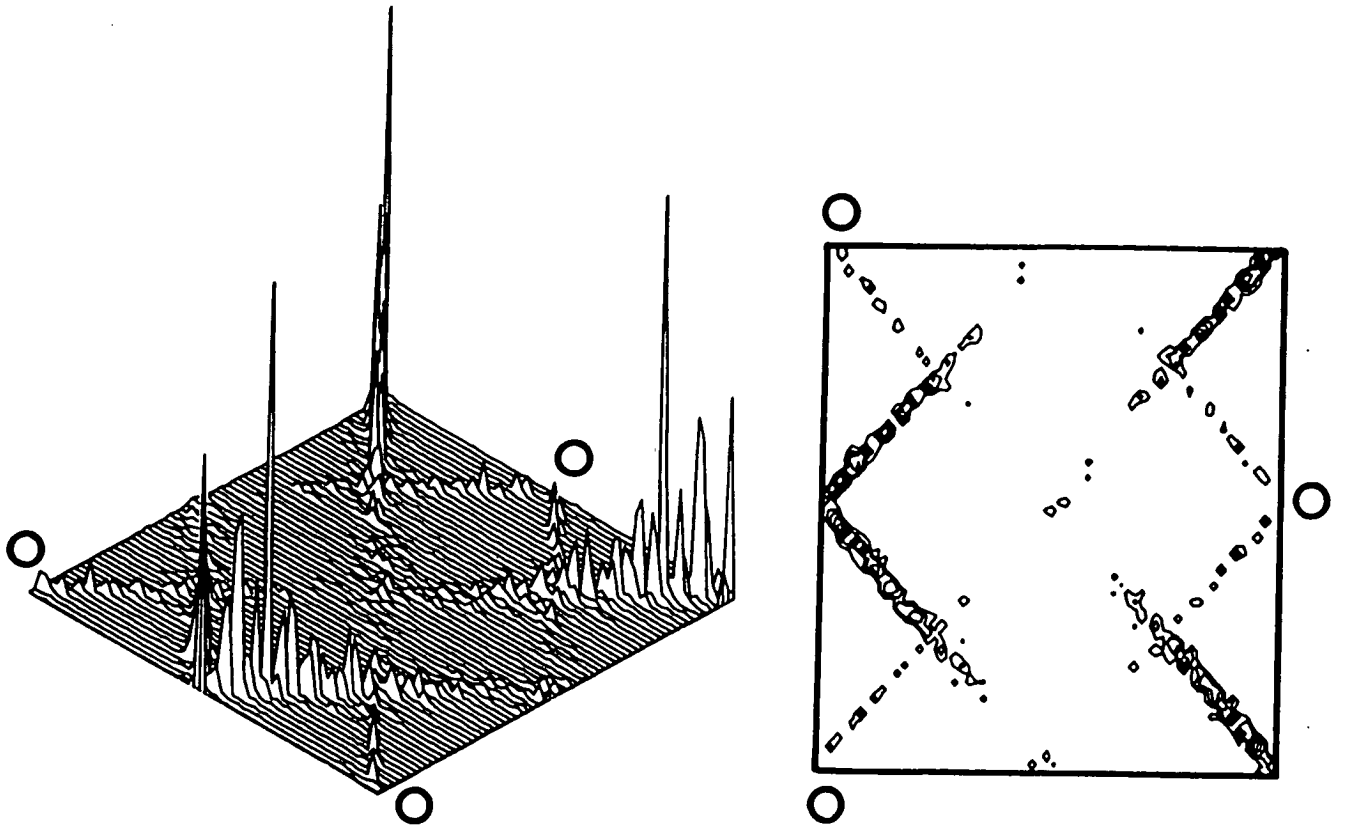

Fig. 12. — Fourier transform of the configuration of Figure 11, in which the variable used is the angle of the central C-C bond with the direction AB. The diagram on the right is exactly to scale with the configuration of Figure 11.

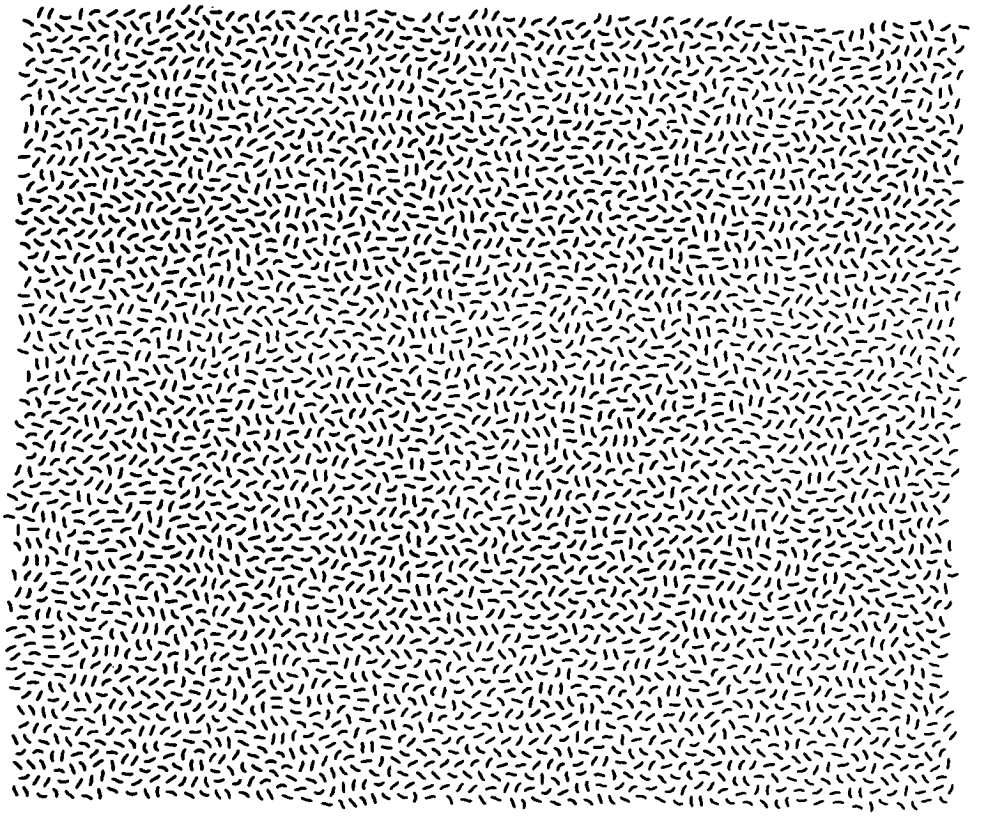

ig. 13. — As Figure 11 but for 14 K. The domain walls are now not discernible to the eye, and so are examined through the use of the transform.

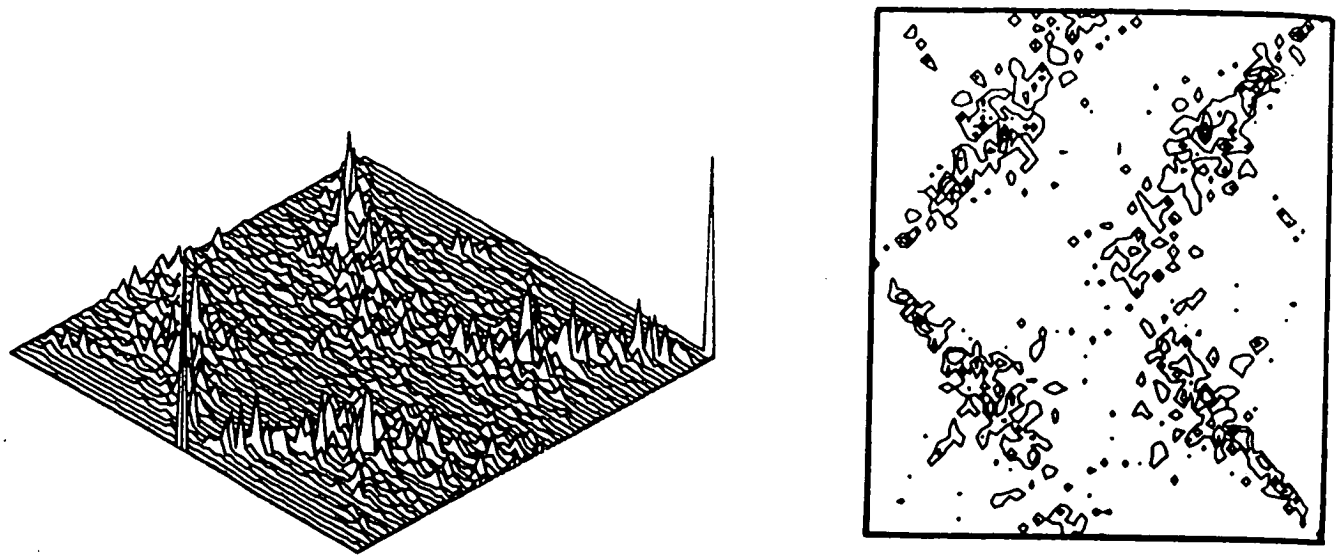

Fig. 14. — As Figure 12 but for 14 K. The features in the transform associated with the domain walls are still clearly apparent.

can be chosen as a model variable, and the height of the barrier at $\theta = 0$ is another model variable. Only preliminary results are presented here for simulations which are not always exactly at zero pressure. No numerical details are given for these results, so the temperature values must be interpreted as simply defining a scale.

At 3 K a single crystal of herringbone structure persists for a long time (in MD terms), but a clear change sets in at 5 K as shown in Figure 11. This latter configuration has been investigated via the Fourier transform of the single variable – the angle of the central quaternane bond with the horizontal line AB. The transform is shown in Figure 12, where Figure 12 (b) is exactly to scale for the reciprocal space of Figure 11.

During the time before Figure 11 it was clear from the transform that systematic disordering was building up, and earlier configurations show domain walls of little more than one molecule thick. These walls were found not to move in a soliton fashion, but simply grew in thickness until the point where Figure 11 was plotted, after which no noticeable change occurred. The Fourier transform clearly shows lines of intensity at right-angles to the directions of the domain walls. Equivalent reciprocal space origins are denoted by 0 in Figure 12 (a), and it should be realised that these points have zero intensity in the fully ordered case as the chosen variable has an antiferromagnetic form and therefore has a mean value of zero.

A most interesting point to notice is the structure in the regions where two walls intersect. The structure here is closely related to the structure in a wall, and is reminiscent of a smectic liquid crystal. This model thus probably has many of the features for a two-dimensional liquid crystal, and we plan to do further simulations on configurations which allow this structure to exist over the whole MD sample.

Finally let us look at the result obtained at 14 K, shown in Figures 13 and 14. Figure 13 does not show domain walls even to the practised eye, and might be described as liquid-like. Nevertheless the Fourier transform contradicts this conclusion as Figure 14 clearly shows. The same peaks appear as in Figure 12, albeit smaller, and we have found that even at higher temperatures the domain wall "signal" is noticeable above the noise. We presume that melting takes place when this signal disappears but have not yet reached this point in our work.

Finale

We regard the pattern recognition required within these configurations as a taxing task in information technology and foresee a growing demand for the development of the necessary algorithms as the computing power available increases. Molecular dynamics, along with Monte Carlo, is already a major user of computing resource, and now that realistic modelling is feasible the future for this work is bright indeed.

Acknowledgements

We thank Professors Robert Pick and Salvatore Califano for inviting us to contribute to this issue. Thanks are also due to the Science and Engineering Research Council (UK) for support both of our DAP facility and of three of the authors.

References

(1) H. Gostick. — I.C.L. Tech. Jour., 1979, 1, 116-135. R.W. Hockney & C.R. Jesshope. — *Parallel Computers*, Adam Hilger Ltd., Bristol, 1981.
(2) M. Parrinello & A. Rahman. — *Phys. Rev. Letters*, 1980, 45, 1196-1199.
(3) G.S. Pawley & G.W. Thomas. — *Phys. Rev. Letters*, 1982, 48, 410-413.
(4) R.G. Della-Valle & G.S. Pawley. — *Acta Cryst.*, 1984, A40, 297-305.
(5) D. Beeman. — *J. Compout. Phys.*, 1976, 20, 130-139.
(6) D.J. Evans. — *Mol. Phys.*, 1977, 34, 317-323.
(7) P. Du Val. — *Homographies, Quaternions and Rotations*, (Oxford Mathematical Monograph), 1964.
(8) G.S. Pawley. — *Mol. Phys.*, 1981, 43, 1321-1330.
(9) K. Refson & G.S. Pawley. — In preparation.
(10) H.J.C. Berendsen and W.F. Van Gunsteren. — *In Proc. NATO Advanced Study Inst.* On Superionic Conductors, Odense, Denmark, 1981, Plenum Press, 1983.
(11) M.T. Dove and G.S. Pawley. — *J. Phys. C*, 1983, 16, 5969-5983.
(12) M.T. Dove and G.S. Pawley. — *J. Phys. C*, 1984, 17, 6581-6599.

(13) G. Dolling, B.M. Powell and V.F. Sears. – *Molec. Phys.*, 1979, 37, 1859.
(14) G. Raynerd, G.J. Tatlock and J.A. Venables. – *Acta Cryst.*, 1982, B38, 1896.
(15) G.S. Pawley and M.T. Dove. – *Chem. Phys. Letters*, 1983, 99, 45-48.
(16) B.M. Powell. – Private communication.
(17) Ph. Pruzan, D.H. Leibenberg and R.L. Mills. – *Phys. Rev. Letters*, 1982, 48, 1200.
(18) G.S. Pawley. – Solid State Communications, 1985, 53, 817-821.
(19) E.F. Sheka, E.L. Bokhenkov, B. Dorner, J. Kalus, G.A. Mackenzie, I. Natkaniec, G.S. Pawley and U. Schmelzer. – *J. Phys., C*, 1984, 17, 5893-5914.
(20) J.A. Ripmeester and R.K. Boyd. – *J. Chem. Phys.*, 1979, 71, 5167 ; J.A. Ripmeester, A.H. Reddoch and N.S. Dalal. – *J. Chem. Phys.*, 1981, 74, 1526.
(21) M.L. Cangeloni and V. Schettino. – *Mol. Cryst. Liq. Cryst.* 1975, 31, 219.
(22) G.S. Pawley and G.W. Thomas. – *J. Comput. Phys.*, 1982, 47, 165-178.
(23) J.G. Aston and G.H. Messerly. – *J. Amer. Chem. Soc.*, 1940, 62, 1917.
(24) M.J.R. Hoch. – *J. Chem. Phys.*, 1976, 65, 2522.
(25) P. Bak. – *Rep. Prog. Phys.*, 1982, 45, 587.